

DB white dwarfs in the Sloan Digital Sky Survey Data Release 10 and 12

D. Koester¹ and S.O. Kepler²

¹ Institut für Theoretische Physik und Astrophysik, Universität Kiel, 24098 Kiel, Germany
e-mail: koester@astrophysik.uni-kiel.de

² Instituto de Física, Universidade Federal do Rio Grande do Sul, 91501-900 Porto-Alegre, RS, Brazil

Sep 21, 2015

ABSTRACT

Aims. White dwarfs with helium-dominated atmospheres (spectral types DO, DB) comprise approximately 20% of all white dwarfs. There are fewer studies than of their hydrogen-rich counterparts (DA) and thus several questions remain open. Among these are the total masses and the origin of the hydrogen traces observed in a large number and the nature of the deficit of DBs in the range from 30 000 - 45 000 K. We use the largest-ever sample (by a factor of 10) provided by the Sloan Digital Sky Survey (SDSS) to study these questions.

Methods. The photometric and spectroscopic data of 1107 helium-rich objects from the SDSS are analyzed using theoretical model atmospheres. Along with the effective temperature and surface gravity, we also determine hydrogen and calcium abundances or upper limits for all objects. The atmosphere models are extended with envelope calculations to determine the extent of the helium convection zones and thus the total amount of hydrogen and calcium present.

Results. When accounting for problems in determining surface gravities at low T_{eff} , we find an average mass for helium-dominated white dwarfs of $0.606 \pm 0.004 M_{\odot}$, which is very similar to the latest determinations for DAs. There are 32% of the sample with detected hydrogen, but this increases to 75% if only the objects with the highest signal-to-noise ratios are considered. In addition, 10-12% show traces of calcium, which must come from an external source. The interstellar medium (ISM) is ruled out by the fact that all polluted objects show a Ca/H ratio that is much larger than solar. We also present arguments that demonstrate that the hydrogen is very likely not accreted from the ISM but is the result of convective mixing of a residual thin hydrogen layer with the developing helium convection zone. It is very important to carefully consider the bias from observational selection effects when drawing these conclusions.

Key words. white dwarfs – Stars: atmospheres – Stars: abundances – convection – accretion

1. Introduction

Approximately 20% of all white dwarfs have atmospheres dominated by helium. Above $T_{\text{eff}} \approx 40\,000$ K, He II lines are strong and the stars are classified as spectral type DO or DOA if, in addition, Balmer lines of hydrogen are visible, or as DAO if these are dominant. Below this temperature He I lines are dominant and the spectral type is DB. If traces of other elements are present, more letters are added to the type, e.g., A for hydrogen, Z for metals (Sion et al. 1983). The existence of almost pure hydrogen (DA) and almost pure helium atmospheres as a result of gravitational settling is well understood, with the lightest element present floating to the top of the outer layers (Schatzman 1948). Helium-rich white dwarfs must have almost completely lost their outer hydrogen layer in a previous evolutionary phase; the currently accepted scenario is the born again or late thermal pulse scenario (Iben et al. 1983).

Questions remain as to the so-called DB gap and the origin of hydrogen traces in a large number, perhaps the majority, of DB white dwarfs. The deficit of DBs between 30 000 and 45 000 K was first identified by Liebert et al. (1986) and explained in terms of diffusion and convective mixing by Fontaine & Wesemael (1987). Eisenstein et al. (2006) and Kleinman et al. (2013) found several objects within the gap, but the number was still smaller than expected from the simple cooling rates without changes of spectral types. In principle, the ob-

served traces of hydrogen could be explained by two competing theories: accretion of interstellar matter (ISM) or convective mixing with a (thin) hydrogen layer left over from the previous evolution (which, at the same time, could also explain the DB gap).

Two recent studies have analyzed large samples of helium-rich white dwarfs. Voss et al. (2007) used data for 71 objects from the Supernova Ia Progenitor Survey (SPY, Napiwotzki et al. 2003). The typical resolution (depending on the seeing) was $\sim 0.4 \text{ \AA}$, with the signal-to-noise ratio (S/N) varying but > 15 . The study by Bergeron et al. (2011, henceforth BW11) is the largest so far with 108 objects. The resolution from two different spectrographs was 3–6 \AA , with the S/N mostly above 50. In this work we use a sample of 1107 DB (and DBA or DBZ) stars, thus increasing the sample more than tenfold the largest previous ones. The resolution is $\sim 2.5 \text{ \AA}$, the S/N ranges from 10 to 75 with an average of 20. The average quality of the spectra is inferior to the BW11 sample in S/N and in resolution to the SPY sample. However, this is compensated for by the huge size and homogeneity, which allows us to study statistical properties of the helium-rich white dwarfs with unprecedented quality.

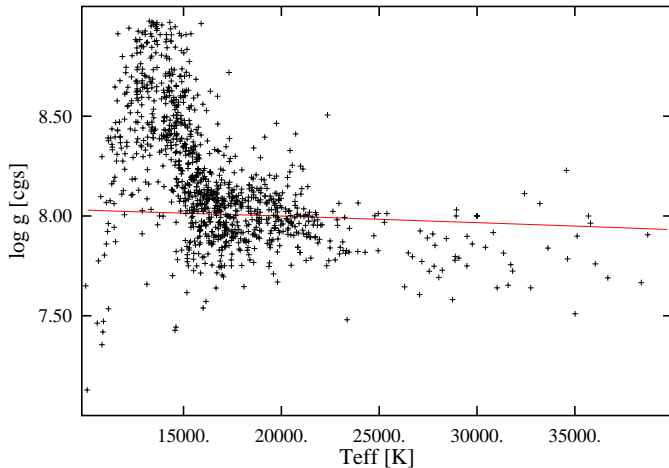


Fig. 1. Surface gravity $\log g$ as a function of effective temperature. The continuous (red) line is the sequence for a constant mass of $0.6 M_{\odot}$.

2. The sample

Data Release 7 (Kleinman et al. 2013, DR7) of the Sloan Digital Sky Survey (SDSS) contained spectra of 923 stars classified as DB (helium atmospheres). DR10 (Kepler et al. 2015) added another 450 (including subtypes DBA with hydrogen traces and DBZ with metals), and DR12 (Kepler et al. 2015a) added 121 more, all of which are new detections. The number of spectra is larger since several have two or three spectra in the database. From this database we first selected all those with S/N greater than 10.

After a first tentative fit with model spectra (see below for details) and a visual inspection we eliminated all objects with peculiarities, such as a red unresolved companion (DB+dM), presence of He II lines (DO), obvious magnetic splitting of spectral lines, very marginal or invisible He lines (DC), or spectra with strong artifacts. We did not eliminate DB stars with traces of hydrogen (DBA) or calcium H+K lines (DBZ). This left us with a sample of 1267 spectra of 1107 different objects, of which 13 had three and 136 had two spectra. In addition to the spectra, we used the SDSS photometry, available for each object in the sample.

3. Atmospheric parameters

Atmospheric parameters T_{eff} , $\log g$, abundances, or upper limits of hydrogen and calcium were determined by a comparison of observations with several grids of theoretical model atmospheres. The input physics and procedures used are described in Koester (2010). We use the mixing-length approximation for convection in the version ML2 (Fontaine et al. 1981; Tassoul et al. 1990) with a mixing length equal to 1.25 pressure scale heights. A pure helium grid – for technical reasons the logarithmic abundance ratio of hydrogen to helium, $\log N_{\text{H}}/N_{\text{He}}$ (abbreviated [H/He] henceforth) is -20.0 – covers effective temperatures from 10 000 to 50 000 K, with step widths ranging from 250 to 500 K from low to high effective temperatures. The surface gravity $\log g$ ranged from 6.00 to 9.50, with step width 0.25. In addition to the pure helium grid above, we also calculated grids with various [H/He] ratios: -6.0 , -5.5 , -5.0 , -4.5 , -4.0 , -3.5 , and -3.0 . These grids covered the same T_{eff} and $\log g$ values, except that the $\log g$ range only covered from 7.0 to 9.0. Details of the analysis are described in the following.

3.1. Photometry

From the synthetic spectra we calculated theoretical photometry in the SDSS system. The effect of the surface gravity on the photometry is small; in the first step of the fitting procedure, we thus kept this parameter fixed at the canonical value of 8.0. A possible concern for the fainter objects at greater distance is interstellar reddening, which leads to lower apparent temperatures. We determined three different fit results: one assuming that the reddening is negligible, a second that assumes the maximum reddening from the Schlafly & Finkbeiner (2011) extinction map, and a third value that uses an iterative procedure as described in Tremblay et al. (2011) and Genest-Beaulieu & Bergeron (2014). Basically, this method assumes that the extinction is negligible within 100 pc, and from there it increases linearly to the maximum value at a vertical height $z = 250$ pc above the Galactic plane. This approach also gives the best approximation for the distance and z , although it should be kept in mind at this step a fixed radius corresponding to $\log g = 8.0$ and a pure He atmosphere is assumed for all objects.

3.2. Spectroscopy

As a next step the observed spectra were fitted with the pure He grid, to determine T_{eff} and $\log g$. A well known problem in many cases is that there are two possible solutions corresponding to local χ^2 minima, one below and one above the region of $T_{\text{eff}} = 24\,000 - 26\,000$ K, where the He lines reach their maximum strength. The χ^2 values of the two solutions are usually very similar or even identical and cannot be trusted to select the correct solution. We used the photometric fits, which do not have this problem, as well as visual inspection of all fits, to minimize wrong choices.

Then, in all spectra we used an automatic measuring procedure to determine H α equivalent widths and uncertainties, or alternatively upper limits; all positive and negative detections were confirmed by visual inspection. These measurements were compared to theoretical equivalent widths from the grids with various hydrogen traces as described above, and hydrogen abundances [H/He], uncertainties, or upper limits were determined. With this additional knowledge, the spectral fits were repeated with the grid that matched to the measured abundance most closely, and this whole procedure was iterated until the parameters were determined with (almost) fully consistent theoretical models. As a final step, the photometric fit was repeated, but now keeping all parameters from the spectroscopic results fixed and solving only for the consistent distance and Galactic position. Table 1 (online only) contains the final results of this analysis.

4. Analysis

4.1. Surface gravity and masses

Figure 1 shows the surface gravity versus effective temperature for all objects, except for a few low temperature DBs, where the spectroscopic fitting did not converge on a $\log g$ within the grid; Table 1 shows more detail in numerical form. Some features of this result are immediately apparent:

- the $\log g$ and masses are significantly higher below 16 000 K than for the hotter objects. This effect has been observed before, e.g., by Kepler et al. (2007), BW11, and Kepler et al. (2015). BW11 tentatively conclude that the large mass spread might be real for $T_{\text{eff}} > 13\,000$ K, given the presence of larger and smaller $\log g$ determinations in the same

Table 2. Average surface gravity $\log g$ as a function of effective temperature T_{eff} in 19 intervals. Second column: average $\log g$ and, in parentheses, 1σ width of the distribution. Third column: average mass, error of the average and 1σ width of the distribution. N is the number of objects in the interval. BR is the number normalized with the cooling time through the interval and the luminosity to the $3/2$ power.

T_{eff} [K]	$\log g$ [cgs]	M [M_{\odot}]	N	BR
10000 - 12000	8.166 (0.379)	0.696 (0.029,0.208)	52	2.092
12000 - 13000	8.564 (0.234)	0.928 (0.017,0.142)	69	4.018
13000 - 14000	8.577 (0.290)	0.937 (0.019,0.173)	83	3.928
14000 - 14500	8.535 (0.236)	0.914 (0.017,0.141)	69	5.595
14500 - 15000	8.384 (0.283)	0.825 (0.018,0.165)	81	6.125
15000 - 15500	8.250 (0.276)	0.741 (0.017,0.165)	94	6.287
15500 - 16000	8.137 (0.228)	0.673 (0.015,0.135)	84	5.284
16000 - 16500	8.046 (0.175)	0.621 (0.012,0.098)	71	4.013
16500 - 17000	8.021 (0.169)	0.607 (0.011,0.095)	72	3.865
17000 - 17500	8.015 (0.171)	0.605 (0.012,0.097)	62	3.089
17500 - 18000	8.014 (0.113)	0.603 (0.009,0.062)	44	2.093
18000 - 19000	8.007 (0.128)	0.601 (0.008,0.070)	70	1.471
19000 - 20000	8.011 (0.138)	0.605 (0.009,0.077)	65	1.165
20000 - 22000	7.991 (0.119)	0.597 (0.007,0.066)	79	0.595
22000 - 24000	7.898 (0.175)	0.556 (0.019,0.095)	24	0.161
24000 - 26000	7.934 (0.079)	0.574 (0.016,0.042)	7	0.046
26000 - 28000	7.789 (0.099)	0.509 (0.014,0.045)	11	0.074
28000 - 30000	7.828 (0.132)	0.532 (0.018,0.063)	12	0.087
30000 - 40000	7.841 (0.171)	0.550 (0.016,0.079)	23	0.063

temperature interval and a comparison of spectroscopic and parallax distances of 11 objects. Only one of the 11 objects has a really large spectroscopic mass, and for this one the two distances show a large discrepancy; the authors admit that at these low temperatures the limit of the spectroscopic method may have been reached, because of the weakness of the He lines. We believe that the systematic change in our sample (Fig. 1) is caused by an imperfect implementation of line broadening by neutral helium, which dominates the broadening below 16 000 K.

- There is also a significant increase in the width of the $\log g$ distribution, in addition to this systematic effect. The explanation is most likely the decreasing strength of the helium lines in conjunction with the moderate resolution and S/N of the SDSS spectra, which increase the errors of the individual parameter determinations. Because of these results, we only use the solution with $\log g$ fixed at 8.0 for $T_{\text{eff}} < 16\,000$ K and assume an error for $\log g$ of 0.25.
- The average mass in Table 2 shows little variation in the range $16\,000 \leq T_{\text{eff}} \leq 22\,000$ K with an average over this whole range of $0.606 \pm 0.004 M_{\odot}$. In six of the seven highly populated intervals, the average agrees with this value within the 1σ errors, and in the other within 2σ , which is close to expectation, if the average mass is indeed constant. We conclude that this is a realistic estimate of the average mass of DB (including DBA, DBZ) white dwarfs and that any averaging that includes cooler or hotter objects will necessarily lead to erroneous results. For example, for our complete sample we get an unreliable average of $0.706 \pm 0.006 M_{\odot}$.
- DBs at 10 000 K are approximately 5×10^8 years older than at 30 000 K. They may originate from more massive progenitor stars on the main sequence and end up as higher mass white dwarfs. Using data from Salaris et al. (2009) and Pietrinferni et al. (2004), we estimate that this effect could account for a difference of about $0.05 M_{\odot}$ over the observed range. This could explain the slightly lower mass at the high T_{eff} end, but certainly not the large increase below 16 000 K.

- Both Fig. 1 and Table 2 show a deficiency of objects – almost a gap – in the interval 24 000–26 000 K, in comparison to both neighboring intervals. To demonstrate that such a gap is not expected from evolution or observational effects, we calculated the quantity BR in the last column of the table. This is the number of objects divided by the cooling time during the interval and by the luminosity $L^{3/2}$, and scaled by an arbitrary constant for easier comparison. The first factor takes the different times spent in each interval during the cooling into account, and the second the larger observation volume for intrinsically brighter objects. If the observations were complete and a magnitude-limited sample, this number would be proportional to the birthrate of DB white dwarfs, and thus be a constant, if all DBs originate at high T_{eff} and only evolve through the range of our sample (see below). Obviously these conditions are not fulfilled; nevertheless, even with these numbers, the gap 24 000–26 000 K is significant. (We note that the apparent gap is centered on 26 000 K, and the argument would be even more convincing had we used the interval 25 000–27 000 K.)

Our explanation of the last point is as follows: This temperature region is exactly where the helium lines have their maximum strength as a function of effective temperature. If the predicted line strengths are greater than attained by the observed objects, then the fitting procedure will force them to a solution on either side of the maximum. BW11 also discuss this possibility and conclude that a mixing-length parameter $\alpha = 1.25$ (which is also our choice) provides the smoothest distribution of stars over the temperature range. However, because of their smaller sample, there are only ~ 20 objects between 20 000 and 30 000 K, compared to 134 in our sample. Judging by Fig. 2 in BW11, a slightly larger α would probably give a more plausible distribution for our sample.

An alternative suggestion, made by the referee, is a possible small error in the SDSS flux calibration (see below for further discussion). A possible indication for this is that two of the

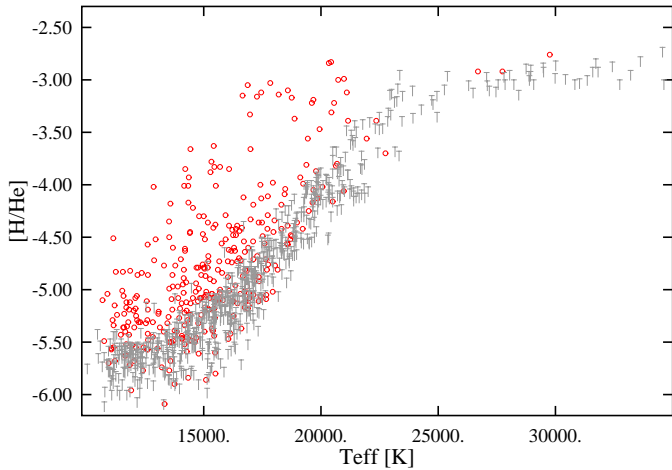


Fig. 2. Logarithmic hydrogen abundance $[H/He]$ as a function of T_{eff} . Red circles indicate detected abundances, black symbols indicate upper limits.

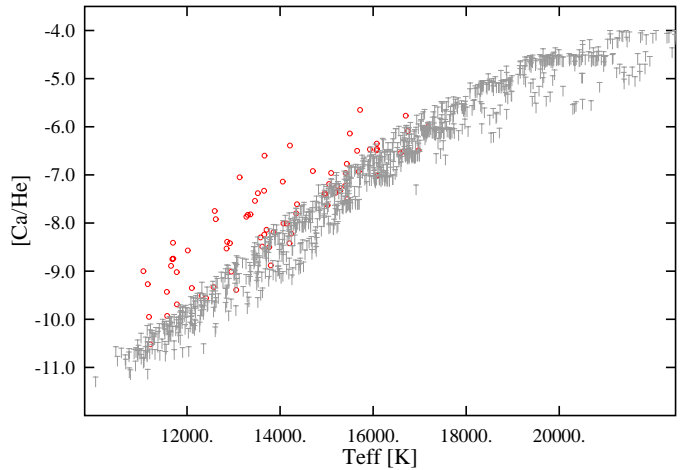


Fig. 4. Logarithmic calcium abundance $[Ca/He]$ as a function of T_{eff} . Red circles represent detected abundances, and black symbols the upper limits.

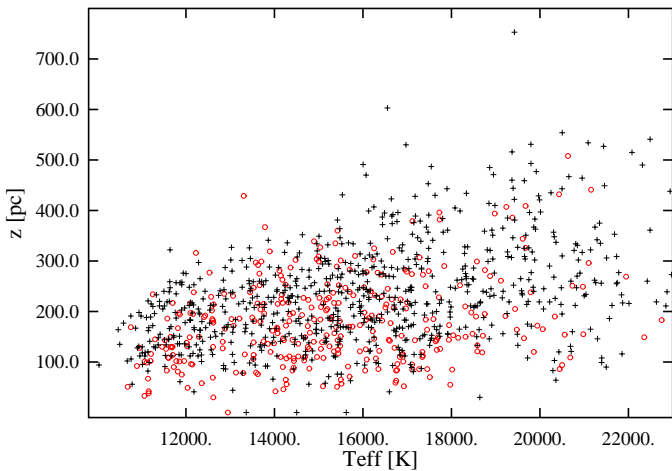


Fig. 3. Distribution of DBAs (red circles) and DBs (black crosses) with height z above the Galactic plane. The general decrease of distances towards lower T_{eff} is very likely caused by the lower luminosity of the cooler objects.

common objects between the BW11 and our sample have $T_{\text{eff}} \sim 26\,000$ K in BW11, but 24 000 and 28 000 K in our determination.

4.2. Hydrogen abundance

The hydrogen abundance as a function of T_{eff} is shown in Fig 2. The detection limit is high at high temperatures because the hydrogen spectral lines get weaker. On the other hand, at low temperatures, much smaller abundances can easily be detected. The abundances, however, do not reach the same level as at the high T_{eff} end, because the hydrogen gets diluted by the increasing depth of the convection zone. Out of a total of 1036 objects with $T_{\text{eff}} < 23\,000$ K, 329 or 32% show hydrogen. However, our sample extends over a large range of S/N values and positions in the Galaxy that have an influence on the observed DBA fraction. This is demonstrated in Table 3.

The S/N ratio is an obvious factor influencing the detectability of hydrogen. The percentage of DBAs increases very significantly with increasing S/N, from 37% for the subsample with $z \leq 250$ pc to 75% at the highest S/N. This is even higher than the

Table 3. Dependence of the DBA/(DBA+DB) number ratio on the signal-to-noise (S/N) and position in the Galaxy z . The statistics use only objects with $T_{\text{eff}} \leq 23\,000$ K to minimize observational bias that is due to the low detection probability at higher T_{eff} .

S/N, z [pc]	N(DBA)	N(DB)	%DBA
$S/N \geq 10, z \leq 250$	267	449	37.3
$S/N \geq 10, z > 250$	62	258	19.4
$S/N \geq 20, z \leq 250$	191	179	51.6
$S/N \geq 20, z > 250$	12	27	30.8
$S/N \geq 30, z \leq 250$	106	55	65.8
$S/N \geq 30, z > 250$	0	4	0.0
$S/N \geq 40, z \leq 250$	46	15	75.4
$S/N \geq 40, z > 250$	0	0	0.0
S/N 10 - 15, $z \leq 250$	29	140	17.2
S/N 10 - 15, $z > 250$	25	140	15.2

Table 4. Similar to Table 3 but for Ca: dependence of the DBZ/(DBZ+DB) number ratio on the S/N and position in the Galaxy z . The statistics use only objects with $T_{\text{eff}} \leq 17\,000$ K.

S/N, z [pc]	N(DBZ)	N(DB)	%DBZ
$S/N \geq 10, z \leq 250$	62	484	11.4
$S/N \geq 10, z > 250$	13	144	8.3
$S/N \geq 20, z \leq 250$	34	233	12.7
$S/N \geq 20, z > 250$	0	11	0.0
$S/N \geq 30, z \leq 250$	14	100	12.3
$S/N \geq 30, z > 250$	0	0	0.0
$S/N \geq 40, z \leq 250$	4	41	8.9
$S/N \geq 40, z > 250$	0	0	0.0
S/N 10 - 15, $z \leq 250$	12	124	8.8
S/N 10 - 15, $z > 250$	10	82	10.9

values of 44% found by BW11 and 55% by Voss et al. (2007), regarded as being lower limits in those papers. Our findings suggest that practically all DBs show some trace of hydrogen if the resolution and S/N are high enough.

With the large size of our sample and the excellent SDSS photometry, for the first time we can try to study the position of DBs and DBAs in the Galaxy, in particular the height above the Galactic plane. This is an important quantity for the question: is the hydrogen content due to external processes, e.g., accretion from interstellar gas, or from the remnants of a planetary system, or to an intrinsic process like dilution of an outer hy-

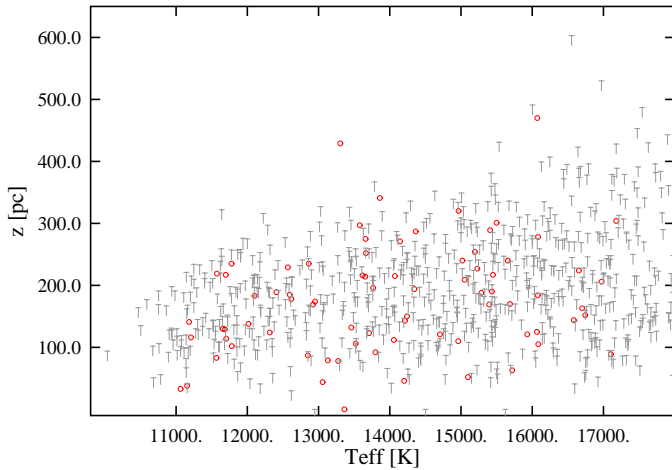


Fig. 5. Distribution of DBZs (red circles) and DBs (black limit symbols) with height z above the Galactic plane.

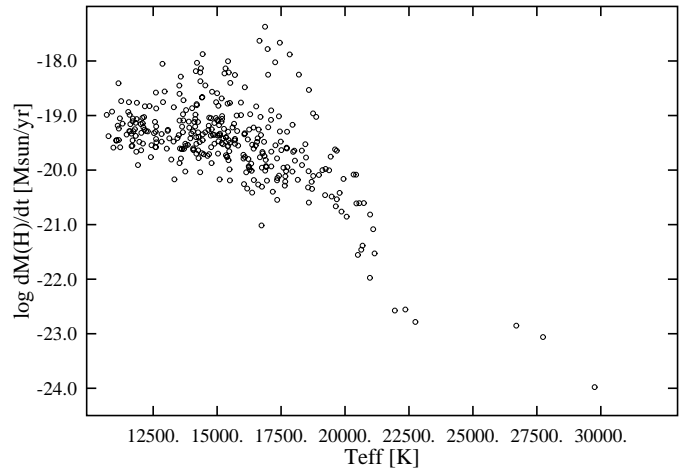


Fig. 7. Average rate for the increase in the total hydrogen mass with age of the white dwarf.

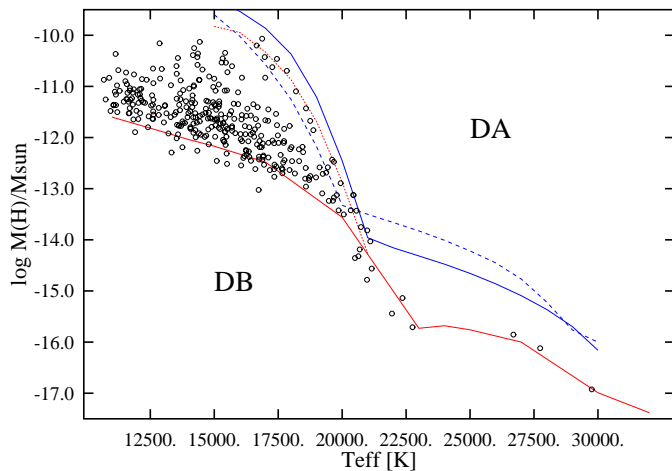


Fig. 6. Total hydrogen mass in the convection zone. The continuous red line is the transformed lower limit to the positive detections in Fig. 2. The dotted red curve is the expected location for an abundance $[H/He] = -3$, which coincides with the continuous red curve at high temperatures. The blue curves indicate the expected hydrogen masses for abundances of -2 (continuous) or -1 (dotted).

drogen envelope in a developing helium convection zone. Figure 3 shows this distribution, which demonstrates a concentration of the DBAs towards the Galactic plane. The effect becomes even clearer in Table 3, which shows a decrease in the DBA percentage with height z . Before jumping to premature conclusions, however, we need to take into account that the group with $z > 250$ pc has on average larger distances and lower S/N, which possibly alone could explain the z dependence. To test this we have taken a progressively smaller limit on the S/N, to make both groups more comparable. Taking only objects with $10 \leq S/N \leq 15$, the average S/N and its distribution become almost identical. For this sample the difference between the two groups disappears (last lines in Table 3): taking samples with comparable S/N, there is no obvious concentration toward the Galactic plane.

4.3. Metals in DBs: the DBZs

Seventy-five objects show the H+K resonance lines of ionized calcium – this is the only metal detected in our sample. Figures 4 and 5 and Table 4 show the distribution of the DBZs with

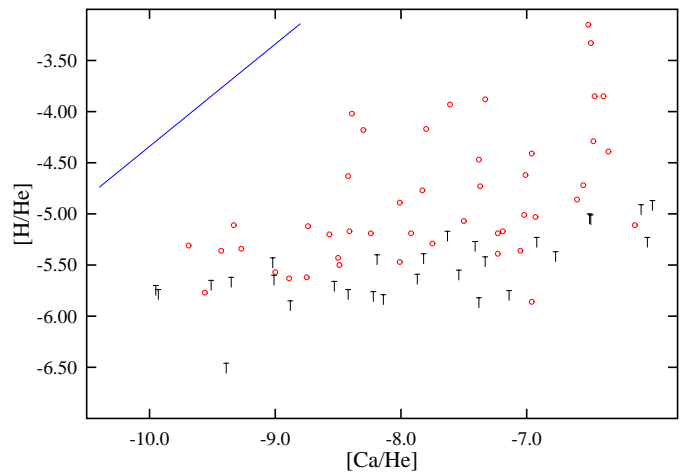


Fig. 8. Hydrogen abundance or upper limit versus Ca abundance in all DBZs. The $[H/He]$ ratio is smaller than the solar value (continuous line) in all objects.

T_{eff} , S/N, and z in the same way as for hydrogen in the previous figures and tables. Surprisingly, the fraction of DBZs shows little variation with the S/N ratio, which might even be explainable by the smaller numbers. The only explanation we can find is that the Ca II lines are much narrower and deeper than $H\alpha$, and therefore easier to detect, even at low S/N. The change of the ratio with z is smaller than that for hydrogen (from 11.4 to 8.3%) and even reverses when using the limited sample with S/N between ten and 15. The numbers are still relatively small, but we can definitely state that they do not prove any preference for accretion of interstellar matter close to the Galactic plane (Fig. 5).

4.4. Error estimates

The errors for T_{eff} and $\log g$ in Table 2 are only formal statistical errors and thus underestimate the real uncertainties. Fortunately we have multiple spectra for 149 objects, leading to 162 pairs of T_{eff} determinations and 72 for $\log g$ (excluding those with fixed 8.0). The average absolute differences are 3.1% for T_{eff} , 0.12 for $\log g$, 0.18 for $[H/He]$, and 0.25 for $[Ca/He]$. Since the models and fitting procedures are exactly the same, these are uncertain-

ties due to the observations caused, for example, by different S/N or reductions.

There are 27 objects in common with the sample of BW11. If we compare only the 17 DBs with $T_{\text{eff}} \geq 16\,000\text{ K}$, where we determine both parameters, the systematic difference for T_{eff} is -1.3%, i.e. our T_{eff} are slightly larger on average). The dispersion is 4.6%, a reasonable number given that our internal uncertainties are already 3.1%. The differences in surface gravity are larger, with a systematic effect of 0.095 dex. In their study of DA white dwarfs, Genest-Beaulieu & Bergeron (2014), Tremblay et al. (2011), and Gianninas et al. (2011) find similar differences between their own spectra and SDSS samples. They conclude that the most likely reason is a small residual calibration error of the SDSS spectra. It is plausible that such an error would also affect the DB spectra. The $\log g$ dispersion between the BW11 and our results for $\log g$ is 0.073 dex. The larger internal error that we obtained above may be influenced by different S/N values for the multiple spectra of the same object.

5. Results and discussion

The overall features of our DB sample are similar to the results of BW11 and Voss et al. (2007): an apparent increase in the masses toward lower temperatures, mean mass around $0.6 M_{\odot}$, several DBs within the so-called DB gap above $30\,000\text{ K}$, and a large number of DBs contaminated with hydrogen abundances $[\text{H}/\text{He}]$ between -6 and -3. Apparent differences may at least be partly attributed to the tenfold increase of the sample size.

We do not find the apparent dichotomy at the very cool end between normal masses and a few very high masses near $1.2 M_{\odot}$, which probably motivated BW11 to exclude only the few objects in this range when determining a mean mass for DBs. In our sample there is clearly a continuous distribution; the increase in masses starts below $16\,000\text{ K}$. Since the convection zone develops near $30\,000\text{ K}$ and deepens significantly below $20\,000\text{ K}$, we think that neutral broadening is a more likely explanation than the convection theory, which is thought to be the reason behind a similar effect in the DAs (Tremblay et al. 2013). For the averaging, we thus use the intervals between $16\,000$ and $22\,000\text{ K}$, with many objects and a constant mass throughout, which results in a lower mean mass of $0.606 \pm 0.004 M_{\odot}$ compared to $0.671 M_{\odot}$ in BW11. The mean masses of Voss et al. (2007) agree approximately with our current result, but since different mixing-length parameters and different intervals for the averaging were used, the comparison is not very meaningful. We emphasize again that, as long as the reason for the $\log g$ increase at the low T_{eff} end is not understood, it is very important to only compare mean masses for well-defined T_{eff} intervals. If we use our complete sample, we obtain a mean mass of $0.706 M_{\odot}$, which is even higher than the BW11 result. Our preferred result agrees with the most recent determination of 0.603 ± 0.002 for DA white dwarfs from DR12 by Kepler et al. (2015a), but the caveat above also applies to the DA vs. DB comparison.

5.1. Hydrogen

Our result for the highest S/N objects indicates that at least 75% – and perhaps all DBs – show some contamination with hydrogen. The difference between DBs and DBAs is very likely just a question of the quality of the observations and we no longer distinguish the mean masses for the two groups. Since hydrogen lines are detected much more easily at low T_{eff} , the detections and upper limits go down to abundances around -6. High abundances, as found at high T_{eff} , are not detected in this range,

although they would be found easily. The obvious reason is the deepening of the convection zone below $\sim 18\,000\text{ K}$, and indeed, if multiplied with the mass in the convection zone, the total hydrogen masses seem to increase towards lower T_{eff} (Fig. 6). As a reminder, all hydrogen originally present or accreted from any source should always stay at the top of the envelope, in this case within the outer helium convection zone. The total hydrogen mass in an object can thus never decrease with time.

Continuous accretion from the interstellar medium could explain such an increase; dividing the hydrogen masses by the cooling age of the white dwarf indicates time-averaged accretion rates of 10^{-17} to $10^{-24} M_{\odot}/\text{yr}$ (Fig. 7). The size of these average rates is reasonable (Dupuis et al. 1993), although the huge spread and the increase toward lower temperatures might be difficult to explain. An alternative proposal, the continuous accretion of comets from an Oort cloud (Veras et al. 2014), could also explain such an increase toward older white dwarfs, but this faces the same problems.

To put these results into proper perspective we have to consider the strong observational selection effects apparent in Fig. 2. Transforming the approximate location of the observable lower limits for the detected DBAs into lower limits for the total H mass in the convection zone leads to the continuous red line in Fig. 6; because of the spread in S/N and range in $\log g$, there is a transition region and some objects are still found below our chosen curve. Below the red line we do not expect to find hydrogen in the objects of our sample. The region is of course not empty but filled with DBs with upper limits to the hydrogen mass between 10^{-16} and $10^{-12} M_{\odot}$, depending on T_{eff} .

At the hot end all abundances are $[\text{H}/\text{He}] \approx -3.0$; we have continued the (theoretical) location for this abundance with the dotted red curve toward lower T_{eff} . Almost all of our objects are confined to the region between these two red curves. Larger abundances are not found, but with our model calculations we can predict their location in Fig. 6. For abundances larger than ~ -2 the convection zones in the atmosphere become tiny or absent. Such models are not realistic because the hydrogen would diffuse upward immediately and turn the star into a hydrogen-rich DA – and thus out of our sample. In the upper right part we do not expect to find any DBAs as this region is occupied by DAs. The upper left part also seems sparsely populated. Rare objects like GD16 could fit in there with $11\,000\text{ K}$ and $\log M_{\text{H}}/M_{\odot} \approx -9$ (Koester et al. 2005, Gentile-Fusillo et al. in prep), but these can easily be misclassified as a DA.

In summary: we find exactly those objects that can exist in our sample, given the observational constraints and the physics of gravitational settling. The morphology of Fig. 7 is very similar to Fig. 6, because the cooling ages change only by 1.5 dex over the whole range of the figure, and the remarks concerning the observable objects are also applicable to the hypothetical accretion rates. The conclusion from this discussion is that Figs. 6 and 7 do not prove that there is any increase in the total hydrogen mass with time. The descendants of the hot DBAs with $M_{\text{H}}/M_{\odot} = 10^{-16}$ are not the observed cool DBAs but are lost from sight when the H abundance goes below the observable limit. This has to be taken into account when trying to derive conclusions about the origin of hydrogen in DBs from our present results.

Although our approach and presentation are completely different from the theoretical calculations of Macdonald & Vennes (1991), we agree with their prediction that helium-rich DBs with a hydrogen mass $> 10^{-14} M_{\odot}$ can only appear below $20\,000 - 22\,000\text{ K}$, depending slightly on the version of the mixing-length theory applied. According to their Fig. 1 and Ta-

ble 1, higher hydrogen masses appear at progressively lower T_{eff} , where they change from a pure hydrogen object into a DBA (or possibly a DB). If we look closely at the details, however, significant differences appear. To take a specific example: a DA with $M_{\text{H}}/M_{\odot} = 10^{-12}$ should turn into a DBA only at 11,300 K, whereas we already find such objects around 19 000 K. These problems led BW11 to the hypothesis that hydrogen might not be completely mixed within the He convection zone, but floating only near the top. This would decrease the total amount of H present for a given abundance and effective temperature, thus allowing for a dredge-up at higher T_{eff} . We consider this scenario unlikely since the convection velocities in the highly turbulent convection zone are many orders of magnitude larger than the diffusion velocities of hydrogen in helium. Instead, we prefer to speculate that the discrepancies are due to our imperfect description of convection with the mixing-length theory. Nature somehow seems to manage a complete mixing at 20 000 K, although theory predicts it only happens at 11 300 K.

Does this mean that the origin of hydrogen in DBAs is the mixing of a residual small hydrogen layer in the range 30 000 - 40 000 K, which is left over from the previous evolution? In the framework of interstellar accretion as a source of the hydrogen, one would have to assume a typical average hydrogen accretion rate of $10^{-19} M_{\odot}/\text{yr}$ for the majority of the cool objects. In 10^5 years the star would accumulate an outer H layer of $10^{-14} M_{\odot}$, enough to become a DA. This is a very short time compared to the cooling age at 30 000 K, and for the later evolution it makes no essential difference if the DA arrives with a thin evolutionary H layer or acquires it almost instantaneously through accretion. Both scenarios require that a significant fraction of DA white dwarfs near $T_{\text{eff}} = 30\,000$ K have thin hydrogen envelopes in the range of $10^{-16} - 10^{-10} M_{\odot}$. It also requires that many DB/DBA white dwarfs are only borne around 20 000 K and, thus, that their space density, corrected for cooling times (i.e., the luminosity function), is smaller at higher T_{eff} . This is exactly what was found by BW11: the DB to DA ratio of all white dwarfs in the Palomar-Green sample increases sharply around 20 000 K during the cooling sequence.

A decision about the origin of hydrogen then boils down to the question of whether it is more likely for stars to have environments at 30 000 K that lead to accretion rates differing by six orders of magnitude or to have residual hydrogen layers from the previous evolution between 10^{-16} and $10^{-10} M_{\odot}$. In view of the absence of any correlation between the occurrence of the DBAs and height above the Galactic plane, we favor the second alternative.

As a result of the existence of cool DBs without any visible hydrogen, BW11 concluded that there must be two channels for DBs. One channel consists of DAs that are transformed into DBs through convective mixing, and the other of DBs that never change during evolution. If we accept the view that the hydrogen is residual hydrogen from the previous evolution, then a more natural explanation would be that the hydrogen mass (in DBs) extends from $\sim 10^{-10} M_{\odot}$ not just down to $10^{-16} M_{\odot}$, but even lower. The very existence of DBs in the so-called DB gap that exists between 30 000 and 45 000 K proves this. In connection with this it is interesting that the hydrogen layer masses in the ZZ Ceti (DA!) white dwarfs, which are determined by pulsational properties (Romero et al. 2012; Castanheira & Kepler 2009), cover the range from $\sim 10^{-4}$ to a lower limit of $\sim 10^{-10} M_{\odot}$. It is tempting to wonder if we really need two different scenarios for the origin of the hydrogen-rich versus the helium-rich white dwarf sequences or whether have to accept a continuum of hydrogen layer thickness from the canon-

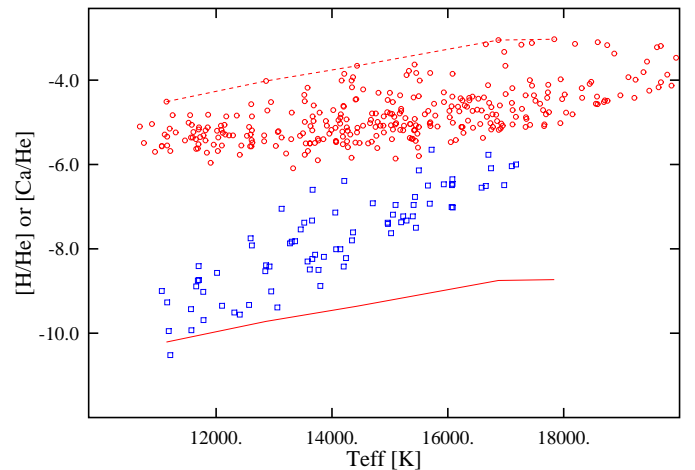


Fig. 9. Hydrogen (red circles) and Ca (blue squares) abundance versus T_{eff} . The red dotted line is an empirical upper limit to H abundances, drawn through those objects with the highest abundances. The continuous line is shifted downward by 5.7 dex, the solar H/Ca ratio. Stars with a solar or higher H/Ca would be found below this line, which is, however, below the visibility limit of Ca for all but the coolest stars.

ical DA value of $10^{-4} M_{\odot}$ down to zero, but such considerations are beyond the scope of this work.

5.2. Calcium

Unlike hydrogen, calcium does not accumulate in the outer layers with time but diffuses downward with a timescale that is much shorter than the cooling timescale. The origin therefore must be external. If accretion from the ISM (gas and dust) were the source for both hydrogen and calcium, we would thus expect that the Ca/H ratio is always smaller than the solar (ISM) value. On the contrary, Fig. 8 shows the opposite: the ratio in all objects is at least a factor of ten larger than solar. This is a well known fact in many metal-polluted white dwarfs and has always been a problem for the ISM accretion hypothesis. Again, however, selection effects are important in this respect and may lead to wrong conclusions: Fig. 9 demonstrates that there is only a very slim chance of finding such objects at the lowest T_{eff} with the solar ratio in our sample. They must exist, since eventually the calcium will completely diffuse out of the atmosphere, but at this time we cannot find them any more. That we find many objects with Ca is significant and means that, at least in all of these objects, the accretion is currently of extremely hydrogen-poor material. Together with the missing correlation between DBZs and Galactic position, this adds more weight to the hypothesis that ISM accretion cannot explain the observed facts, which leaves the currently favored accretion from a circumstellar dust disk as remnant of a planetary system as the only viable scenario.

The total mass of calcium within the convection zone (Fig. 10) shows the opposite behavior from that of hydrogen – the total amount decreases significantly toward lower temperatures, confirming our assumption that no accumulation occurs with time. It is thus not meaningful to calculate average rates as done for hydrogen, but instead the important timescale for metals would be the diffusion timescale. Assuming equilibrium between diffusion and accretion, we can calculate the calcium accretion flux (Koester 2009). This is presented in Fig. 11, where we have changed the accretion flux unit to g/s, the preferred

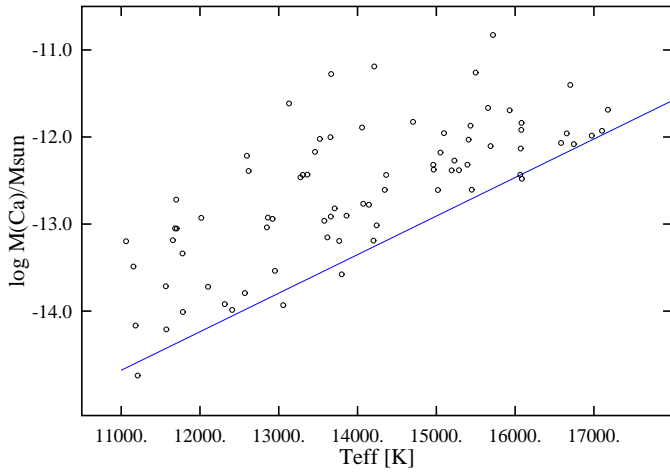


Fig. 10. Total calcium mass within the convection zone. The blue continuous line indicates the approximate lower limits, transformed from Fig. 4.

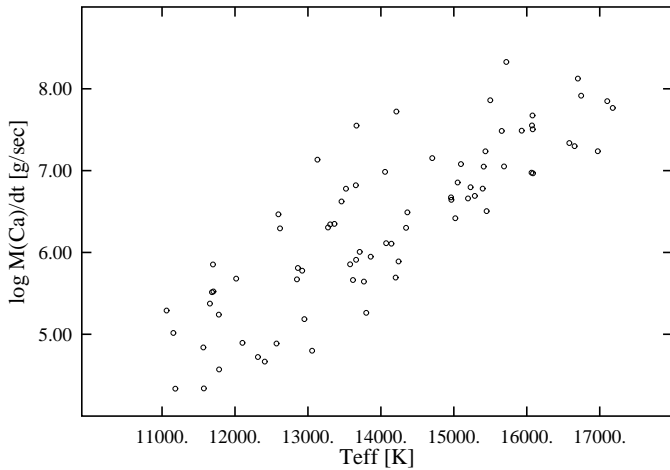


Fig. 11. Accretion rate of Ca in g/s, assuming equilibrium between accretion and diffusion.

choice in the case of metal polluted white dwarfs. The lower limit is obtained from the lower limit to the observed abundances in Fig. 4. The strong decline with decreasing T_{eff} is not easy to understand in the currently favored explanation of accretion from a circumstellar disk. If indeed most of the objects are in an equilibrium state between diffusion and accretion, we would expect, on average, constant accretion rates from high to low temperatures, as has been found for metal pollution in DAs (see Fig. 8 in Koester et al. 2014). The problem is already visible in the abundance distribution of Fig. 4; the change of 4.5 orders of magnitude is much more than could be explained by dilution in the He convection zone, which changes only by 1.6 orders over this range. This leads us to ask how accurate our calculations of the convection zone depth are.

5.3. The depth of the helium convection zone

Our envelope code starts at some specific position in the atmosphere model (usually $\tau_{\text{Ross}} = 100$) and integrates the stellar structure equations inward. The equation of state (EOS) used for hydrogen and helium models is that of Saumon et al. (1995). For a model with $T_{\text{eff}} = 10\,000$ K, $\log g = 8.0$ the base of the convection zone is reached at density (g cm^{-3}) $\log \rho = 2.76$ and

temperature (K) $\log T = 6.56$. The zone runs through the region of pressure ionization of He (see Fig. 2 of the paper cited above), which is not treated explicitly but bridged by an interpolation scheme. The most important quantity for the envelope structure is the adiabatic gradient, since the convection zone is very nearly adiabatic. Looking at Fig. 23 in Saumon et al. (1995), it is obvious that different EOS give different results for the adiabatic gradient. Considerable scatter is also apparent, which is probably caused by the numerical calculation of second derivatives in the free-energy minimization procedure. As a test of the sensitivity of our envelope structure, we have made a calculation with the adiabatic gradient artificially set to 0.4 everywhere. This decreases the mass in the convection zone by almost three orders of magnitude. While this is certainly an extreme assumption, the extent of the convection zone, and with it the derived total masses of hydrogen and calcium, as well as the diffusion timescales, depend very sensitively on details of the EOS used and could be uncertain by large factors.

6. Conclusions

We analyzed photometry and spectra of the largest sample of helium-rich stars studied so far. The estimated masses show a significant increase below $T_{\text{eff}} = 16\,000$ K, which we attributed to imperfect implementation of line broadening by neutral helium atoms. Using the range from 16 000 to 22 000, where the average mass does not change, we find an average of 0.606 ± 0.004 , which is identical to the latest determination for DAs from DR12 (Kepler et al. 2015a).

At least 75% of the helium-rich stars show contamination with hydrogen. The total amount of hydrogen is larger at low T_{eff} than at the hot end. However, we show that when selection effects are taken into account this does not prove that the hydrogen in any single object increases with time. The unavoidable conclusion is that a significant number of DAs must appear at 30 000 K with thin hydrogen layers. Whether (i) these are always $\sim 10^{-16} M_{\odot}$ and then increase during evolution by average accretion rates, which have to span the range from $10^{-23} - 10^{-17} M_{\odot}/\text{yr}$, or whether (ii) the evolutionary hydrogen layer mass spans the range from $10^{-17} - 10^{-10} M_{\odot}$ and further accretion is unimportant cannot be distinguished from the current data. Given that there is no correlation of the DBA numbers with distance above the Galactic plane and also that the observed metals cannot be explained by ISM accretion, we prefer the thin H-layer alternative. We admit that the current theoretical calculations predict the existence of stable DBA models with M_{H} from $10^{-14} - 10^{-10} M_{\odot}$ between 15 000 and 21 000 K, but not any evolutionary path that would lead there. The solution to this puzzle might be a more physically sound treatment of convection and convective mixing.

About 10-12% of the DBs are contaminated by traces of calcium. This can only be accreted from an external source, and it is very clear that, in all cases, the accreted matter is extremely hydrogen-poor. ISM accretion with solar abundances can be ruled out, and the currently favored model of accretion from a dust disk is supported. If we assume equilibrium between accretion and downward diffusion at the bottom of the convection zone we find calcium accretion rates that decrease strongly with decreasing T_{eff} . We have currently no explanation for this and it might indicate that the extreme physical conditions in the pressure ionization region of helium are not yet adequately described.

Acknowledgements. DK gratefully acknowledges support from the program Science without Borders, MCIT/MEC-Brazil, which provided the opportunity for

extended visits to Porto Alegre. Funding for SDSS-III has been provided by the Alfred P. Sloan Foundation, the Participating Institutions, the National Science Foundation, and the U.S. Department of Energy Office of Science. The SDSS-III web site is <http://www.sdss3.org/>. SDSS-III is managed by the Astrophysical Research Consortium for the Participating Institutions of the SDSS-III Collaboration including the University of Arizona, the Brazilian Participation Group, Brookhaven National Laboratory, Carnegie Mellon University, University of Florida, the French Participation Group, the German Participation Group, Harvard University, the Instituto de Astrofísica de Canarias, the Michigan State/Notre Dame/JINA Participation Group, Johns Hopkins University, Lawrence Berkeley National Laboratory, Max Planck Institute for Astrophysics, Max Planck Institute for Extraterrestrial Physics, New Mexico State University, New York University, Ohio State University, Pennsylvania State University, University of Portsmouth, Princeton University, the Spanish Participation Group, University of Tokyo, University of Utah, Vanderbilt University, University of Virginia, University of Washington, and Yale University.

References

- Bergeron, P., Wesemael, F., Dufour, P., et al. 2011, *ApJ*, 737, 28
 Castanheira, B. G. & Kepler, S. O. 2009, *MNRAS*, 396, 1709
 Dupuis, J., Fontaine, G., Pelletier, C., & Wesemael, F. 1993, *ApJS*, 84, 73
 Eisenstein, D. J., Liebert, J., Koester, D., et al. 2006, *AJ*, 132, 676
 Fontaine, G., Villeneuve, B., & Wilson, J. 1981, *ApJ*, 243, 550
 Fontaine, G. & Wesemael, F. 1987, in Conference on Faint Blue Stars, 2nd, Tucson, AZ, June 1-5, 1987, Proceedings (A89-17526 05-90). Schenectady, NY, L. Davis Press, Inc., 1987, p. 319-326; Discussion, p. 327, 328. NSERC-supported research., 319-326
 Genest-Beaulieu, C. & Bergeron, P. 2014, *ApJ*, 796, 128
 Gianninas, A., Bergeron, P., & Ruiz, M. T. 2011, *ApJ*, 743, 138
 Iben, Jr., I., Kaler, J. B., Truran, J. W., & Renzini, A. 1983, *ApJ*, 264, 605
 Kepler, S. O., Kleinman, S. J., Nitta, A., et al. 2007, *MNRAS*, 375, 1315
 Kepler, S. O., Pelisoli, I., Koester, D., et al. 2015, *MNRAS*, 446, 4078
 Kepler, S. O. et al. 2015a, submitted to *MNRAS*
 Kleinman, S. J., Kepler, S. O., Koester, D., et al. 2013, *ApJS*, 204, 5
 Koester, D. 2009, *A&A*, 498, 517
 Koester, D. 2010, *Mem. Soc. Astron. Italiana*, 81, 921
 Koester, D., Gänsicke, B. T., & Farihi, J. 2014, *A&A*, 566, A34
 Koester, D., Napiwotzki, R., Voss, B., Homeier, D., & Reimers, D. 2005, *A&A*, 439, 317
 Liebert, J., Wesemael, F., Hansen, C. J., et al. 1986, *ApJ*, 309, 241
 Macdonald, J. & Vennes, S. 1991, *ApJ*, 371, 719
 Napiwotzki, R., Christlieb, N., Drechsel, H., et al. 2003, *The Messenger*, 112, 25
 Pietrinferni, A., Cassisi, S., Salaris, M., & Castellì, F. 2004, *ApJ*, 612, 168
 Romero, A. D., Córscico, A. H., Althaus, L. G., et al. 2012, *MNRAS*, 420, 1462
 Salaris, M., Serenelli, A., Weiss, A., & Miller Bertolami, M. 2009, *ApJ*, 692, 1013
 Saumon, D., Chabrier, G., & van Horn, H. M. 1995, *ApJS*, 99, 713
 Schatzman, E. 1948, *Nature*, 161, 61
 Schlafly, E. F. & Finkbeiner, D. P. 2011, *ApJ*, 737, 103
 Sion, E. M., Greenstein, J. L., Landstreet, J. D., et al. 1983, *ApJ*, 269, 253
 Tassoul, M., Fontaine, G., & Winget, D. E. 1990, *ApJS*, 72, 335
 Tremblay, P.-E., Bergeron, P., & Gianninas, A. 2011, *ApJ*, 730, 128
 Tremblay, P.-E., Ludwig, H.-G., Steffen, M., & Freytag, B. 2013, *A&A*, 559, A104
 Veras, D., Shannon, A., & Gänsicke, B. T. 2014, *MNRAS*, 445, 4175
 Voss, B., Koester, D., Napiwotzki, R., Christlieb, N., & Reimers, D. 2007, *A&A*, 470, 1079

Table 1. Stellar parameters for the sample effective temperature (T_{eff}), surface gravity ($\log g$), S/N, distance (d), distance above Galactic plane (z), and logarithmic abundances of H and Ca. Numbers in parentheses are formal errors from the fit; a zero means that $\log g$ was kept fixed at 8.00 or, for the abundances, that these are upper limits.

SDSSJ	T_{eff} [K]	$\log g$ [cgs]	S/N	d [pc]	z [pc]	[H/He]	[Ca/He]
000116.49+000204.45	10985 (130)	8.000 (0.000)	23.2	220	191	-5.74 (0.00)	-10.62 (0.00)
000106.22+250330.00	15194 (75)	8.000 (0.000)	15.4	428	254	-4.73 (0.30)	-7.37 (0.30)
000223.06+272358.50	16886 (42)	7.950 (0.028)	45.1	219	123	-5.48 (0.00)	-6.56 (0.00)
000515.58+071313.71	18650 (86)	8.024 (0.033)	30.5	269	217	-4.70 (0.00)	-5.09 (0.00)
000720.22-002325.40	19276 (240)	7.863 (0.068)	14.9	353	309	-4.21 (0.00)	-4.97 (0.00)
000742.62+252422.50	19916 (320)	7.851 (0.085)	11.0	804	477	-3.85 (0.00)	-4.36 (0.00)
000730.75+275111.90	16048 (180)	7.795 (0.132)	10.1	546	305	-4.84 (0.00)	-6.36 (0.00)
000816.26+154609.44	13547 (79)	8.000 (0.000)	18.4	253	181	-5.50 (0.55)	-8.68 (0.00)
001830.96-095644.50	15514 (18)	8.000 (0.000)	60.3	61	57	-4.01 (0.10)	-7.58 (0.00)
002001.81+135248.00	17973 (48)	8.049 (0.022)	48.7	74	55	-4.45 (0.11)	-5.60 (0.00)
002153.33+083141.82	16780 (123)	7.967 (0.082)	15.4	353	284	-4.90 (0.00)	-6.16 (0.00)
002458.42+245834.26	20691 (162)	8.073 (0.028)	32.7	213	131	-4.20 (0.00)	-4.55 (0.00)
002846.59+235312.16	21291 (529)	7.907 (0.068)	12.5	549	342	-3.48 (0.00)	-4.01 (0.00)
003003.28+152628.37	16065 (47)	8.102 (0.036)	35.0	171	125	-4.62 (0.15)	-7.01 (0.08)
003115.10+083004.83	13448 (102)	8.000 (0.000)	15.1	295	238	-5.32 (0.36)	-8.62 (0.00)
003340.91-182032.30	14685 (26)	8.000 (0.000)	53.0	111	110	-5.46 (0.13)	-8.55 (0.00)
003436.66+003141.60	15999 (92)	8.000 (0.000)	13.5	317	280	-5.07 (0.00)	-6.65 (0.00)
003436.33+072014.00	15476 (61)	8.000 (0.000)	18.8	304	250	-5.28 (0.00)	-7.33 (0.00)
003533.09+080324.26	12102 (102)	8.000 (0.000)	18.4	268	218	-5.72 (0.00)	-9.88 (0.00)
003833.66+242022.40	15962 (51)	8.000 (0.000)	23.9	340	211	-5.41 (0.00)	-7.02 (0.00)
004200.48+241647.20	15920 (54)	8.000 (0.000)	22.6	354	220	-5.39 (0.00)	-7.02 (0.00)
004900.48-094203.00	18195 (263)	7.879 (0.105)	11.1	418	399	-4.33 (0.00)	-5.15 (0.00)
005151.24+063935.49	14959 (100)	8.000 (0.000)	13.1	402	334	-5.20 (0.00)	-7.32 (0.00)
010532.40+064234.18	13661 (93)	8.000 (0.000)	16.1	314	260	-5.53 (0.00)	-8.50 (0.00)
010608.43+063123.27	11624 (113)	8.000 (0.000)	18.6	265	220	-5.67 (0.00)	-10.15 (0.00)
010901.58+083354.67	16016 (104)	8.090 (0.073)	18.8	305	247	-5.21 (0.00)	-6.85 (0.00)
011023.82+223716.25	12609 (102)	8.000 (0.000)	16.8	283	182	-5.57 (0.80)	-9.41 (0.00)
011341.04+190020.52	13489 (56)	8.000 (0.000)	26.4	227	156	-5.81 (0.00)	-9.04 (0.00)
011356.38+301514.62	17453 (46)	8.119 (0.031)	36.1	161	86	-4.13 (0.09)	-6.05 (0.00)
011415.03+261822.60	17968 (106)	8.134 (0.049)	23.2	337	199	-4.88 (0.00)	-5.54 (0.00)
011409.86+272739.42	17715 (117)	8.074 (0.063)	17.3	398	228	-4.42 (0.42)	-5.73 (0.00)
011420.50+312027.20	10673 (179)	8.000 (0.000)	20.3	196	102	-5.69 (0.00)	-10.74 (0.00)
011535.52+004543.40	19428 (374)	8.100 (0.093)	10.7	433	381	-4.00 (0.00)	-4.51 (0.00)
011607.92+330154.29	20476 (261)	8.002 (0.046)	18.7	434	214	-4.01 (0.00)	-4.51 (0.00)
011721.58+061601.13	15618 (47)	8.000 (0.000)	25.9	272	226	-5.51 (0.00)	-7.45 (0.00)
012044.78-004159.10	12102 (132)	8.000 (0.000)	14.3	206	183	-5.62 (0.00)	-9.35 (0.24)
012148.24-001053.00	15864 (26)	8.000 (0.000)	46.8	110	97	-5.74 (0.00)	-7.14 (0.00)
012118.42+384606.90	17664 (160)	7.909 (0.082)	13.4	498	200	-4.60 (0.00)	-5.58 (0.00)
012413.08+072246.90	12224 (163)	8.000 (0.000)	11.2	388	316	-5.31 (0.39)	-9.46 (0.00)
012426.34+400357.40	20733 (481)	8.411 (0.065)	13.5	422	160	-3.80 (0.00)	-4.36 (0.00)
012732.97+133030.10	13771 (147)	8.000 (0.000)	10.4	278	208	-5.31 (0.00)	-8.12 (0.00)
012921.39+404428.50	11143 (74)	8.000 (0.000)	26.2	184	67	-4.51 (0.16)	-10.68 (0.00)
013025.42+232805.48	16898 (42)	8.235 (0.030)	41.5	187	116	-4.60 (0.11)	-6.54 (0.00)
013224.03+245612.52	16751 (66)	8.461 (0.053)	26.6	105	63	-4.64 (0.09)	-6.52 (0.00)
013553.05+070315.10	18338 (197)	7.806 (0.072)	13.0	535	434	-4.26 (0.00)	-5.07 (0.00)
014049.00-010302.70	18848 (137)	7.894 (0.055)	18.0	472	414	-4.45 (0.00)	-5.29 (0.00)
014200.46+073350.69	16032 (68)	8.190 (0.048)	26.7	248	198	-4.88 (0.23)	-7.01 (0.00)
014245.37+131546.40	12160 (60)	8.000 (0.000)	30.2	159	117	-6.03 (0.00)	-10.00 (0.00)
014618.90-005150.50	10504 (176)	8.000 (0.000)	19.3	155	135	-5.61 (0.00)	-10.77 (0.00)
014722.59-083100.21	14407 (30)	8.000 (0.000)	42.7	156	144	-4.46 (0.10)	-8.78 (0.00)
014852.15-083137.40	16454 (113)	7.754 (0.083)	16.1	299	275	-5.04 (0.00)	-6.51 (0.00)
014812.13+220558.52	14404 (29)	8.000 (0.000)	46.4	132	83	-5.48 (0.18)	-8.86 (0.00)
014945.65+223016.49	18474 (258)	8.092 (0.099)	10.7	427	265	-4.20 (0.00)	-4.90 (0.00)
015157.07-093341.86	13629 (87)	8.000 (0.000)	16.5	316	292	-5.09 (0.40)	-8.53 (0.00)
015348.07-005929.44	14112 (139)	8.000 (0.000)	10.3	325	281	-4.95 (0.39)	-7.84 (0.00)
015629.58+131744.70	16908 (109)	7.890 (0.075)	17.4	282	205	-5.01 (0.00)	-6.30 (0.00)
015935.01+130023.50	11524 (83)	8.000 (0.000)	24.5	126	91	-5.86 (0.00)	-10.46 (0.00)

Table 1. continued.

SDSSJ	T_{eff} [K]	$\log g$ [cgs]	S/N	d [pc]	z [pc]	[H/He]	[Ca/He]
015904.10+144151.04	13704 (66)	8.000 (0.000)	22.4	262	185	-5.70 (0.00)	-8.73 (0.00)
020409.84+212948.58	20980 (107)	8.250 (0.026)	31.8	251	155	-2.99 (0.13)	-4.54 (0.00)
020527.47+143553.80	13349 (95)	8.000 (0.000)	16.0	248	174	-5.61 (0.00)	-8.82 (0.00)
021258.62+074953.00	16019 (102)	8.024 (0.072)	19.4	302	231	-5.24 (0.00)	-6.91 (0.00)
021614.17-001309.20	15246 (95)	8.000 (0.000)	12.5	290	241	-5.18 (0.00)	-7.14 (0.00)
022524.28-080301.80	14095 (95)	8.000 (0.000)	15.6	329	287	-5.52 (0.00)	-8.22 (0.00)
023154.82+251259.50	15395 (70)	8.000 (0.000)	18.1	317	169	-5.39 (0.40)	-7.23 (0.30)
023333.42-092325.30	17837 (54)	7.834 (0.040)	24.7	334	290	-3.03 (0.10)	-6.08 (0.00)
023402.50+243352.20	29758 (547)	7.860 (0.061)	16.6	498	269	-2.76 (0.08)	-4.00 (0.00)
023617.32-073500.72	13503 (103)	8.000 (0.000)	15.2	266	227	-5.57 (0.00)	-8.64 (0.00)
023614.44-080804.90	11214 (227)	8.000 (0.000)	10.6	251	215	-5.40 (0.00)	-10.10 (0.00)
023823.22+271451.80	16721 (191)	8.150 (0.129)	10.4	410	204	-4.78 (0.00)	-5.97 (0.00)
024232.63-050954.75	14657 (63)	8.000 (0.000)	20.8	275	227	-5.02 (0.26)	-7.99 (0.00)
024433.59-042326.04	15778 (100)	8.000 (0.000)	12.9	409	334	-5.05 (0.00)	-6.71 (0.00)
025005.76-022258.56	11404 (168)	8.000 (0.000)	13.4	278	220	-5.51 (0.00)	-10.09 (0.00)
025150.40+351548.30	16706 (166)	7.715 (0.120)	11.1	583	213	-4.71 (0.00)	-5.98 (0.00)
025341.93-025658.59	13075 (77)	8.000 (0.000)	19.8	218	172	-5.21 (0.23)	-9.15 (0.00)
025352.96+332803.60	27557 (333)	7.723 (0.043)	22.5	554	214	-3.00 (0.00)	-4.00 (0.00)
025934.98-072134.20	15433 (74)	8.000 (0.000)	17.3	235	190	-5.37 (0.00)	-6.77 (0.22)
030253.10-010833.80	15097 (20)	8.000 (0.000)	55.7	68	52	-5.86 (0.40)	-6.96 (0.10)
030922.06+010556.30	16727 (94)	8.135 (0.061)	20.5	315	228	-5.11 (0.00)	-6.46 (0.00)
032452.83+045106.70	15527 (116)	8.000 (0.000)	10.9	417	274	-5.04 (0.00)	-6.80 (0.00)
032742.88+002503.00	12535 (115)	8.000 (0.000)	15.2	257	177	-5.65 (0.00)	-9.48 (0.00)
034153.03-054905.90	21730 (265)	7.897 (0.033)	26.5	366	255	-3.68 (0.00)	-4.70 (0.00)
035617.50-063109.60	12921 (91)	8.000 (0.000)	18.6	255	169	-5.74 (0.00)	-8.42 (0.20)
040836.75+155149.40	18318 (198)	8.094 (0.070)	15.7	346	150	-4.42 (0.42)	-5.09 (0.00)
041621.04+065613.50	15377 (273)	8.913 (0.158)	10.3	221	110	-5.08 (0.00)	-6.92 (0.00)
042042.78+072637.80	28949 (580)	8.031 (0.077)	11.5	595	286	-2.86 (0.00)	-4.00 (0.00)
044109.80-050329.80	12829 (90)	8.000 (0.000)	18.4	271	140	-5.31 (0.24)	-9.36 (0.00)
044745.75-054215.00	17947 (100)	8.040 (0.055)	21.0	346	173	-3.98 (0.18)	-5.54 (0.00)
052941.58+603806.80	17138 (107)	7.944 (0.072)	18.7	331	81	-5.01 (0.00)	-6.03 (0.00)
053607.02+615409.80	11062 (91)	8.000 (0.000)	27.3	125	33	-5.57 (0.20)	-9.00 (0.10)
054326.73+834056.20	17390 (190)	8.288 (0.115)	10.9	455	193	-4.65 (0.00)	-5.59 (0.00)
055531.33+830732.80	33623 (663)	7.839 (0.094)	12.3	895	382	-2.78 (0.00)	-4.00 (0.00)
064452.30+371144.30	15510 (55)	8.000 (0.000)	22.5	300	76	-5.50 (0.00)	-7.47 (0.00)
064813.95+382042.20	18625 (232)	7.837 (0.087)	11.5	601	164	-4.20 (0.00)	-4.96 (0.00)
065026.82+280419.30	17075 (200)	8.043 (0.120)	10.3	453	95	-4.63 (0.00)	-5.69 (0.00)
065146.32+271927.40	35800 (433)	7.964 (0.045)	24.5	505	106	-2.85 (0.00)	-4.00 (0.00)
065221.16+374917.90	17269 (49)	8.001 (0.034)	25.2	304	86	-3.16 (0.10)	-6.03 (0.00)
070916.40+394039.80	16597 (28)	8.037 (0.017)	68.6	120	41	-5.67 (0.00)	-6.73 (0.00)
071159.16+382846.40	23361 (756)	7.480 (0.096)	10.4	818	283	-2.91 (0.00)	-4.00 (0.00)
072459.83+365625.60	17772 (191)	7.951 (0.095)	11.9	590	223	-4.53 (0.00)	-5.43 (0.00)
072414.86+391003.36	14659 (76)	8.000 (0.000)	16.2	379	146	-5.14 (0.00)	-7.75 (0.00)
072707.40+351429.40	14696 (96)	8.000 (0.000)	15.0	394	148	-5.42 (0.00)	-7.77 (0.00)
072758.87+420714.48	11680 (124)	8.000 (0.000)	17.2	274	112	-5.64 (0.00)	-10.07 (0.00)
072959.11+455121.50	16297 (77)	7.865 (0.054)	23.9	230	99	-5.32 (0.00)	-6.98 (0.00)
073029.07+345613.40	11155 (72)	8.000 (0.000)	33.9	99	38	-5.34 (0.16)	-9.27 (0.08)
073217.01+274641.30	12849 (88)	8.000 (0.000)	18.4	248	87	-5.66 (0.00)	-8.53 (0.21)
073223.60+433628.51	20839 (301)	7.842 (0.054)	15.6	631	270	-3.74 (0.00)	-4.34 (0.00)
073416.92+444801.21	15267 (76)	8.000 (0.000)	14.9	422	185	-4.90 (0.37)	-7.18 (0.00)
073512.67+163804.10	14704 (107)	8.000 (0.000)	12.0	413	121	-5.23 (0.00)	-6.92 (0.28)
073842.57+183509.60	15719 (34)	8.000 (0.000)	36.2	198	63	-5.66 (0.00)	-5.65 (0.10)
073847.48+463844.74	17915 (83)	7.886 (0.040)	25.7	343	156	-4.85 (0.00)	-5.95 (0.00)
073916.80+242513.69	12349 (128)	8.000 (0.000)	14.3	321	114	-5.56 (0.00)	-9.47 (0.00)
073935.14+244505.27	21498 (200)	7.893 (0.022)	36.4	250	90	-4.08 (0.00)	-4.93 (0.00)
073939.13+670916.50	19805 (137)	7.992 (0.034)	28.2	349	171	-4.40 (0.00)	-5.28 (0.00)
074120.75+281245.60	13460 (95)	8.000 (0.000)	15.2	343	132	-5.55 (0.00)	-7.54 (0.14)

Table 1. continued.

SDSSJ	T_{eff} [K]	$\log g$ [cgs]	S/N	d [pc]	z [pc]	[H/He]	[Ca/He]
074253.65+185306.70	15224 (31)	8.000 (0.000)	37.2	213	71	-5.79 (0.00)	-8.01 (0.00)
074233.59+272238.80	13688 (96)	8.000 (0.000)	15.6	349	134	-5.55 (0.00)	-8.51 (0.00)
074249.21+280745.70	16527 (121)	7.871 (0.088)	14.3	551	214	-4.44 (0.39)	-6.33 (0.00)
074257.30+390618.20	14468 (119)	8.000 (0.000)	11.5	329	145	-5.25 (0.00)	-7.65 (0.00)
074257.18+423029.44	12555 (141)	8.000 (0.000)	12.4	329	149	-5.50 (0.00)	-9.21 (0.00)
074345.08+384953.51	14948 (62)	8.000 (0.000)	19.9	352	156	-5.48 (0.00)	-7.70 (0.00)
074351.32+385615.80	17549 (131)	7.890 (0.068)	16.6	332	147	-4.77 (0.00)	-5.85 (0.00)
074443.40+164851.10	17156 (86)	7.865 (0.053)	23.9	351	115	-5.08 (0.00)	-6.05 (0.00)
074507.43+194000.50	17722 (171)	8.071 (0.086)	13.2	451	157	-4.62 (0.00)	-5.56 (0.00)
074508.80+311659.44	17573 (183)	8.091 (0.100)	11.9	478	197	-4.56 (0.00)	-5.48 (0.00)
074624.34+335214.56	13982 (92)	8.000 (0.000)	15.3	348	149	-5.22 (0.00)	-8.20 (0.00)
074713.07+184719.80	15762 (100)	8.000 (0.000)	10.6	486	170	-4.56 (0.55)	-6.59 (0.00)
074823.27+221311.30	12233 (146)	8.000 (0.000)	12.7	357	134	-5.57 (0.00)	-9.57 (0.00)
074925.15+195039.94	19720 (115)	7.973 (0.029)	32.9	297	108	-4.46 (0.00)	-5.37 (0.00)
074903.16+273204.20	11854 (178)	8.000 (0.000)	10.8	249	101	-5.12 (0.43)	-9.70 (0.00)
075035.65+200332.20	15107 (86)	8.000 (0.000)	12.8	294	108	-5.02 (0.38)	-7.25 (0.00)
075156.89+131018.30	13275 (101)	8.000 (0.000)	15.2	239	78	-5.59 (0.00)	-7.87 (0.23)
075132.16+200226.77	16749 (62)	8.046 (0.044)	30.9	224	83	-5.17 (0.25)	-6.53 (0.00)
075140.41+411244.26	15669 (102)	8.000 (0.000)	12.3	354	168	-5.07 (0.00)	-6.79 (0.00)
075129.01+460131.19	14611 (61)	8.000 (0.000)	19.4	313	152	-5.50 (0.00)	-7.92 (0.00)
075212.14+141244.83	17740 (144)	7.970 (0.075)	14.5	506	171	-4.59 (0.00)	-5.54 (0.00)
075224.32+150352.34	13966 (46)	8.000 (0.000)	32.3	192	66	-5.90 (0.00)	-8.89 (0.00)
075452.85+194907.00	21300 (252)	7.896 (0.032)	25.3	380	146	-4.01 (0.00)	-4.70 (0.00)
075453.84+291114.17	13889 (90)	8.000 (0.000)	15.4	383	166	-5.45 (0.00)	-8.24 (0.00)
075520.71+091757.70	13020 (146)	8.000 (0.000)	11.6	441	139	-5.46 (0.00)	-8.82 (0.00)
075523.87+172825.20	27180 (197)	7.772 (0.027)	33.1	403	149	-3.06 (0.00)	-4.00 (0.00)
075556.00+240113.70	15405 (75)	8.000 (0.000)	16.6	393	161	-5.32 (0.00)	-7.28 (0.00)
075608.44+490239.73	16208 (116)	8.088 (0.078)	16.7	361	183	-5.11 (0.00)	-6.62 (0.00)
080127.11+141454.88	15697 (36)	8.000 (0.000)	30.8	193	71	-5.00 (0.19)	-7.51 (0.00)
080136.87+201011.13	16745 (146)	8.328 (0.088)	14.1	373	152	-4.91 (0.00)	-6.09 (0.30)
080257.89+060740.40	20706 (242)	8.053 (0.043)	21.6	379	121	-4.06 (0.00)	-4.52 (0.00)
080228.14+105450.10	17113 (72)	7.950 (0.053)	21.5	271	95	-4.19 (0.30)	-6.06 (0.00)
080236.92+154813.58	21395 (174)	7.972 (0.022)	37.6	256	99	-4.11 (0.00)	-5.01 (0.00)
080234.16+405015.19	14672 (39)	8.000 (0.000)	30.8	204	103	-4.94 (0.15)	-8.28 (0.00)
080345.75+074422.00	17512 (51)	8.099 (0.027)	39.7	210	70	-4.49 (0.13)	-6.05 (0.00)
080349.15+085532.70	21855 (334)	7.981 (0.047)	19.7	338	116	-3.76 (0.00)	-4.44 (0.00)
080348.49+393115.00	18581 (118)	7.767 (0.045)	22.4	265	133	-4.61 (0.00)	-5.62 (0.00)
080459.55+351327.60	12093 (149)	8.000 (0.000)	13.0	228	112	-5.58 (0.00)	-9.69 (0.00)
080413.06+390451.43	14895 (84)	8.000 (0.000)	14.1	366	184	-5.24 (3.65)	-7.43 (0.00)
080513.13+540615.60	13799 (55)	8.000 (0.000)	26.9	173	92	-5.85 (0.00)	-8.88 (0.32)
080630.85+271750.92	11854 (157)	8.000 (0.000)	12.5	295	136	-5.50 (0.00)	-9.76 (0.00)
080611.67+334425.56	15416 (25)	8.000 (0.000)	44.7	105	51	-5.19 (0.13)	-7.59 (0.00)
080653.76+361014.20	17038 (159)	7.695 (0.100)	12.0	570	285	-4.59 (0.00)	-5.73 (0.00)
080717.72+431241.80	12612 (114)	8.000 (0.000)	14.9	249	130	-5.42 (0.76)	-9.35 (0.00)
080841.72-072852.80	16948 (117)	7.751 (0.074)	16.5	485	112	-4.92 (0.00)	-6.19 (0.00)
080830.78+264054.74	17734 (97)	8.025 (0.047)	22.4	324	151	-4.87 (0.00)	-5.94 (0.00)
080942.84+080853.50	16292 (92)	7.899 (0.071)	18.9	300	107	-4.60 (0.35)	-6.75 (0.00)
080902.06+202955.60	11608 (87)	8.000 (0.000)	23.2	247	108	-5.23 (0.20)	-10.32 (0.00)
080949.94+310642.00	11782 (135)	8.000 (0.000)	14.3	208	102	-5.31 (0.31)	-9.69 (0.26)
080939.34+334543.05	17102 (128)	7.904 (0.080)	15.3	495	248	-4.80 (0.00)	-5.97 (0.00)
081040.75+191811.95	20335 (281)	7.908 (0.050)	17.8	437	190	-2.84 (0.20)	-4.64 (0.00)
081011.15+214540.40	19719 (271)	8.000 (0.066)	14.1	392	175	-4.07 (0.00)	-4.52 (0.00)
081058.71+501145.89	15342 (34)	8.000 (0.000)	34.7	206	112	-5.70 (0.00)	-7.59 (0.00)
081137.18+162115.30	10683 (107)	8.000 (0.000)	24.2	122	51	-5.10 (0.19)	-10.83 (0.00)
081307.29+153635.81	11844 (136)	8.000 (0.000)	14.4	274	115	-5.56 (0.00)	-9.85 (0.00)
081345.43+365140.50	27065 (437)	7.606 (0.060)	16.1	692	362	-2.93 (0.00)	-4.00 (0.00)
081442.62+102329.70	16937 (187)	7.801 (0.121)	10.4	466	183	-4.62 (0.00)	-5.76 (0.00)

Table 1. continued.

SDSSJ	T_{eff} [K]	$\log g$ [cgs]	S/N	d [pc]	z [pc]	[H/He]	[Ca/He]
081453.56+300734.90	22632 (632)	8.023 (0.050)	15.8	435	219	-3.42 (0.00)	-4.01 (0.00)
081627.93+005028.70	16672 (117)	8.016 (0.075)	17.0	284	93	-5.06 (0.00)	-6.41 (0.00)
081656.17+204946.10	27463 (182)	7.890 (0.025)	35.6	253	117	-3.07 (0.00)	-4.00 (0.00)
081739.38+134951.11	16839 (79)	8.204 (0.050)	24.4	268	114	-5.18 (0.00)	-6.50 (0.00)
081751.55+245923.27	11724 (148)	8.000 (0.000)	14.0	305	149	-5.53 (0.00)	-9.90 (0.00)
081952.23+142013.40	18086 (263)	7.646 (0.102)	10.3	563	246	-4.23 (0.00)	-5.09 (0.00)
081958.05+284109.28	11958 (84)	8.000 (0.000)	23.0	199	102	-5.53 (0.21)	-10.11 (0.00)
081904.19+354255.80	23134 (639)	7.870 (0.070)	12.2	377	202	-3.17 (0.00)	-4.00 (0.00)
082004.96+213135.69	20700 (301)	7.946 (0.052)	16.6	542	260	-3.85 (0.00)	-4.46 (0.00)
082019.50+253035.15	13130 (39)	8.000 (0.000)	39.1	158	79	-5.36 (0.14)	-7.05 (0.13)
082216.14+133822.60	14538 (82)	8.000 (0.000)	15.6	253	111	-4.22 (0.19)	-7.89 (0.00)
082316.33+233317.70	19861 (120)	8.083 (0.025)	35.2	241	120	-4.13 (0.22)	-4.58 (0.00)
082323.20+360834.79	15387 (80)	8.000 (0.000)	14.7	378	207	-5.19 (0.00)	-7.09 (0.00)
082457.54+285241.73	19788 (279)	8.040 (0.058)	15.0	450	238	-3.87 (0.61)	-4.51 (0.00)
082543.11+430640.93	15438 (42)	8.000 (0.000)	28.5	235	134	-5.58 (0.00)	-7.52 (0.00)
082659.83+111845.44	16778 (49)	7.936 (0.032)	36.7	217	96	-5.11 (0.33)	-6.54 (0.00)
082614.97+402234.82	20215 (340)	8.035 (0.060)	14.4	510	290	-3.90 (0.00)	-4.48 (0.00)
082623.76+474814.83	15247 (51)	8.000 (0.000)	21.8	323	187	-5.47 (0.00)	-7.55 (0.00)
082710.07+442951.10	14306 (122)	8.000 (0.000)	11.5	395	228	-5.29 (0.00)	-7.78 (0.00)
082834.81+090547.80	14653 (75)	8.000 (0.000)	17.7	250	108	-5.51 (0.00)	-7.91 (0.00)
082852.82+305603.49	15108 (95)	8.000 (0.000)	11.8	389	214	-5.09 (0.00)	-7.09 (0.00)
082829.17+363418.69	16350 (49)	7.970 (0.036)	36.6	171	97	-5.52 (0.00)	-7.02 (0.00)
082916.83+123744.46	11894 (110)	8.000 (0.000)	18.2	250	114	-5.68 (0.00)	-9.99 (0.00)
082931.60+282836.27	19168 (247)	8.100 (0.063)	15.4	444	240	-4.22 (0.00)	-4.63 (0.00)
083021.84-035805.90	17089 (129)	7.958 (0.078)	15.6	508	172	-4.87 (0.00)	-6.01 (0.00)
083059.35+193214.30	15435 (95)	8.000 (0.000)	12.9	361	182	-5.14 (0.00)	-7.00 (0.00)
083056.94+253853.80	16922 (136)	7.743 (0.087)	13.5	535	286	-4.78 (0.00)	-6.01 (0.00)
083024.17+455206.02	14836 (73)	8.000 (0.000)	15.9	354	208	-5.08 (0.35)	-7.58 (0.00)
083035.14+564459.40	26487 (237)	7.815 (0.032)	27.4	288	169	-3.08 (0.00)	-4.00 (0.00)
083342.06+045252.10	15623 (107)	8.000 (0.000)	11.6	329	0	-5.06 (0.00)	-6.78 (0.00)
083317.64+051201.47	12314 (112)	8.000 (0.000)	16.6	295	124	-5.65 (0.00)	-9.51 (0.23)
083344.04+252229.90	15125 (90)	8.000 (0.000)	13.0	443	240	-5.22 (0.00)	-7.25 (0.00)
083345.84+434328.70	14316 (91)	8.000 (0.000)	14.2	369	218	-5.29 (0.47)	-7.88 (0.00)
083317.40+531335.50	11525 (129)	8.000 (0.000)	16.2	241	143	-5.01 (0.19)	-10.20 (0.00)
083457.61+081144.20	17615 (207)	8.063 (0.107)	10.6	379	170	-4.51 (0.00)	-5.40 (0.00)
083421.14+242212.90	11704 (91)	8.000 (0.000)	22.8	212	114	-5.12 (0.16)	-8.74 (0.15)
083415.45+254819.90	22846 (652)	7.981 (0.056)	14.9	386	211	-3.35 (0.00)	-4.00 (0.00)
083407.27+385057.60	17989 (192)	8.067 (0.093)	12.5	358	209	-4.53 (0.00)	-5.37 (0.00)
083409.05+410700.90	12144 (75)	8.000 (0.000)	24.6	161	95	-5.06 (0.13)	-10.09 (0.00)
083412.05+513707.60	12815 (142)	8.000 (0.000)	12.0	262	156	-5.51 (0.00)	-9.03 (0.00)
083542.23+040817.50	14022 (36)	8.000 (0.000)	39.9	100	42	-4.71 (0.09)	-9.05 (0.00)
083606.48+041005.46	16745 (112)	8.091 (0.069)	17.2	377	160	-4.99 (0.00)	-6.25 (0.00)
083647.58+045951.04	21261 (527)	7.777 (0.059)	14.3	593	257	-3.57 (0.00)	-4.16 (0.00)
083855.76+184946.50	18583 (228)	8.106 (0.090)	11.8	400	211	-4.29 (0.00)	-5.00 (0.00)
083905.08+255338.40	13068 (128)	8.000 (0.000)	12.6	301	169	-5.51 (0.00)	-8.86 (0.00)
083930.08+261804.90	18195 (126)	7.867 (0.075)	11.9	446	252	-3.14 (0.25)	-5.20 (0.00)
083906.11+432459.40	13796 (136)	8.000 (0.000)	11.6	246	149	-5.38 (0.00)	-8.21 (0.00)
084036.73+063721.55	11972 (145)	8.000 (0.000)	14.0	297	136	-5.56 (0.00)	-9.76 (0.00)
084040.43+551113.40	16591 (159)	8.039 (0.097)	12.8	445	270	-4.89 (0.00)	-6.18 (0.00)
084104.07+055406.16	12083 (159)	8.000 (0.000)	11.7	329	149	-5.08 (0.32)	-9.53 (0.00)
084155.03+372311.90	13521 (66)	8.000 (0.000)	23.6	176	106	-5.82 (0.00)	-7.38 (0.11)
084211.30+461819.00	24778 (423)	8.001 (0.040)	20.5	406	250	-3.19 (0.00)	-4.00 (0.00)
084303.44+160719.40	15714 (89)	8.000 (0.000)	14.0	303	159	-5.15 (0.00)	-6.89 (0.00)
084350.85+361419.50	20428 (176)	8.026 (0.031)	29.8	197	120	-4.26 (0.00)	-4.55 (0.00)
084424.51+105044.00	17666 (149)	8.002 (0.074)	14.9	328	164	-4.69 (0.00)	-5.68 (0.00)
084539.18+225728.00	20360 (139)	7.971 (0.024)	40.8	113	64	-4.09 (0.00)	-5.48 (0.00)
084521.51+511559.36	13859 (130)	8.000 (0.000)	11.4	367	228	-5.28 (0.00)	-8.03 (0.00)

Table 1. continued.

SDSSJ	T_{eff} [K]	$\log g$ [cgs]	S/N	d [pc]	z [pc]	[H/He]	[Ca/He]
084614.90+193515.40	20559 (196)	8.254 (0.048)	17.3	277	154	-3.22 (0.24)	-4.51 (0.00)
084734.75+095706.70	17030 (169)	8.078 (0.102)	12.1	338	170	-4.74 (0.00)	-5.85 (0.00)
084717.71+322209.40	12884 (146)	8.000 (0.000)	10.9	273	166	-4.72 (0.41)	-8.88 (0.00)
084716.21+484220.40	15480 (52)	8.000 (0.000)	24.2	232	145	-5.55 (0.00)	-7.51 (0.00)
084835.69+062848.10	17105 (194)	7.848 (0.116)	10.4	568	274	-4.54 (0.53)	-5.64 (0.00)
084952.82+471248.78	17321 (40)	8.141 (0.024)	49.0	138	87	-5.35 (0.00)	-6.07 (0.00)
085253.92+000739.23	22976 (535)	7.810 (0.058)	15.5	606	273	-3.29 (0.00)	-4.00 (0.00)
085205.50+031413.93	15144 (31)	8.000 (0.000)	37.8	296	139	-5.81 (0.00)	-8.02 (0.00)
085202.44+213036.50	24946 (507)	7.826 (0.045)	18.2	423	246	-3.11 (0.00)	-4.00 (0.00)
085413.95+050843.70	20344 (379)	7.939 (0.071)	14.1	458	226	-3.93 (0.00)	-4.53 (0.00)
085427.99+380841.80	14067 (54)	8.000 (0.000)	25.5	258	165	-5.44 (0.26)	-8.65 (0.00)
085707.25+120336.29	14063 (114)	8.000 (0.000)	12.3	359	197	-5.31 (0.00)	-7.95 (0.00)
085720.19+360142.80	16777 (104)	7.896 (0.065)	18.4	382	246	-5.05 (0.00)	-6.39 (0.00)
085934.17+112309.39	16078 (93)	8.197 (0.069)	18.6	333	184	-4.39 (0.23)	-6.35 (0.27)
085919.96+350730.80	16826 (66)	8.033 (0.042)	27.3	192	124	-5.08 (0.00)	-6.52 (0.00)
085953.78+464036.10	17471 (201)	7.809 (0.112)	10.6	465	305	-4.50 (0.00)	-5.48 (0.00)
085957.20+573249.90	15656 (110)	8.000 (0.000)	11.0	376	240	-5.00 (0.00)	-6.50 (0.34)
090146.63+094029.80	15417 (108)	8.000 (0.000)	11.7	315	173	-5.11 (0.00)	-6.95 (0.00)
090232.18+071930.00	28749 (614)	7.581 (0.092)	10.9	662	354	-2.85 (0.00)	-4.00 (0.00)
090235.69+134306.00	16801 (193)	8.323 (0.111)	10.8	338	195	-4.79 (0.00)	-5.91 (0.00)
090239.74+364458.00	16956 (77)	7.842 (0.049)	25.2	217	143	-5.16 (0.00)	-6.51 (0.00)
090339.72+103213.10	16770 (32)	8.078 (0.020)	56.2	150	84	-4.81 (0.14)	-6.57 (0.00)
090331.28+140049.07	15147 (22)	8.000 (0.000)	50.1	99	58	-5.94 (0.00)	-8.04 (0.00)
090315.40+204743.80	16873 (43)	7.774 (0.032)	27.5	247	152	-3.05 (0.17)	-6.52 (0.00)
090336.00+212214.02	14826 (115)	8.000 (0.000)	10.7	406	251	-5.08 (0.00)	-7.21 (0.00)
090322.43+834550.00	29986 (233)	8.000 (0.000)	24.4	497	251	-2.94 (0.00)	-4.00 (0.00)
090409.04+012741.00	21143 (396)	7.910 (0.053)	17.5	332	165	-3.86 (0.00)	-4.50 (0.00)
090456.13+525029.90	38725 (794)	7.906 (0.089)	13.0	825	544	-2.70 (0.00)	-4.00 (0.00)
090529.44+104257.38	16020 (88)	8.187 (0.062)	21.3	313	178	-5.22 (0.00)	-6.97 (0.00)
090538.46+290610.40	19501 (121)	7.874 (0.032)	30.6	205	133	-4.52 (0.00)	-5.51 (0.00)
090542.42+510455.50	15076 (39)	8.000 (0.000)	28.5	209	139	-4.87 (0.20)	-8.00 (0.00)
090957.47+111111.29	14549 (65)	8.000 (0.000)	19.1	319	186	-5.51 (0.00)	-7.97 (0.00)
091058.73+044934.40	15933 (99)	8.000 (0.000)	11.7	318	173	-4.52 (0.46)	-6.59 (0.00)
091044.00+084029.70	15436 (99)	8.000 (0.000)	11.9	353	201	-5.10 (0.00)	-6.94 (0.00)
091029.42+090205.10	16039 (53)	7.967 (0.039)	33.8	165	94	-5.57 (0.00)	-7.04 (0.00)
091113.01+031127.00	13843 (65)	8.000 (0.000)	23.7	172	92	-5.78 (0.00)	-8.78 (0.00)
091125.32+193541.80	20502 (456)	7.753 (0.085)	11.2	489	310	-3.64 (0.00)	-4.21 (0.00)
091131.38+302709.50	14906 (93)	8.000 (0.000)	13.6	383	257	-5.28 (0.00)	-7.46 (0.00)
091322.22+254514.70	15096 (110)	8.000 (0.000)	10.5	326	216	-5.05 (0.70)	-7.08 (0.00)
091448.53+424033.50	11695 (124)	8.000 (0.000)	17.5	187	130	-5.52 (0.35)	-10.15 (0.00)
091541.95+431250.20	12951 (115)	8.000 (0.000)	14.7	252	174	-5.60 (0.00)	-9.01 (0.24)
091651.97+414703.80	15178 (93)	8.000 (0.000)	12.5	321	224	-5.18 (0.40)	-7.18 (0.00)
091755.64+003351.80	17732 (196)	7.915 (0.102)	11.1	404	216	-4.48 (0.00)	-5.38 (0.00)
091828.56+224022.60	11778 (134)	8.000 (0.000)	15.3	281	187	-5.63 (0.00)	-10.01 (0.00)
091827.89+305237.00	19370 (296)	7.747 (0.084)	11.6	746	516	-4.00 (0.00)	-4.64 (0.00)
091905.82+202316.70	17507 (84)	7.954 (0.044)	25.9	202	133	-5.05 (0.00)	-6.29 (0.00)
092001.29+404728.26	11201 (188)	8.000 (0.000)	13.3	269	189	-5.51 (0.00)	-10.22 (0.00)
092106.43+140736.70	22358 (242)	8.506 (0.027)	30.3	234	149	-3.39 (0.25)	-4.05 (0.00)
092116.04+372943.38	11579 (132)	8.000 (0.000)	15.9	263	186	-5.06 (0.28)	-10.10 (0.00)
092200.98+000834.40	22872 (795)	7.953 (0.067)	13.1	440	239	-3.27 (0.00)	-4.00 (0.00)
092239.15+012726.00	12377 (119)	8.000 (0.000)	14.8	254	141	-5.64 (0.00)	-9.57 (0.00)
092235.07+402059.30	12291 (93)	8.000 (0.000)	20.1	211	150	-5.31 (0.20)	-9.81 (0.00)
092355.26+085717.30	20501 (148)	7.963 (0.022)	38.5	154	94	-4.16 (0.15)	-5.43 (0.00)
092313.66+112910.10	17348 (94)	8.388 (0.052)	21.6	180	113	-4.88 (0.33)	-6.02 (0.00)
092326.10+230228.00	15038 (50)	8.000 (0.000)	23.2	270	184	-4.80 (0.23)	-7.86 (0.00)
092452.74+020712.30	14330 (97)	8.000 (0.000)	14.9	274	156	-5.47 (0.00)	-8.02 (0.00)
092414.62+090940.20	15947 (106)	8.000 (0.000)	11.5	319	196	-4.97 (0.00)	-6.53 (0.00)

Table 1. continued.

SDSSJ	T_{eff} [K]	$\log g$ [cgs]	S/N	d [pc]	z [pc]	[H/He]	[Ca/He]
092539.11+345445.70	16850 (114)	8.027 (0.075)	16.2	314	224	-4.97 (2.68)	-6.25 (0.00)
092654.51-013111.01	19257 (142)	8.060 (0.037)	27.9	360	196	-4.52 (0.00)	-4.73 (0.00)
092917.88+162637.46	15447 (76)	8.000 (0.000)	15.6	355	239	-5.22 (0.00)	-7.11 (0.00)
093031.00+061852.90	16583 (56)	8.025 (0.041)	31.0	234	144	-4.72 (0.26)	-6.55 (0.10)
093024.62+083406.67	11811 (87)	8.000 (0.000)	21.8	216	136	-5.69 (0.00)	-10.16 (0.00)
093130.31+073054.60	11778 (196)	8.000 (0.000)	10.5	375	235	-5.43 (0.00)	-9.02 (0.26)
093329.42+090554.58	16125 (98)	8.185 (0.067)	19.7	264	169	-5.23 (0.00)	-6.82 (0.00)
093356.79+653026.00	15320 (83)	8.000 (0.000)	14.8	278	182	-5.26 (0.00)	-7.22 (0.00)
093444.55+092443.31	17342 (51)	8.273 (0.028)	36.9	171	110	-4.36 (0.14)	-6.05 (0.00)
093454.24+304106.50	16972 (136)	7.704 (0.085)	13.2	722	530	-4.73 (0.00)	-5.94 (0.00)
093416.09+483239.35	13065 (129)	8.000 (0.000)	11.7	319	231	-5.23 (0.52)	-8.68 (0.00)
093512.70+003857.12	12569 (67)	8.000 (0.000)	26.1	212	124	-5.55 (0.00)	-9.75 (0.00)
093512.70+104001.20	14239 (94)	8.000 (0.000)	14.8	384	252	-5.41 (0.00)	-7.99 (0.00)
093529.43+133702.39	11289 (130)	8.000 (0.000)	16.7	291	196	-5.38 (0.00)	-10.29 (0.00)
093610.22+303049.30	17323 (213)	8.719 (0.111)	10.4	386	284	-4.70 (0.00)	-5.56 (0.00)
093628.93+400451.10	17072 (117)	8.086 (0.074)	16.1	333	248	-4.62 (0.00)	-6.01 (0.00)
093759.52+091653.30	29494 (470)	7.898 (0.062)	14.2	515	338	-2.88 (0.00)	-4.00 (0.00)
093708.92+284205.70	15213 (112)	8.000 (0.000)	10.2	410	301	-5.04 (0.00)	-6.95 (0.00)
093806.30+032242.53	18434 (123)	8.038 (0.046)	22.4	342	211	-4.63 (0.00)	-5.09 (0.00)
093849.68+363839.88	18790 (96)	8.033 (0.037)	27.5	318	238	-4.63 (0.00)	-5.06 (0.00)
093844.81+391321.67	13333 (69)	8.000 (0.000)	22.7	215	160	-5.77 (0.00)	-9.07 (0.00)
093924.25+001145.70	18910 (161)	8.069 (0.062)	16.9	289	173	-4.44 (0.00)	-5.02 (0.00)
094026.86-021234.88	19490 (117)	8.083 (0.029)	32.1	267	155	-4.51 (0.00)	-4.63 (0.00)
094023.58+185837.24	13516 (60)	8.000 (0.000)	25.2	254	181	-5.81 (0.00)	-9.01 (0.00)
094029.90+221802.80	11661 (175)	8.000 (0.000)	12.2	234	170	-5.53 (0.00)	-9.95 (0.00)
094049.57+335853.00	16177 (100)	8.109 (0.069)	19.6	247	185	-5.25 (0.00)	-6.85 (0.00)
094105.41+013140.60	15848 (74)	8.000 (0.000)	17.1	236	144	-5.24 (0.00)	-6.98 (0.00)
094431.28-003933.70	14057 (62)	8.000 (0.000)	23.5	186	112	-5.75 (0.00)	-7.14 (0.11)
094551.02+194013.19	19161 (254)	8.099 (0.063)	15.7	500	365	-4.26 (0.00)	-4.65 (0.00)
094534.50+343455.50	18894 (130)	7.928 (0.053)	19.0	321	245	-4.49 (0.00)	-5.32 (0.00)
094547.51+482314.57	10470 (249)	8.000 (0.000)	14.4	220	164	-5.38 (0.00)	-10.57 (0.00)
094826.42+040730.80	14432 (51)	8.000 (0.000)	26.1	136	89	-5.24 (0.28)	-8.43 (0.00)
094957.05-011609.45	16251 (56)	8.143 (0.042)	30.8	243	149	-5.06 (0.00)	-7.01 (0.00)
095027.87+000535.70	20087 (369)	7.922 (0.067)	13.7	391	245	-3.96 (0.00)	-4.55 (0.00)
095035.51+483758.70	13448 (128)	8.000 (0.000)	12.0	287	217	-5.44 (0.00)	-8.49 (0.00)
095102.23+010432.60	16923 (35)	8.087 (0.023)	51.3	82	52	-5.03 (0.11)	-7.21 (0.00)
095141.89+501715.80	17465 (85)	8.076 (0.048)	24.6	286	215	-5.03 (0.00)	-6.02 (0.00)
095256.69+015407.70	33206 (263)	8.062 (0.037)	27.3	314	203	-2.91 (0.00)	-4.00 (0.00)
095207.88+090953.40	18694 (99)	8.091 (0.034)	30.1	171	119	-4.52 (0.26)	-5.09 (0.00)
095353.91+074246.10	19940 (222)	8.051 (0.049)	19.2	250	172	-3.47 (0.25)	-4.53 (0.00)
095449.30+181454.78	12617 (86)	8.000 (0.000)	19.9	237	178	-5.19 (0.18)	-7.92 (0.13)
095455.12+440330.30	19847 (263)	8.078 (0.066)	14.9	319	248	-4.09 (0.00)	-4.52 (0.00)
095426.18+484700.50	17437 (106)	7.780 (0.060)	20.0	283	215	-4.92 (0.00)	-6.12 (0.00)
095600.58+224810.70	11302 (135)	8.000 (0.000)	15.9	189	145	-5.24 (0.22)	-10.31 (0.00)
095749.40+335923.60	24953 (338)	8.012 (0.032)	25.6	277	219	-3.31 (0.00)	-4.00 (0.00)
095723.13+571350.30	14691 (34)	8.000 (0.000)	35.9	204	149	-4.79 (0.15)	-8.42 (0.00)
095854.97+055020.83	11684 (83)	8.000 (0.000)	25.1	187	129	-5.62 (0.40)	-8.75 (0.11)
095820.52+600234.91	14070 (59)	8.000 (0.000)	22.4	219	157	-5.46 (0.73)	-8.46 (0.00)
095926.99+010327.90	16559 (79)	7.893 (0.055)	24.1	371	245	-5.04 (0.30)	-6.57 (0.00)
095923.47+023143.62	15499 (97)	8.000 (0.000)	12.3	398	267	-5.07 (0.00)	-6.85 (0.00)
095902.38+044653.02	20315 (336)	8.193 (0.054)	16.1	392	268	-3.98 (0.00)	-4.50 (0.00)
100001.26+442015.72	14345 (55)	8.000 (0.000)	23.3	247	194	-4.17 (0.13)	-7.80 (0.25)
100140.17+025853.19	18555 (124)	8.186 (0.043)	23.0	279	190	-4.56 (0.40)	-5.08 (0.00)
100156.61+452004.30	13701 (92)	8.000 (0.000)	16.6	220	173	-5.60 (0.00)	-8.58 (0.00)
100209.64+035327.30	17174 (117)	8.347 (0.067)	17.6	208	143	-4.87 (0.30)	-6.02 (0.00)
100442.48+533150.00	20220 (255)	8.022 (0.045)	19.8	288	219	-4.12 (0.00)	-4.53 (0.00)
100621.42+250445.00	16252 (124)	8.103 (0.088)	13.7	406	325	-4.48 (0.30)	-6.52 (0.00)

Table 1. continued.

SDSSJ	T_{eff} [K]	$\log g$ [cgs]	S/N	d [pc]	z [pc]	[H/He]	[Ca/He]
100646.07+413306.60	13057 (104)	8.000 (0.000)	15.7	198	159	-5.64 (0.00)	-9.07 (0.00)
100755.84+213117.40	19763 (258)	8.112 (0.064)	14.6	499	396	-4.05 (0.00)	-4.51 (0.00)
100728.41+611103.40	13710 (86)	8.000 (0.000)	17.4	360	259	-5.58 (0.00)	-8.54 (0.00)
100852.01+225937.20	11312 (72)	8.000 (0.000)	30.4	162	128	-5.92 (0.00)	-10.63 (0.00)
100809.13+425657.84	16648 (117)	8.053 (0.072)	16.7	357	287	-4.99 (0.00)	-6.29 (0.00)
100817.04+434931.80	11209 (118)	8.000 (0.000)	20.5	145	116	-5.68 (4.89)	-10.52 (0.30)
100926.60+154236.54	15002 (66)	8.000 (0.000)	16.5	386	299	-4.79 (0.35)	-7.50 (0.00)
100922.96+410505.17	13911 (38)	8.000 (0.000)	36.0	148	120	-5.08 (0.12)	-9.01 (0.00)
101022.37+272239.30	16003 (163)	8.023 (0.110)	12.5	339	275	-5.03 (0.00)	-6.58 (0.00)
101149.93+024105.82	16484 (178)	8.089 (0.122)	10.9	410	288	-4.77 (0.00)	-6.04 (0.00)
101208.09+283244.90	19377 (347)	8.078 (0.074)	12.1	472	386	-3.81 (0.58)	-4.52 (0.00)
101249.63+412311.05	16735 (39)	8.600 (0.023)	50.0	73	59	-5.02 (0.11)	-6.57 (0.00)
101259.43+541912.68	15725 (65)	8.000 (0.000)	17.8	383	295	-5.22 (0.00)	-7.00 (0.00)
101247.94+622736.30	15287 (39)	8.000 (0.000)	25.4	260	188	-3.88 (0.18)	-7.33 (0.19)
101316.02+075915.20	19985 (259)	8.088 (0.056)	16.2	295	219	-4.10 (0.00)	-4.52 (0.00)
101342.58+085121.28	21459 (517)	7.894 (0.057)	14.5	600	449	-3.55 (0.00)	-4.14 (0.00)
101357.19+234533.00	11840 (104)	8.000 (0.000)	19.7	243	197	-5.72 (0.30)	-10.08 (0.00)
101320.07+354116.80	16003 (130)	7.539 (0.102)	13.6	596	491	-4.98 (0.00)	-6.62 (0.00)
101427.06+132657.34	16268 (80)	8.174 (0.054)	23.5	231	179	-5.31 (0.00)	-6.91 (0.00)
101545.92+400214.99	18575 (140)	8.093 (0.046)	20.7	363	299	-4.39 (0.33)	-5.06 (0.00)
101502.95+464835.30	23457 (367)	7.819 (0.041)	19.7	503	405	-3.35 (0.00)	-4.00 (0.00)
101636.81+074951.40	18873 (115)	7.964 (0.077)	11.4	360	270	-3.37 (0.29)	-4.87 (0.00)
101727.85+184705.96	13952 (46)	8.000 (0.000)	32.0	171	138	-5.20 (0.00)	-8.90 (0.00)
101716.69+465232.40	12569 (103)	8.000 (0.000)	16.2	283	229	-5.11 (0.30)	-9.33 (0.26)
101821.19+140507.00	14193 (98)	8.000 (0.000)	15.1	232	183	-5.50 (0.00)	-8.13 (0.00)
101800.81+370840.64	15020 (55)	8.000 (0.000)	19.8	289	240	-5.17 (0.00)	-7.63 (0.30)
101904.85+052256.30	10945 (118)	8.000 (0.000)	22.8	173	128	-5.70 (0.73)	-10.65 (0.00)
101951.55+290100.70	21145 (369)	8.036 (0.049)	17.9	385	322	-3.86 (0.00)	-4.18 (0.00)
101929.78+375218.90	12540 (119)	8.000 (0.000)	14.2	244	203	-5.12 (0.00)	-9.41 (0.00)
102044.06+090617.10	20500 (191)	7.965 (0.032)	25.7	578	443	-4.12 (0.00)	-4.89 (0.00)
102106.66+082724.48	21629 (162)	7.955 (0.021)	39.1	278	212	-4.08 (0.00)	-4.96 (0.00)
102100.92+564644.70	20972 (194)	8.001 (0.030)	29.1	325	249	-4.06 (0.36)	-4.53 (0.00)
102218.91+261502.75	14337 (35)	8.000 (0.000)	37.7	132	111	-5.84 (0.97)	-8.77 (0.00)
102216.66+514149.33	14166 (92)	8.000 (0.000)	14.1	292	233	-4.01 (0.24)	-7.98 (0.00)
102251.35+520304.84	15409 (81)	8.000 (0.000)	13.2	363	289	-4.41 (0.43)	-6.96 (0.30)
102312.63+051039.60	18729 (113)	7.895 (0.044)	22.4	252	188	-4.59 (0.00)	-5.55 (0.00)
102618.50+013646.46	18914 (167)	8.019 (0.065)	15.9	495	361	-4.32 (0.00)	-5.01 (0.00)
102616.80+081258.90	14229 (108)	8.000 (0.000)	12.8	409	317	-5.35 (0.00)	-7.91 (0.00)
102651.55+091347.50	28227 (258)	7.728 (0.037)	26.6	623	487	-3.00 (0.00)	-4.00 (0.00)
102655.38+530610.09	36687 (487)	7.690 (0.046)	22.9	676	540	-3.00 (0.00)	-4.00 (0.00)
102600.36+591424.68	18710 (88)	8.206 (0.030)	32.4	200	152	-4.48 (0.15)	-5.09 (0.00)
102718.79+275539.51	20734 (147)	8.106 (0.035)	23.5	295	251	-3.00 (0.04)	-4.52 (0.00)
102701.87+583142.64	12435 (92)	8.000 (0.000)	19.2	251	192	-5.55 (0.41)	-9.64 (0.00)
102807.83-013552.94	13617 (79)	8.000 (0.000)	19.6	305	216	-5.50 (0.31)	-8.49 (0.35)
102816.83+490200.70	17420 (73)	8.063 (0.041)	27.1	226	184	-5.06 (0.33)	-6.02 (0.00)
102953.32+020812.45	14152 (72)	8.000 (0.000)	18.7	304	225	-4.81 (0.25)	-8.27 (0.00)
102941.17+451810.20	12074 (104)	8.000 (0.000)	18.0	254	212	-5.67 (0.00)	-9.85 (0.00)
103026.29+075607.50	18864 (234)	7.991 (0.094)	10.2	620	485	-4.09 (0.00)	-4.74 (0.00)
103056.39+233831.80	13295 (42)	8.000 (0.000)	36.2	259	220	-6.05 (0.00)	-9.44 (0.00)
103033.20+385447.59	20323 (287)	8.150 (0.047)	18.8	409	348	-4.05 (0.00)	-4.52 (0.00)
103110.42+080059.40	21439 (640)	8.019 (0.083)	10.7	671	527	-3.39 (0.00)	-4.00 (0.00)
103238.12+532710.59	15000 (69)	8.000 (0.000)	16.1	355	285	-5.32 (0.00)	-7.46 (0.00)
103340.76+131159.53	15042 (92)	8.000 (0.000)	12.6	374	306	-5.21 (0.00)	-7.28 (0.00)
103453.66+393127.80	16434 (86)	8.211 (0.061)	20.5	212	182	-5.13 (0.50)	-6.72 (0.00)
103536.44-011849.17	27094 (371)	7.925 (0.039)	23.4	527	384	-3.01 (0.00)	-4.00 (0.00)
103517.85+273934.30	12737 (165)	8.000 (0.000)	10.8	269	232	-5.46 (0.00)	-9.02 (0.00)
103555.52+421043.75	45741 (136)	7.909 (0.060)	19.0	788	673	-2.65 (0.00)	-4.00 (0.00)

Table 1. continued.

SDSSJ	T_{eff} [K]	$\log g$ [cgs]	S/N	d [pc]	z [pc]	[H/He]	[Ca/He]
103610.50+052329.57	17488 (161)	7.959 (0.091)	12.3	502	391	-4.54 (0.00)	-5.51 (0.00)
103611.53+181453.20	13030 (76)	8.000 (0.000)	20.7	219	185	-5.56 (0.33)	-9.25 (0.00)
103729.48-003111.17	16169 (46)	8.064 (0.032)	40.7	166	122	-5.54 (0.00)	-7.04 (0.00)
103710.16+663201.40	15343 (35)	8.000 (0.000)	32.2	170	121	-5.37 (0.30)	-7.57 (0.00)
103902.40+024326.62	12431 (143)	8.000 (0.000)	12.8	314	240	-5.51 (0.00)	-9.33 (0.00)
103923.87+264822.90	13955 (49)	8.000 (0.000)	28.3	186	162	-5.27 (0.24)	-8.79 (0.00)
103955.45+310643.53	13529 (74)	8.000 (0.000)	19.3	133	114	-4.50 (0.18)	-8.81 (0.00)
103910.92+345235.95	11866 (148)	8.000 (0.000)	14.0	295	257	-5.55 (0.00)	-9.82 (0.00)
103959.55+400225.10	19565 (166)	7.881 (0.043)	21.7	306	265	-4.33 (0.00)	-5.16 (0.00)
103942.95+422718.70	12168 (160)	8.000 (0.000)	12.7	248	213	-5.57 (0.00)	-9.62 (0.00)
104036.41+095358.60	13774 (120)	8.000 (0.000)	12.8	262	214	-5.04 (0.00)	-8.30 (0.00)
104052.58+284856.70	16879 (42)	8.051 (0.027)	42.4	131	114	-5.18 (0.21)	-6.55 (0.00)
104043.86+375306.50	16553 (197)	8.081 (0.121)	10.2	395	344	-4.75 (0.00)	-5.99 (0.00)
104117.42+231036.40	21244 (287)	8.007 (0.037)	22.5	422	367	-3.95 (0.00)	-4.15 (0.00)
104115.77+262153.56	11905 (42)	8.000 (0.000)	44.0	85	75	-5.96 (0.61)	-10.59 (0.00)
104219.93-015223.03	13806 (107)	8.000 (0.000)	14.3	354	261	-5.45 (0.00)	-8.28 (0.00)
104318.16+492320.10	16594 (116)	8.333 (0.067)	18.6	273	228	-5.12 (0.00)	-6.47 (0.00)
104441.54+011041.40	14354 (126)	8.000 (0.000)	11.5	354	271	-5.24 (0.00)	-7.70 (0.00)
104423.24+565506.78	29073 (417)	7.789 (0.056)	14.9	764	607	-3.00 (0.00)	-4.00 (0.00)
104657.99-005045.70	18534 (62)	7.906 (0.026)	40.5	279	211	-4.89 (0.00)	-6.13 (0.00)
104832.64-020112.29	14778 (17)	8.000 (0.000)	74.3	75	56	-7.08 (0.00)	-8.49 (0.00)
104819.30+180052.78	14893 (87)	8.000 (0.000)	13.2	391	339	-4.86 (0.40)	-7.38 (0.00)
104908.33-001529.30	22490 (662)	7.875 (0.071)	12.8	708	541	-3.31 (0.00)	-4.00 (0.00)
105001.57+000541.40	15535 (107)	8.000 (0.000)	11.7	561	431	-5.07 (0.00)	-6.84 (0.00)
105113.66+043516.91	14503 (27)	8.000 (0.000)	48.7	117	0	-6.24 (0.00)	-8.81 (0.00)
105149.10+110112.70	19859 (208)	7.928 (0.052)	18.8	284	240	-4.19 (0.00)	-4.94 (0.00)
105100.62+283715.40	15229 (56)	8.000 (0.000)	20.2	253	227	-5.19 (0.33)	-7.23 (0.37)
105344.44+201415.30	38395 (640)	7.666 (0.065)	19.1	581	514	-2.80 (0.00)	-4.00 (0.00)
105443.45+042923.70	16146 (139)	7.572 (0.114)	12.8	385	312	-4.94 (0.00)	-6.50 (0.00)
105423.95+211057.58	22012 (283)	7.954 (0.026)	32.9	243	216	-4.02 (0.00)	-4.06 (0.00)
105404.68+443819.90	27807 (552)	7.748 (0.071)	15.3	496	433	-2.93 (0.00)	-4.00 (0.00)
105528.58+621903.64	14363 (90)	8.000 (0.000)	13.5	375	287	-3.93 (0.26)	-7.61 (0.32)
105604.14+045634.13	16694 (54)	8.110 (0.041)	27.9	254	207	-4.12 (0.13)	-6.53 (0.00)
105635.40+391757.55	19269 (225)	8.069 (0.055)	17.1	431	385	-4.26 (0.00)	-4.61 (0.00)
105842.69+521823.13	12862 (92)	8.000 (0.000)	16.6	280	235	-4.02 (0.34)	-8.39 (0.20)
105829.24+655227.20	15770 (79)	8.000 (0.000)	15.3	347	256	-5.15 (0.00)	-6.87 (0.00)
105925.46+341451.40	12037 (38)	8.000 (0.000)	46.0	54	49	-5.36 (0.08)	-10.57 (0.00)
105929.60+554039.30	19881 (224)	8.079 (0.046)	18.7	368	302	-3.98 (0.00)	-4.53 (0.00)
110030.22+552238.00	11651 (90)	8.000 (0.000)	22.1	184	150	-5.40 (0.25)	-10.26 (0.00)
110235.85+623416.10	23158 (259)	7.827 (0.029)	27.8	344	264	-3.64 (0.00)	-4.00 (0.00)
110342.78+220333.80	19117 (157)	8.181 (0.034)	27.2	288	261	-3.93 (0.23)	-4.91 (0.00)
110438.39+071129.80	11182 (135)	8.000 (0.000)	18.4	167	141	-5.70 (0.00)	-9.95 (0.16)
110520.35+092324.97	16653 (125)	8.016 (0.079)	15.7	452	389	-4.97 (0.00)	-6.26 (0.00)
110559.21+371725.50	11641 (107)	8.000 (0.000)	19.4	271	247	-5.75 (0.00)	-10.24 (0.00)
110611.71+125835.00	19678 (230)	8.114 (0.048)	18.5	371	326	-4.05 (0.49)	-4.54 (0.00)
110649.88+374655.90	13608 (61)	8.000 (0.000)	25.7	252	230	-5.85 (0.00)	-9.02 (0.00)
110737.03+142527.20	12359 (102)	8.000 (0.000)	17.8	202	180	-5.74 (0.00)	-9.72 (0.00)
110700.55-164721.20	18746 (232)	7.979 (0.097)	10.6	567	359	-4.15 (0.00)	-4.83 (0.00)
110708.12+361631.57	20363 (283)	8.024 (0.051)	17.3	369	337	-4.00 (0.00)	-4.51 (0.00)
110817.58+132049.10	17279 (103)	8.000 (0.000)	13.3	347	307	-4.68 (0.60)	-5.80 (0.00)
110834.77+575403.40	15497 (37)	8.000 (0.000)	31.0	186	151	-4.38 (0.14)	-7.52 (0.00)
110957.82+131827.90	16081 (130)	8.057 (0.102)	11.6	314	278	-3.85 (0.33)	-6.46 (0.50)
110959.94+261845.40	15421 (61)	8.000 (0.000)	18.3	83	76	-5.30 (0.00)	-7.24 (0.00)
110901.01+454309.60	14577 (45)	8.000 (0.000)	29.3	199	176	-5.77 (0.00)	-8.37 (0.00)
111004.40+300918.40	15499 (62)	8.000 (0.000)	17.8	325	301	-5.11 (0.30)	-6.14 (0.15)
111010.94+385700.30	16426 (59)	8.107 (0.044)	29.8	252	230	-4.39 (0.14)	-7.00 (0.00)
111023.02+592234.10	12279 (79)	8.000 (0.000)	22.3	256	205	-5.84 (0.00)	-9.92 (0.00)

Table 1. continued.

SDSSJ	T_{eff} [K]	$\log g$ [cgs]	S/N	d [pc]	z [pc]	[H/He]	[Ca/He]
111158.10-153503.30	16249 (139)	7.810 (0.107)	13.5	441	289	-5.00 (0.00)	-6.48 (0.00)
111137.92+184938.63	11249 (142)	8.000 (0.000)	15.8	257	234	-4.83 (0.26)	-10.27 (0.00)
111203.60+215747.46	13704 (75)	8.000 (0.000)	19.1	326	299	-5.49 (0.83)	-8.60 (0.00)
111201.75+420403.52	14291 (88)	8.000 (0.000)	15.0	371	336	-5.40 (0.00)	-7.95 (0.00)
111335.92+014534.05	34567 (668)	8.228 (0.096)	10.9	687	566	-2.69 (0.00)	-4.00 (0.00)
111310.23+202916.40	13522 (26)	8.000 (0.000)	53.9	115	106	-4.35 (0.09)	-9.55 (0.00)
111348.39+600229.30	16993 (54)	7.907 (0.042)	25.8	349	279	-3.66 (0.13)	-6.47 (0.00)
111435.44+244743.03	15935 (74)	8.000 (0.000)	16.5	339	314	-5.16 (0.00)	-6.81 (0.00)
111447.80+293249.60	12532 (103)	8.000 (0.000)	16.8	298	277	-5.32 (0.22)	-9.48 (0.00)
111650.24+493903.57	15474 (38)	8.000 (0.000)	29.2	207	181	-5.27 (0.29)	-7.52 (0.00)
111822.68+153334.50	22750 (161)	7.780 (0.028)	36.0	201	183	-3.70 (0.31)	-4.80 (0.00)
111911.27-130649.80	14692 (86)	8.000 (0.000)	14.5	354	246	-5.36 (0.00)	-7.68 (0.00)
111946.75+673631.10	15428 (29)	8.000 (0.000)	41.9	195	143	-4.92 (0.22)	-7.57 (0.00)
112009.89+085642.00	16673 (137)	8.108 (0.093)	14.2	361	318	-4.87 (0.57)	-6.23 (0.00)
112022.38+141026.70	12086 (99)	8.000 (0.000)	18.9	202	183	-5.75 (0.00)	-9.94 (0.00)
112013.34+665259.90	15442 (79)	8.000 (0.000)	16.3	384	285	-5.31 (0.00)	-7.23 (0.00)
112154.14+542503.40	20308 (237)	7.980 (0.042)	20.5	420	357	-4.07 (0.00)	-4.52 (0.00)
112223.42+113641.47	22080 (706)	7.956 (0.061)	13.3	574	515	-3.36 (0.00)	-4.00 (0.00)
112225.21+153527.13	15425 (70)	8.000 (0.000)	15.0	393	360	-3.63 (0.26)	-7.09 (0.00)
112506.49+452814.00	14766 (44)	8.000 (0.000)	27.2	247	223	-5.32 (0.27)	-8.08 (0.00)
112632.69-073837.30	16677 (172)	8.169 (0.117)	11.1	515	392	-4.81 (0.00)	-6.02 (0.00)
112615.92+454154.91	14500 (67)	8.000 (0.000)	18.7	277	251	-5.51 (0.00)	-7.99 (0.00)
112711.72+325229.70	15088 (94)	8.000 (0.000)	12.5	311	294	-5.12 (0.00)	-7.27 (0.00)
112752.92+553522.05	19638 (89)	8.188 (0.019)	46.6	176	147	-4.17 (0.13)	-4.65 (0.00)
112839.69+415140.70	20846 (331)	7.844 (0.061)	15.1	358	331	-3.81 (0.00)	-4.43 (0.00)
112920.58+011604.71	16687 (91)	8.003 (0.058)	21.2	319	269	-5.11 (0.00)	-6.50 (0.00)
112900.85+151119.75	16507 (60)	8.105 (0.042)	28.9	226	208	-4.70 (0.19)	-6.83 (0.00)
113028.62+301120.70	13894 (92)	8.000 (0.000)	15.1	337	319	-4.97 (0.32)	-8.27 (0.00)
113011.86+621926.20	16992 (65)	8.088 (0.038)	29.3	176	144	-5.20 (0.00)	-6.51 (0.00)
113143.40+370128.10	12895 (45)	8.000 (0.000)	36.8	92	86	-6.32 (0.00)	-9.83 (0.00)
113153.32+481852.30	18180 (62)	7.975 (0.024)	42.7	184	165	-5.02 (0.00)	-5.44 (0.00)
113155.92+645703.79	15454 (55)	8.000 (0.000)	18.4	329	252	-3.83 (0.24)	-7.24 (0.00)
113213.56+202518.50	18960 (88)	8.139 (0.035)	28.6	246	232	-4.62 (0.00)	-5.05 (0.00)
113247.25+283519.00	25265 (605)	7.968 (0.048)	17.3	484	462	-3.05 (0.00)	-4.00 (0.00)
113325.85-012829.24	14536 (34)	8.000 (0.000)	39.0	164	136	-5.08 (0.18)	-8.56 (0.00)
113316.54+035652.59	15354 (27)	8.000 (0.000)	42.0	181	157	-5.04 (0.16)	-7.61 (0.00)
113425.11+644305.35	16137 (70)	8.045 (0.047)	27.9	242	187	-5.42 (0.30)	-7.01 (0.00)
113527.68-000844.40	19497 (206)	8.032 (0.054)	19.7	390	327	-4.32 (0.00)	-4.59 (0.00)
113529.60+425339.84	15207 (77)	8.000 (0.000)	14.3	358	332	-5.20 (0.00)	-7.19 (0.00)
113654.22+070336.18	18585 (61)	8.341 (0.021)	47.0	135	121	-4.57 (0.15)	-5.15 (0.00)
113623.54+320403.80	32427 (448)	8.112 (0.054)	15.1	516	494	-2.83 (0.00)	-4.00 (0.00)
113747.78+354421.70	16443 (162)	7.921 (0.117)	10.9	391	372	-4.79 (0.00)	-6.12 (0.00)
113752.01+561715.59	11854 (68)	8.000 (0.000)	28.5	178	151	-5.93 (0.00)	-10.33 (0.00)
113751.45+661002.14	11161 (116)	8.000 (0.000)	20.3	221	168	-5.69 (0.00)	-10.47 (0.00)
113811.94+545947.60	18810 (147)	8.077 (0.055)	17.5	375	322	-4.41 (0.00)	-5.02 (0.00)
114039.37-004949.70	23905 (656)	7.822 (0.072)	12.4	544	457	-3.06 (0.00)	-4.00 (0.00)
114022.27+143002.77	13352 (66)	8.000 (0.000)	23.8	179	167	-5.75 (0.00)	-9.11 (0.00)
114051.66+663950.10	17090 (89)	8.052 (0.054)	23.2	321	242	-5.12 (0.00)	-6.08 (0.00)
114245.28+290432.60	12091 (96)	8.000 (0.000)	19.6	224	216	-5.18 (0.16)	-9.93 (0.00)
114238.69+572747.50	19149 (175)	8.395 (0.047)	20.3	270	227	-4.46 (0.00)	-4.73 (0.00)
114350.12+272733.22	18081 (181)	7.875 (0.069)	15.2	420	405	-4.52 (0.00)	-5.21 (0.00)
114428.49+143146.34	18983 (172)	8.184 (0.067)	14.2	437	410	-4.26 (0.00)	-4.94 (0.00)
114446.39+254122.36	48409 (249)	8.001 (0.063)	29.9	544	525	-3.00 (0.00)	-4.00 (0.00)
114552.73+033218.71	14053 (71)	8.000 (0.000)	19.0	273	240	-5.58 (0.00)	-8.34 (0.00)
114850.90+350425.02	15281 (35)	8.000 (0.000)	35.2	176	170	-5.73 (0.00)	-7.72 (0.00)
114912.80+304531.20	11862 (107)	8.000 (0.000)	18.3	200	194	-4.82 (0.17)	-10.07 (0.00)
114909.26+431758.48	13208 (55)	8.000 (0.000)	27.8	199	186	-5.74 (0.74)	-9.32 (0.00)

Table 1. continued.

SDSSJ	T_{eff} [K]	$\log g$ [cgs]	S/N	d [pc]	z [pc]	[H/He]	[Ca/He]
114933.01+451043.59	12001 (136)	8.000 (0.000)	14.4	297	275	-5.58 (0.00)	-9.76 (0.00)
115153.98+111809.04	13268 (95)	8.000 (0.000)	15.2	322	301	-5.53 (0.00)	-8.75 (0.00)
115114.92+194346.63	18152 (80)	8.079 (0.028)	37.5	153	148	-4.81 (0.22)	-5.45 (0.00)
115130.77+403455.49	17644 (51)	8.299 (0.026)	41.7	149	141	-4.71 (0.16)	-6.05 (0.00)
115141.89+593430.60	14320 (104)	8.000 (0.000)	13.5	265	219	-5.39 (0.00)	-7.92 (0.00)
115326.63+223752.23	16439 (99)	7.856 (0.071)	17.9	399	387	-5.06 (0.00)	-6.52 (0.00)
115307.40+312737.73	20954 (261)	7.817 (0.046)	17.8	477	464	-3.82 (0.00)	-4.44 (0.00)
115418.62+014137.90	19653 (259)	7.952 (0.067)	15.3	353	309	-4.13 (0.00)	-4.38 (0.00)
115416.86+045104.10	17286 (75)	8.054 (0.042)	28.7	163	146	-5.17 (0.00)	-6.04 (0.00)
115426.67+251755.60	21869 (186)	7.865 (0.022)	38.6	222	217	-4.08 (0.00)	-4.09 (0.00)
115553.69+242737.00	15674 (145)	7.750 (0.116)	13.0	345	336	-5.09 (0.00)	-6.85 (0.00)
115538.57+254135.20	34626 (534)	7.785 (0.080)	13.2	814	798	-3.00 (0.00)	-4.00 (0.00)
115503.66+314825.80	16134 (89)	7.958 (0.068)	20.4	234	228	-5.29 (0.00)	-6.95 (0.00)
115705.53+452011.10	17544 (142)	7.891 (0.072)	14.8	522	487	-4.64 (0.00)	-5.67 (0.00)
115959.91+500554.20	12159 (69)	8.000 (0.000)	27.0	215	195	-5.29 (0.14)	-10.13 (0.00)
120043.67+592601.02	15209 (54)	8.000 (0.000)	21.5	224	187	-5.50 (0.00)	-7.61 (0.00)
120101.04+673004.90	17942 (61)	7.918 (0.027)	37.0	192	144	-5.02 (0.40)	-5.58 (0.00)
120203.13+285647.07	17294 (153)	8.157 (0.086)	13.1	386	379	-4.69 (0.00)	-5.69 (0.00)
120350.03+102242.17	11478 (175)	8.000 (0.000)	12.8	218	205	-5.47 (0.00)	-10.00 (0.00)
120319.78+243955.70	14141 (43)	8.000 (0.000)	33.4	112	110	-5.03 (0.11)	-8.86 (0.00)
120524.67+063010.00	19702 (179)	8.031 (0.045)	21.6	233	214	-4.31 (0.00)	-4.56 (0.00)
120658.14-003336.80	21733 (210)	7.891 (0.029)	31.4	356	309	-4.05 (0.00)	-4.85 (0.00)
120735.19+225905.70	19899 (224)	7.916 (0.055)	17.4	369	363	-4.12 (0.00)	-4.82 (0.00)
120706.08+314030.10	20013 (342)	8.042 (0.062)	14.8	404	397	-4.04 (0.00)	-4.51 (0.00)
120817.49+482022.30	14783 (92)	8.000 (0.000)	13.6	306	282	-5.30 (0.00)	-7.55 (0.00)
121037.50+193200.60	18714 (66)	7.943 (0.027)	39.0	245	240	-4.82 (0.00)	-6.03 (0.00)
121031.40+214430.10	19388 (189)	7.879 (0.053)	18.3	352	346	-4.29 (0.00)	-5.09 (0.00)
121108.46+053249.80	15819 (108)	8.000 (0.000)	11.6	306	280	-5.01 (0.00)	-6.63 (0.00)
121312.75+500441.60	16790 (97)	7.902 (0.062)	20.1	434	396	-5.09 (0.00)	-6.47 (0.00)
121527.51+373009.13	16247 (125)	8.039 (0.084)	15.7	417	407	-5.05 (0.00)	-6.52 (0.00)
121754.60-024323.40	17979 (174)	8.231 (0.085)	13.7	289	248	-4.61 (0.00)	-5.47 (0.00)
121735.00+244308.50	13042 (131)	8.000 (0.000)	12.1	283	280	-5.49 (0.00)	-8.84 (0.00)
121813.58+461806.10	41561 (522)	7.972 (0.050)	23.5	596	559	-3.00 (0.00)	-4.00 (0.00)
121939.35+094956.42	31357 (234)	7.814 (0.029)	31.2	484	458	-2.96 (0.00)	-4.00 (0.00)
122025.21+384127.90	16661 (119)	7.639 (0.082)	14.9	385	374	-4.90 (0.00)	-6.28 (0.00)
122002.19+592643.69	14475 (64)	8.000 (0.000)	18.7	259	218	-4.94 (0.00)	-7.98 (0.00)
122241.28-003614.40	27740 (387)	7.910 (0.035)	28.7	413	363	-2.92 (0.06)	-4.00 (0.00)
122259.40+503645.30	17814 (152)	7.866 (0.068)	16.2	391	357	-4.63 (0.00)	-5.53 (0.00)
122250.15+684314.25	13956 (79)	8.000 (0.000)	16.3	239	178	-5.46 (0.00)	-8.22 (0.00)
122314.26+435009.20	20634 (356)	7.903 (0.051)	15.7	534	508	-3.82 (0.64)	-4.44 (0.00)
122444.73+174145.85	14476 (72)	8.000 (0.000)	18.0	308	302	-5.49 (0.62)	-7.99 (0.00)
122529.70+065033.43	19646 (231)	8.053 (0.057)	16.3	493	459	-4.13 (0.00)	-4.53 (0.00)
122555.17+225057.30	18366 (222)	8.155 (0.074)	13.2	330	328	-4.42 (0.00)	-5.04 (0.00)
122526.22+621552.50	14144 (79)	8.000 (0.000)	16.5	332	271	-4.89 (0.42)	-8.01 (0.24)
122555.85+663903.47	19992 (318)	7.975 (0.080)	12.2	548	421	-3.84 (0.00)	-4.40 (0.00)
122655.92-010454.80	12324 (100)	8.000 (0.000)	17.9	186	163	-5.73 (0.00)	-9.74 (0.00)
122626.13+531716.30	17802 (160)	8.103 (0.074)	14.3	429	384	-4.59 (0.00)	-5.49 (0.00)
122929.47+243544.00	14378 (104)	8.000 (0.000)	13.8	232	231	-5.42 (0.00)	-7.93 (0.00)
123006.36+114826.53	15424 (80)	8.000 (0.000)	14.4	396	381	-5.17 (0.00)	-7.04 (0.00)
123045.65+162138.59	14632 (80)	8.000 (0.000)	16.1	360	352	-5.40 (0.00)	-7.77 (0.00)
123032.75+443729.90	14021 (72)	8.000 (0.000)	19.5	286	272	-5.61 (0.00)	-8.42 (0.00)
123051.52+532721.90	15710 (64)	8.000 (0.000)	18.1	314	280	-5.25 (0.00)	-7.05 (0.00)
123108.33-011438.10	11462 (103)	8.000 (0.000)	21.2	149	130	-5.43 (0.24)	-10.41 (0.00)
123114.72+321352.00	11251 (96)	8.000 (0.000)	23.3	212	210	-5.78 (0.00)	-10.52 (0.00)
123230.41+035036.70	18827 (162)	7.972 (0.065)	15.3	327	299	-4.37 (0.00)	-5.16 (0.00)
123341.16+451642.80	13684 (54)	8.000 (0.000)	26.8	215	204	-4.60 (0.14)	-8.95 (0.00)
123427.23+033900.30	15312 (78)	8.000 (0.000)	16.1	297	272	-5.32 (0.00)	-7.32 (0.00)

Table 1. continued.

SDSSJ	T_{eff} [K]	$\log g$ [cgs]	S/N	d [pc]	z [pc]	[H/He]	[Ca/He]
123407.08+482011.22	21090 (560)	7.929 (0.070)	11.3	574	534	-3.44 (0.00)	-4.00 (0.00)
123432.64+560643.10	12595 (86)	8.000 (0.000)	20.4	212	185	-5.29 (0.20)	-7.75 (0.13)
123552.27+073134.30	14251 (91)	8.000 (0.000)	14.7	270	253	-4.93 (0.41)	-8.05 (0.00)
123654.96+170918.70	26298 (399)	7.645 (0.050)	19.7	465	0	-3.01 (0.00)	-4.00 (0.00)
123735.52+602833.00	15821 (63)	8.000 (0.000)	18.9	373	310	-5.10 (0.42)	-7.01 (0.00)
123819.28+080309.70	14439 (31)	8.000 (0.000)	43.0	108	102	-5.13 (0.10)	-8.84 (0.00)
123914.29+321058.60	14954 (68)	8.000 (0.000)	17.4	306	304	-4.76 (0.26)	-7.59 (0.00)
124058.69+532623.64	17308 (127)	8.111 (0.066)	16.8	378	339	-4.84 (0.00)	-5.92 (0.00)
124112.99+122613.70	15160 (44)	8.000 (0.000)	27.2	153	147	-5.66 (0.00)	-7.92 (0.00)
124206.06+194305.63	16269 (73)	8.083 (0.049)	24.9	234	232	-5.25 (0.34)	-6.95 (0.00)
124306.09+205708.86	14782 (31)	8.000 (0.000)	39.5	127	126	-5.61 (0.23)	-8.21 (0.00)
124304.32+500928.60	16947 (70)	8.181 (0.046)	26.6	308	283	-5.08 (0.39)	-6.51 (0.00)
124341.18+615422.95	11331 (147)	8.000 (0.000)	15.2	284	233	-5.54 (0.00)	-10.17 (0.00)
124320.57+645256.27	14188 (37)	8.000 (0.000)	40.8	114	90	-5.34 (0.11)	-8.96 (0.00)
124415.10+201657.29	15699 (50)	8.000 (0.000)	22.2	285	283	-5.09 (0.50)	-7.25 (0.00)
124403.03+444532.01	15482 (67)	8.000 (0.000)	17.3	363	346	-5.28 (0.00)	-7.17 (0.00)
124538.21-073138.40	20868 (160)	7.914 (0.027)	33.0	368	302	-4.19 (0.00)	-5.08 (0.00)
124519.55-084525.70	17150 (132)	7.845 (0.088)	15.1	465	376	-4.82 (0.00)	-6.00 (0.00)
124746.77+470550.80	19367 (320)	8.031 (0.083)	12.2	490	460	-4.04 (0.00)	-4.52 (0.00)
124703.29+493424.05	16085 (36)	8.111 (0.025)	50.6	113	105	-5.01 (0.12)	-7.02 (0.04)
124847.81-001846.03	20250 (358)	7.987 (0.067)	14.3	490	435	-3.91 (0.00)	-4.50 (0.00)
124810.23+100541.20	15688 (41)	8.000 (0.000)	27.2	178	170	-5.03 (0.24)	-6.93 (0.32)
124920.37+290454.20	16234 (73)	8.126 (0.053)	24.4	304	303	-5.11 (0.41)	-6.94 (0.00)
125030.26+594932.66	16129 (119)	7.910 (0.090)	15.6	474	399	-5.12 (0.00)	-6.69 (0.00)
125140.10+284955.16	15695 (32)	8.000 (0.000)	33.8	239	239	-3.83 (0.15)	-7.51 (0.00)
125138.06+490053.60	16221 (191)	8.082 (0.133)	10.4	332	308	-4.87 (0.00)	-6.27 (0.00)
125132.70+621918.30	16555 (68)	8.084 (0.042)	28.9	244	199	-5.33 (0.00)	-6.61 (0.00)
125205.66+662902.80	11626 (174)	8.000 (0.000)	11.9	215	166	-5.51 (0.00)	-9.95 (0.00)
125353.84+180837.90	14966 (99)	8.000 (0.000)	13.3	324	320	-5.27 (0.00)	-7.41 (0.30)
125410.02+121406.58	14624 (43)	8.000 (0.000)	29.8	200	193	-5.50 (0.50)	-8.32 (0.00)
125424.62+582500.14	16175 (132)	8.528 (0.084)	14.9	281	240	-4.63 (0.36)	-6.54 (0.00)
125524.52+151758.00	11149 (134)	8.000 (0.000)	18.0	165	162	-5.68 (0.00)	-10.47 (0.00)
125751.83+263621.50	20654 (452)	8.000 (0.000)	11.1	467	467	-3.64 (0.00)	-4.19 (0.00)
125752.77+425255.10	16252 (46)	8.133 (0.032)	38.5	152	146	-5.11 (0.16)	-7.03 (0.00)
125724.13+592236.00	14060 (38)	8.000 (0.000)	38.2	198	168	-5.13 (0.12)	-9.01 (0.00)
125955.17+240541.71	11573 (107)	8.000 (0.000)	20.6	219	219	-5.74 (0.00)	-9.93 (0.26)
125901.54+303238.80	13530 (68)	8.000 (0.000)	21.8	248	247	-4.99 (0.19)	-8.88 (0.00)
130041.85+234038.30	15328 (62)	8.000 (0.000)	17.4	238	237	-3.78 (0.25)	-7.38 (0.00)
130153.12+233106.13	15377 (57)	8.000 (0.000)	20.7	336	335	-5.39 (0.33)	-7.44 (0.00)
130541.22+081540.90	23330 (268)	7.826 (0.031)	27.9	252	238	-3.68 (0.00)	-4.00 (0.00)
130516.52+405640.90	20828 (249)	8.009 (0.045)	21.6	255	247	-4.06 (0.00)	-4.52 (0.00)
130728.60+144417.05	14756 (30)	8.000 (0.000)	39.7	134	130	-4.79 (0.10)	-8.42 (0.00)
130742.44+622956.80	24281 (436)	7.818 (0.038)	21.1	561	457	-3.24 (0.00)	-4.00 (0.00)
130830.53+470017.90	17187 (117)	7.871 (0.068)	17.4	414	389	-4.85 (0.00)	-6.00 (0.00)
130911.16-013946.80	18361 (182)	8.136 (0.071)	15.7	274	239	-4.56 (0.00)	-5.08 (0.00)
130947.54+121241.80	12075 (115)	8.000 (0.000)	16.6	257	248	-5.65 (0.00)	-9.81 (0.00)
131038.32+063406.60	14529 (85)	8.000 (0.000)	16.1	245	229	-5.48 (0.00)	-7.92 (0.00)
131009.73+240356.79	13010 (117)	8.000 (0.000)	13.8	238	237	-5.57 (0.00)	-8.99 (0.00)
131012.29+444728.40	11722 (67)	8.000 (0.000)	30.0	160	152	-5.96 (0.00)	-10.45 (0.00)
131055.30+680255.23	11972 (141)	8.000 (0.000)	14.0	274	207	-5.53 (0.00)	-9.71 (0.00)
131148.50+053847.60	21000 (316)	8.110 (0.040)	21.5	249	231	-4.02 (0.00)	-4.52 (0.00)
131130.50+124843.42	10035 (125)	8.000 (0.000)	34.7	98	94	-5.71 (0.00)	-11.20 (0.00)
131119.92+275812.65	17630 (76)	7.932 (0.039)	27.7	431	430	-5.01 (0.00)	-6.02 (0.00)
131133.00+485812.20	12139 (154)	8.000 (0.000)	12.3	212	197	-5.51 (0.00)	-9.56 (0.00)
131351.71+051054.42	31818 (368)	7.724 (0.045)	20.9	660	610	-2.88 (0.00)	-4.00 (0.00)
131351.30+124007.93	18587 (32)	7.910 (0.022)	40.2	138	133	-3.10 (0.07)	-6.12 (0.00)
131349.21+503724.09	17914 (135)	8.055 (0.062)	17.5	395	361	-4.68 (0.00)	-5.52 (0.00)

Table 1. continued.

SDSSJ	T_{eff} [K]	$\log g$ [cgs]	S/N	d [pc]	z [pc]	[H/He]	[Ca/He]
131343.91+570404.05	17415 (60)	8.050 (0.039)	27.2	290	250	-4.00 (0.20)	-6.03 (0.00)
131329.44+613359.72	17486 (101)	8.090 (0.053)	19.5	341	280	-4.36 (0.33)	-5.92 (0.00)
131425.19+083648.88	11502 (141)	8.000 (0.000)	14.5	254	240	-5.57 (0.00)	-10.10 (0.00)
131446.17+483124.90	17486 (106)	8.129 (0.060)	18.4	351	325	-4.85 (0.00)	-5.91 (0.00)
131406.75+522350.80	11656 (85)	8.000 (0.000)	25.1	145	130	-5.63 (0.28)	-8.89 (0.11)
131402.01+635552.00	13755 (40)	8.000 (0.000)	36.9	176	141	-5.90 (1.44)	-9.11 (0.00)
131618.55+161332.05	18756 (142)	8.010 (0.049)	20.8	289	282	-4.49 (0.28)	-5.04 (0.00)
131658.16+305148.00	19795 (230)	7.820 (0.060)	15.3	535	531	-4.04 (0.00)	-4.52 (0.00)
131646.02+414639.00	21844 (243)	7.953 (0.032)	26.7	242	233	-3.99 (0.00)	-4.70 (0.00)
131717.02-021945.60	17567 (171)	7.992 (0.099)	12.6	312	270	-4.64 (0.00)	-5.64 (0.00)
131745.60+420930.54	13990 (40)	8.000 (0.000)	34.7	142	137	-5.18 (0.14)	-8.95 (0.00)
131930.81+333554.53	15229 (48)	8.000 (0.000)	23.3	298	294	-5.52 (0.00)	-7.64 (0.00)
131953.38+430202.00	17118 (114)	8.074 (0.068)	16.5	396	379	-4.71 (0.44)	-6.00 (0.00)
132053.99+135043.10	13851 (48)	8.000 (0.000)	30.4	141	136	-5.40 (0.18)	-8.98 (0.00)
132029.02+174756.18	15034 (60)	8.000 (0.000)	18.2	334	327	-5.40 (0.50)	-7.56 (0.00)
132004.28+664535.80	16373 (90)	8.117 (0.061)	22.1	293	224	-5.28 (0.00)	-6.84 (0.00)
132251.69+165604.20	16419 (65)	7.994 (0.048)	27.6	198	194	-5.38 (0.00)	-7.00 (0.00)
132350.28+272744.14	18303 (130)	8.047 (0.046)	22.8	331	328	-4.58 (0.00)	-5.15 (0.00)
132358.62+280330.42	23479 (682)	7.938 (0.063)	13.2	632	627	-3.11 (0.00)	-4.00 (0.00)
132303.26+332628.43	18949 (181)	8.116 (0.071)	14.5	478	471	-4.27 (0.00)	-4.98 (0.00)
132301.29+355924.48	16319 (163)	8.087 (0.103)	12.2	320	314	-4.95 (0.00)	-6.33 (0.00)
132332.78+362032.00	18317 (160)	8.039 (0.060)	17.7	281	275	-4.61 (0.00)	-5.11 (0.00)
132430.42+055316.33	16553 (73)	7.904 (0.049)	25.2	653	603	-5.23 (0.00)	-6.58 (0.00)
132452.67+144135.30	14239 (80)	8.000 (0.000)	17.5	250	242	-5.56 (0.00)	-8.20 (0.00)
132644.21+314402.66	17179 (124)	7.968 (0.075)	15.4	433	428	-4.78 (0.00)	-5.91 (0.00)
132742.39+153118.48	13434 (95)	8.000 (0.000)	15.8	336	326	-5.41 (0.00)	-8.66 (0.00)
132712.19+631044.91	19675 (112)	8.063 (0.047)	17.6	509	409	-3.19 (0.27)	-4.54 (0.00)
132833.43+045637.40	12099 (124)	8.000 (0.000)	14.7	215	197	-5.55 (0.32)	-9.77 (0.00)
132800.53+061542.02	17342 (37)	8.096 (0.021)	51.8	130	120	-5.11 (0.22)	-6.08 (0.00)
132840.62+260458.10	11107 (109)	8.000 (0.000)	22.6	191	188	-5.76 (0.00)	-10.57 (0.00)
132909.67+231454.35	21155 (227)	7.999 (0.048)	19.1	447	441	-3.39 (0.34)	-4.48 (0.00)
132941.36+375322.10	17475 (139)	7.899 (0.075)	14.5	466	453	-4.70 (0.00)	-5.75 (0.00)
133021.16+222904.74	17578 (117)	8.131 (0.056)	19.1	346	341	-4.84 (0.00)	-5.89 (0.00)
133048.27+560805.80	17824 (198)	7.932 (0.097)	11.8	366	317	-4.51 (0.00)	-5.40 (0.00)
133152.50-000445.21	11621 (147)	8.000 (0.000)	14.2	273	239	-5.54 (0.00)	-9.98 (0.00)
133159.27+574508.87	14788 (22)	8.000 (0.000)	53.0	102	87	-4.99 (0.14)	-8.30 (0.00)
133208.34+211709.28	11416 (65)	8.000 (0.000)	34.1	158	155	-5.96 (0.00)	-10.65 (0.00)
133215.95+640656.30	19825 (313)	7.885 (0.079)	12.5	401	318	-3.97 (0.00)	-4.57 (0.00)
133302.89+582130.49	13529 (48)	8.000 (0.000)	30.4	164	139	-5.77 (1.64)	-9.13 (0.00)
133306.98+634936.40	15449 (37)	8.000 (0.000)	31.3	273	217	-5.07 (0.20)	-7.50 (0.12)
133439.60+155948.80	16834 (47)	7.971 (0.032)	38.3	114	110	-4.82 (0.16)	-6.55 (0.00)
133717.52+083044.90	11641 (167)	8.000 (0.000)	12.2	346	322	-5.51 (0.00)	-9.94 (0.00)
133740.75+213216.80	18506 (101)	7.982 (0.040)	25.4	212	208	-4.71 (0.00)	-5.76 (0.00)
133754.88+344911.20	20809 (346)	8.040 (0.059)	15.2	342	334	-3.83 (0.00)	-4.44 (0.00)
133836.18+133360.00	14179 (97)	8.000 (0.000)	14.1	275	263	-5.22 (0.28)	-8.08 (0.00)
133840.45+451543.21	12886 (114)	8.000 (0.000)	14.8	306	287	-5.56 (0.00)	-9.07 (0.00)
133834.97+505111.63	13886 (125)	8.000 (0.000)	12.6	319	288	-5.37 (0.00)	-8.14 (0.00)
133818.00+602254.71	18232 (117)	7.951 (0.049)	22.5	318	263	-4.70 (0.00)	-5.19 (0.00)
133819.07+624018.70	11376 (153)	8.000 (0.000)	15.1	184	148	-5.62 (0.00)	-10.25 (0.00)
134157.73+032424.17	17356 (103)	8.169 (0.060)	19.2	305	273	-4.92 (0.30)	-6.00 (0.00)
134213.99+452055.20	16605 (49)	8.116 (0.030)	39.2	152	142	-5.37 (0.25)	-6.62 (0.00)
134315.81+100838.80	19424 (315)	7.841 (0.086)	10.9	806	753	-3.96 (0.00)	-4.57 (0.00)
134311.80+224543.85	16897 (72)	7.993 (0.046)	26.2	340	332	-5.16 (0.00)	-6.51 (0.00)
134329.63+670733.20	13660 (99)	8.000 (0.000)	15.0	363	275	-5.19 (0.59)	-8.24 (0.30)
134437.65+183714.40	14887 (30)	8.000 (0.000)	40.0	144	140	-5.08 (0.09)	-8.07 (0.00)
134537.98+274450.30	13305 (130)	8.000 (0.000)	11.9	439	429	-4.77 (0.36)	-7.83 (0.28)
134521.30+551037.16	15174 (55)	8.000 (0.000)	20.4	305	265	-5.50 (0.00)	-7.63 (0.00)

Table 1. continued.

SDSSJ	T_{eff} [K]	$\log g$ [cgs]	S/N	d [pc]	z [pc]	[H/He]	[Ca/He]
134712.54+562110.70	10903 (152)	8.000 (0.000)	18.5	150	128	-5.67 (0.00)	-10.59 (0.00)
134849.25+203011.38	14487 (48)	8.000 (0.000)	27.4	187	181	-5.73 (0.00)	-8.35 (0.00)
134839.62+645746.68	13984 (68)	8.000 (0.000)	22.1	251	195	-5.68 (0.00)	-8.55 (0.00)
134956.22+024309.40	14072 (90)	8.000 (0.000)	15.6	244	215	-5.47 (1.19)	-8.01 (0.32)
135121.92+180411.90	19421 (134)	7.855 (0.038)	25.4	440	422	-4.47 (0.00)	-5.37 (0.00)
135116.60+190006.30	16071 (166)	8.238 (0.114)	12.0	489	470	-5.01 (0.00)	-6.49 (0.03)
135142.59+342144.96	13370 (82)	8.000 (0.000)	18.5	298	288	-5.66 (0.00)	-8.88 (0.00)
135153.48+385652.30	15007 (104)	8.000 (0.000)	11.4	365	349	-5.17 (0.00)	-7.24 (0.00)
135224.27+203005.98	16845 (57)	7.966 (0.036)	33.3	226	218	-5.32 (0.00)	-6.53 (0.00)
135228.45+342906.04	11534 (51)	8.000 (0.000)	40.9	117	113	-6.44 (0.00)	-10.67 (0.00)
135240.43+411943.23	11777 (125)	8.000 (0.000)	15.7	272	257	-5.60 (0.00)	-9.96 (0.00)
135310.01+484020.86	28434 (124)	7.887 (0.018)	51.2	207	188	-3.10 (0.00)	-4.00 (0.00)
135532.42+001124.00	14255 (25)	8.000 (0.000)	52.6	76	65	-5.12 (0.08)	-9.08 (0.00)
135541.70+110031.80	20955 (251)	7.817 (0.046)	19.7	342	317	-4.00 (0.00)	-4.65 (0.00)
135541.21+351441.60	13456 (136)	8.000 (0.000)	11.2	317	305	-5.38 (0.00)	-8.41 (0.00)
135754.50+181058.30	15553 (49)	8.000 (0.000)	25.8	179	170	-5.56 (0.00)	-7.51 (0.00)
135723.99+495903.30	15484 (32)	8.000 (0.000)	37.1	148	132	-5.60 (0.22)	-7.54 (0.00)
135933.24-021715.20	16973 (60)	7.830 (0.047)	21.8	248	206	-3.33 (0.11)	-6.49 (0.30)
135911.39+225212.32	20504 (386)	7.968 (0.064)	13.0	576	554	-3.72 (0.00)	-4.29 (0.00)
140035.81+341440.40	16167 (90)	8.000 (0.000)	14.7	349	335	-5.09 (0.00)	-6.62 (0.00)
140028.40+475644.56	30829 (214)	7.917 (0.026)	34.8	283	257	-3.00 (0.00)	-4.00 (0.00)
140129.62+050130.79	17216 (102)	7.999 (0.062)	18.9	354	313	-4.94 (0.00)	-6.01 (0.00)
140235.99-014925.66	18869 (87)	7.963 (0.036)	28.9	276	230	-4.63 (0.00)	-5.64 (0.00)
140255.43+245313.49	13029 (107)	8.000 (0.000)	15.2	340	327	-5.57 (0.00)	-8.98 (0.00)
140246.26+330323.80	15602 (60)	8.000 (0.000)	18.9	258	247	-4.81 (0.27)	-7.24 (0.00)
140227.20+403922.30	16305 (50)	7.876 (0.035)	35.7	246	231	-5.50 (0.00)	-7.02 (0.00)
140255.58+573157.10	21347 (527)	8.147 (0.059)	13.7	447	375	-3.53 (0.00)	-4.02 (0.00)
140229.38+602117.40	16027 (115)	8.228 (0.086)	14.8	304	248	-4.73 (0.34)	-6.62 (0.00)
140356.97+082047.08	16074 (73)	8.034 (0.049)	26.3	271	244	-5.39 (0.00)	-7.01 (0.00)
140336.35+195455.20	13578 (129)	8.000 (0.000)	11.0	312	297	-4.18 (0.32)	-8.30 (0.30)
140458.60+175804.40	12180 (113)	8.000 (0.000)	16.8	268	253	-5.65 (0.00)	-9.73 (0.00)
140441.32+182437.58	12625 (84)	8.000 (0.000)	20.2	226	214	-5.48 (0.25)	-9.55 (0.00)
140438.26+275747.27	19240 (278)	7.983 (0.068)	15.1	424	407	-3.99 (0.39)	-4.92 (0.00)
140555.56+110336.94	16164 (94)	8.154 (0.065)	20.3	265	242	-5.25 (0.00)	-6.84 (0.00)
140518.57+332340.70	14450 (59)	8.000 (0.000)	25.0	141	135	-5.75 (0.00)	-8.41 (0.00)
140502.12+380956.87	16910 (44)	8.021 (0.028)	41.2	107	101	-5.15 (0.21)	-6.55 (0.00)
140619.96-011932.50	15499 (23)	8.000 (0.000)	52.8	78	65	-5.80 (0.21)	-7.57 (0.00)
140645.47+552340.20	15137 (73)	8.000 (0.000)	14.5	357	305	-5.18 (0.00)	-7.26 (0.00)
140615.80+562725.90	49304 (715)	8.172 (0.157)	12.8	663	560	-2.39 (0.00)	-4.00 (0.00)
140759.50+121533.95	18335 (84)	7.958 (0.033)	31.0	288	265	-4.81 (0.00)	-5.94 (0.00)
140805.16+062326.45	14999 (68)	8.000 (0.000)	16.3	348	309	-4.30 (0.21)	-7.47 (0.00)
140832.57+125426.39	13751 (82)	8.000 (0.000)	18.8	275	253	-5.64 (0.00)	-8.61 (0.00)
140822.36+512318.85	15619 (40)	8.000 (0.000)	29.8	192	169	-5.57 (0.00)	-7.51 (0.00)
140957.76+124352.80	14783 (109)	8.000 (0.000)	11.8	291	268	-5.22 (0.00)	-7.44 (0.00)
141023.40+120552.81	12845 (90)	8.000 (0.000)	19.0	287	262	-5.71 (0.00)	-9.33 (0.00)
141037.54+144544.78	13860 (109)	8.000 (0.000)	13.4	368	341	-5.40 (0.00)	-8.19 (0.30)
141029.97+285146.90	19394 (297)	7.765 (0.083)	11.9	466	444	-4.02 (0.00)	-4.67 (0.00)
141044.61+373544.80	28872 (354)	7.778 (0.051)	17.0	853	803	-2.92 (0.00)	-4.00 (0.00)
141127.09+035429.70	36046 (288)	7.760 (0.029)	35.9	344	298	-2.91 (0.00)	-4.00 (0.00)
141122.50+183036.97	16642 (138)	7.943 (0.091)	13.5	451	423	-4.84 (0.00)	-6.12 (0.00)
141258.17+045602.20	30427 (288)	7.843 (0.036)	24.8	336	293	-2.95 (0.00)	-4.00 (0.00)
141218.72+102157.64	17021 (149)	8.229 (0.087)	13.5	335	303	-4.80 (0.00)	-5.88 (0.00)
141322.31+343047.10	22942 (949)	8.063 (0.079)	10.2	463	438	-3.10 (0.00)	-4.00 (0.00)
141306.65+354928.10	13786 (103)	8.000 (0.000)	13.7	390	367	-4.77 (0.28)	-8.34 (0.00)
141301.64+493957.40	17354 (64)	7.995 (0.036)	32.0	171	152	-5.18 (0.00)	-6.56 (0.00)
141349.46+571716.40	28889 (280)	7.797 (0.040)	22.4	553	461	-2.96 (0.00)	-4.00 (0.00)
141431.59-024008.10	11276 (132)	8.000 (0.000)	16.2	161	130	-5.65 (0.00)	-10.35 (0.00)

Table 1. continued.

SDSSJ	T_{eff} [K]	$\log g$ [cgs]	S/N	d [pc]	z [pc]	[H/He]	[Ca/He]
141445.48+563345.00	15334 (38)	8.000 (0.000)	32.2	231	194	-5.70 (0.00)	-7.59 (0.00)
141539.63+185851.50	12947 (57)	8.000 (0.000)	26.4	175	0	-4.52 (0.11)	-9.58 (0.00)
141621.79+322638.60	35015 (786)	7.510 (0.073)	14.9	719	679	-2.79 (0.00)	-4.00 (0.00)
141759.32+010725.64	17236 (114)	7.909 (0.071)	16.8	414	346	-4.82 (0.00)	-5.96 (0.00)
141739.30+081541.26	22316 (487)	7.751 (0.051)	15.7	554	490	-3.42 (0.00)	-4.06 (0.00)
141755.35+231136.90	17745 (65)	8.077 (0.033)	34.5	134	126	-4.76 (0.22)	-6.04 (0.00)
141859.77+034026.76	14752 (47)	8.000 (0.000)	26.4	200	171	-5.11 (0.24)	-8.15 (0.00)
141854.18+125404.60	15923 (82)	8.000 (0.000)	15.1	272	247	-5.15 (0.00)	-6.81 (0.00)
141803.55+200053.70	16769 (160)	7.882 (0.100)	12.2	406	378	-4.78 (0.00)	-6.02 (0.00)
141825.85+224132.39	17554 (54)	7.986 (0.028)	39.7	163	153	-5.19 (0.00)	-6.59 (0.00)
141920.96+411254.76	14564 (84)	8.000 (0.000)	15.3	343	316	-5.37 (0.00)	-7.77 (0.00)
142202.88-020251.90	16132 (82)	7.956 (0.061)	21.9	279	224	-5.33 (0.00)	-7.00 (0.00)
142240.81+334807.95	21686 (291)	7.975 (0.040)	21.7	377	353	-3.80 (0.00)	-4.48 (0.00)
142204.29+345457.49	11725 (38)	8.000 (0.000)	53.0	96	90	-5.35 (0.09)	-10.63 (0.00)
142356.36+362336.00	21748 (330)	8.017 (0.041)	20.6	277	257	-3.81 (0.00)	-4.05 (0.00)
142307.87+362454.00	13499 (47)	8.000 (0.000)	31.8	203	188	-5.26 (0.17)	-9.19 (0.00)
142321.79+592307.10	15205 (123)	8.000 (0.000)	10.3	311	252	-5.07 (0.00)	-7.01 (0.00)
142405.54+181807.40	30011 (583)	8.000 (0.000)	11.2	583	536	-2.82 (0.00)	-4.00 (0.00)
142447.13+262917.10	28046 (487)	7.692 (0.070)	14.1	615	575	-2.91 (0.00)	-4.00 (0.00)
142446.24+322930.37	18933 (155)	8.292 (0.060)	16.5	376	351	-4.40 (0.00)	-5.01 (0.00)
142608.21+182059.75	12286 (147)	8.000 (0.000)	12.6	324	297	-5.52 (0.00)	-9.45 (0.00)
142632.08+455639.70	11939 (142)	8.000 (0.000)	14.3	309	276	-5.61 (0.00)	-9.85 (0.00)
142825.08+051031.10	17694 (66)	8.099 (0.033)	33.5	175	149	-4.81 (0.19)	-6.03 (0.00)
142810.12+103953.70	16307 (96)	7.984 (0.072)	19.2	212	187	-5.22 (0.00)	-6.78 (0.00)
142833.01+161922.94	15523 (77)	8.000 (0.000)	15.7	368	334	-5.21 (0.00)	-7.06 (0.00)
142842.83+600300.63	14342 (98)	8.000 (0.000)	15.4	282	226	-5.45 (0.00)	-7.99 (0.00)
142907.91+254214.16	10754 (173)	8.000 (0.000)	18.6	206	191	-5.60 (0.00)	-10.61 (0.00)
143149.25+235100.11	21234 (251)	7.953 (0.033)	26.6	285	262	-4.04 (0.00)	-4.78 (0.00)
143239.60-020315.83	13451 (91)	8.000 (0.000)	16.9	306	241	-5.59 (0.00)	-8.71 (0.00)
143350.80+071452.22	11566 (50)	8.000 (0.000)	41.0	97	83	-5.36 (0.19)	-9.43 (0.08)
143452.22+091835.35	13270 (70)	8.000 (0.000)	21.6	287	248	-5.74 (0.00)	-9.07 (0.00)
143458.86+121404.99	17117 (106)	7.941 (0.064)	18.6	401	353	-4.93 (0.00)	-6.02 (0.00)
143639.51-011517.80	12829 (154)	8.000 (0.000)	11.0	267	210	-5.45 (0.00)	-8.95 (0.00)
143732.94+172557.04	17667 (47)	8.027 (0.023)	46.7	138	124	-5.05 (0.19)	-6.06 (0.00)
143802.78+144137.54	18935 (124)	8.081 (0.046)	21.2	344	304	-4.51 (0.00)	-5.03 (0.00)
143846.21+280455.90	16486 (177)	7.860 (0.126)	10.3	431	395	-4.73 (0.00)	-6.04 (0.00)
144139.08+485448.33	17460 (112)	7.923 (0.061)	17.4	347	299	-4.75 (0.00)	-5.84 (0.00)
144119.75+512719.20	15783 (92)	8.000 (0.000)	13.1	274	232	-4.84 (0.37)	-6.79 (0.00)
144230.11+083147.20	16880 (141)	7.957 (0.091)	13.8	378	320	-4.86 (0.00)	-6.09 (0.00)
144212.69+105107.30	14940 (64)	8.000 (0.000)	20.8	191	164	-5.56 (0.00)	-7.85 (0.00)
144205.41+122926.80	31591 (409)	7.653 (0.051)	18.4	527	457	-2.88 (0.00)	-4.00 (0.00)
144428.15+162717.60	15477 (104)	8.000 (0.000)	11.7	413	364	-5.04 (0.00)	-6.82 (0.00)
144426.39+413521.44	13014 (105)	8.000 (0.000)	14.8	340	302	-5.55 (0.00)	-8.96 (0.00)
144518.03+585032.20	14242 (51)	8.000 (0.000)	27.2	189	150	-5.76 (0.00)	-8.22 (0.22)
144651.48-002942.00	16331 (112)	8.313 (0.082)	16.0	357	277	-4.63 (0.27)	-6.58 (0.00)
144650.87+285142.30	23278 (737)	7.813 (0.084)	10.6	544	491	-3.04 (0.00)	-4.00 (0.00)
144601.02+625733.80	10753 (126)	8.000 (0.000)	20.7	198	169	-5.49 (0.33)	-10.68 (0.00)
144814.33+150449.70	20327 (121)	7.930 (0.021)	43.4	119	103	-4.46 (0.00)	-5.52 (0.00)
144837.56+150538.29	15347 (43)	8.000 (0.000)	26.5	250	217	-5.04 (0.24)	-7.54 (0.00)
144819.48+322500.89	20432 (237)	8.221 (0.057)	14.0	480	432	-2.83 (0.24)	-4.40 (0.00)
144826.45+630835.30	15476 (67)	8.000 (0.000)	19.4	187	141	-5.43 (0.00)	-7.39 (0.00)
144816.68+632419.27	19163 (160)	8.158 (0.044)	23.3	207	156	-4.51 (0.00)	-4.79 (0.00)
144936.84+093739.80	19750 (287)	8.200 (0.059)	14.8	314	263	-4.08 (0.00)	-4.52 (0.00)
144952.03+133817.92	10863 (132)	8.000 (0.000)	20.1	195	167	-5.67 (0.00)	-10.62 (0.00)
144912.54+170150.56	21386 (209)	7.975 (0.027)	31.4	293	256	-4.06 (0.00)	-4.87 (0.00)
144930.58+445719.44	17899 (165)	7.828 (0.078)	14.4	509	443	-4.53 (0.00)	-5.46 (0.00)
144939.14+494436.72	14515 (108)	8.000 (0.000)	11.9	360	308	-5.21 (0.00)	-7.57 (0.00)

Table 1. continued.

SDSSJ	T_{eff} [K]	$\log g$ [cgs]	S/N	d [pc]	z [pc]	[H/He]	[Ca/He]
145023.39+005441.00	13365 (79)	8.000 (0.000)	20.1	268	205	-5.74 (0.00)	-9.01 (0.00)
145031.36+600101.03	15262 (73)	8.000 (0.000)	16.4	339	265	-5.29 (0.00)	-7.30 (0.00)
145240.49+614526.40	18311 (109)	8.075 (0.038)	25.9	275	210	-4.19 (0.28)	-5.17 (0.00)
145349.09+195201.60	17207 (144)	7.935 (0.087)	13.8	334	293	-4.78 (0.00)	-5.90 (0.00)
145334.24+201924.40	11144 (259)	8.000 (0.000)	10.5	252	221	-5.40 (0.00)	-10.13 (0.00)
145325.98+294912.80	14947 (61)	8.000 (0.000)	21.8	198	176	-5.58 (0.00)	-7.88 (0.00)
145329.41+363612.90	12300 (131)	8.000 (0.000)	13.7	222	197	-5.60 (0.00)	-9.56 (0.00)
145452.84+084640.66	15444 (29)	8.000 (0.000)	39.8	141	117	-5.44 (0.17)	-7.55 (0.00)
145437.06+445523.59	11634 (134)	8.000 (0.000)	15.3	300	259	-5.59 (0.00)	-10.04 (0.00)
145534.04+103846.68	12311 (101)	8.000 (0.000)	18.0	234	195	-5.70 (0.00)	-9.70 (0.00)
145644.91+011017.60	17472 (189)	7.891 (0.108)	11.0	464	357	-4.51 (0.00)	-5.48 (0.00)
145755.43+015442.95	19602 (111)	8.004 (0.027)	33.2	301	233	-4.50 (0.00)	-4.61 (0.00)
145746.31+330944.95	18978 (137)	7.983 (0.046)	20.7	445	394	-4.36 (0.36)	-5.27 (0.00)
145832.63+100818.10	26695 (322)	7.796 (0.026)	40.2	188	155	-2.92 (0.03)	-4.00 (0.00)
145818.51+102632.96	11818 (74)	8.000 (0.000)	26.4	203	167	-5.19 (0.12)	-10.28 (0.00)
145822.52+435905.80	20063 (219)	8.116 (0.035)	26.2	191	165	-4.02 (0.26)	-4.55 (0.00)
145947.04+003954.60	16712 (128)	8.116 (0.084)	15.6	274	205	-5.02 (0.00)	-6.31 (0.00)
145935.23+192818.59	11982 (91)	8.000 (0.000)	21.6	206	178	-5.79 (0.00)	-9.95 (0.00)
145900.87+202221.20	16414 (140)	7.867 (0.101)	13.1	346	300	-4.94 (0.00)	-6.33 (0.00)
145940.78+244554.20	13584 (37)	8.000 (0.000)	40.8	90	79	-5.68 (0.16)	-9.40 (0.00)
145907.68+553116.60	13756 (89)	8.000 (0.000)	15.7	270	215	-5.39 (1.04)	-8.38 (0.00)
145931.20+613502.77	18499 (159)	8.127 (0.059)	16.9	348	264	-4.50 (0.00)	-5.04 (0.00)
150003.86+002420.00	13926 (134)	8.000 (0.000)	11.2	289	219	-5.32 (0.00)	-8.04 (0.00)
150042.53+061304.30	11400 (139)	8.000 (0.000)	15.9	265	211	-5.58 (0.00)	-10.18 (0.00)
150150.83+131707.10	11249 (179)	8.000 (0.000)	13.3	207	172	-5.54 (0.00)	-10.23 (0.00)
150201.40+102243.00	10934 (138)	8.000 (0.000)	20.5	159	131	-5.74 (0.00)	-10.64 (0.00)
150301.95+053414.05	12772 (118)	8.000 (0.000)	14.3	306	241	-5.56 (0.00)	-9.14 (0.00)
150418.56+120025.98	15243 (38)	8.000 (0.000)	30.5	159	131	-5.08 (0.16)	-7.97 (0.00)
150431.69+162453.50	16825 (75)	7.829 (0.047)	26.1	201	169	-5.21 (0.00)	-6.52 (0.00)
150506.24+383017.39	15049 (30)	8.000 (0.000)	37.6	146	126	-4.52 (0.13)	-8.02 (0.00)
150657.27+004610.59	13767 (63)	8.000 (0.000)	22.9	268	196	-5.43 (0.30)	-8.50 (0.29)
150633.90+531929.60	16367 (119)	8.107 (0.076)	16.4	336	273	-5.05 (0.00)	-6.47 (0.00)
150850.96+013518.47	14188 (77)	8.000 (0.000)	17.6	291	217	-5.52 (0.61)	-8.17 (0.00)
151005.05+050905.80	12865 (100)	8.000 (0.000)	17.1	219	168	-5.70 (0.00)	-9.29 (0.00)
151212.40+155742.31	11904 (149)	8.000 (0.000)	13.2	307	253	-5.52 (0.00)	-9.75 (0.00)
151317.27+003523.06	14433 (31)	8.000 (0.000)	40.3	148	107	-3.66 (0.15)	-8.73 (0.00)
151428.74+112417.00	19861 (339)	7.983 (0.084)	11.4	460	367	-3.90 (0.00)	-4.47 (0.00)
151642.97+004042.70	14961 (28)	8.000 (0.000)	41.1	155	110	-4.47 (0.12)	-7.38 (0.16)
151729.46+433028.70	28934 (377)	8.000 (0.000)	16.4	448	373	-2.92 (0.00)	-4.00 (0.00)
151727.59+552452.60	11901 (134)	8.000 (0.000)	14.8	260	203	-5.58 (0.00)	-9.85 (0.00)
151800.52+370303.40	12829 (62)	8.000 (0.000)	26.2	151	127	-5.45 (0.20)	-9.65 (0.00)
151907.02+464521.50	19969 (258)	7.954 (0.062)	14.7	524	429	-4.00 (0.00)	-4.51 (0.00)
152048.23+153013.70	16821 (132)	7.745 (0.091)	14.1	406	326	-4.86 (0.00)	-6.15 (0.00)
152006.05+580037.00	17434 (123)	7.877 (0.068)	16.3	481	367	-4.73 (0.00)	-5.82 (0.00)
152123.36+382519.25	12408 (78)	8.000 (0.000)	23.0	226	189	-5.77 (1.15)	-9.56 (0.24)
152235.04+165117.80	14315 (71)	8.000 (0.000)	19.5	249	200	-5.61 (0.00)	-8.25 (0.00)
152228.41+354908.44	11909 (149)	8.000 (0.000)	13.0	308	258	-5.51 (0.00)	-9.73 (0.00)
152211.51+404455.70	12183 (121)	8.000 (0.000)	16.0	203	168	-5.68 (0.00)	-9.77 (0.00)
152249.56+553354.00	15894 (81)	8.000 (0.000)	15.6	377	291	-5.14 (0.00)	-6.79 (0.00)
152304.84+051157.60	14842 (87)	8.000 (0.000)	15.3	259	191	-5.41 (0.00)	-7.67 (0.00)
152512.52+020305.73	16204 (175)	8.081 (0.122)	11.1	403	287	-4.84 (0.00)	-6.24 (0.00)
152521.13+042111.02	15522 (131)	8.332 (0.087)	16.1	325	237	-5.24 (0.00)	-7.07 (0.00)
152518.41+173349.00	14136 (59)	8.000 (0.000)	24.6	176	141	-5.77 (0.00)	-8.60 (0.00)
152634.97+485801.30	11551 (65)	8.000 (0.000)	28.1	157	126	-4.83 (0.12)	-10.52 (0.00)
152728.84+204010.80	10939 (192)	8.000 (0.000)	15.9	245	198	-5.54 (0.00)	-10.43 (0.00)
152727.08+233351.25	16299 (45)	8.018 (0.029)	40.9	163	133	-5.42 (0.00)	-7.04 (0.00)
152739.56+314242.00	18351 (206)	8.156 (0.083)	13.2	306	253	-4.48 (0.00)	-5.05 (0.00)

Table 1. continued.

SDSSJ	T_{eff} [K]	$\log g$ [cgs]	S/N	d [pc]	z [pc]	[H/He]	[Ca/He]
152718.20+414835.70	14552 (91)	8.000 (0.000)	14.9	250	205	-5.43 (0.00)	-7.84 (0.00)
152808.20+213847.00	35696 (920)	8.000 (0.000)	10.8	540	437	-2.72 (0.00)	-4.00 (0.00)
153035.52+072800.06	10589 (192)	8.000 (0.000)	16.6	240	177	-5.49 (0.00)	-10.60 (0.00)
153006.10+264923.91	16198 (57)	8.073 (0.043)	29.2	235	192	-4.74 (0.20)	-7.01 (0.00)
153024.23+331549.72	17727 (112)	8.149 (0.071)	16.2	482	396	-4.29 (0.28)	-5.69 (0.00)
153148.42+383911.00	17733 (143)	8.080 (0.087)	12.9	469	382	-4.11 (0.43)	-5.53 (0.00)
153124.48+440420.21	13985 (77)	8.000 (0.000)	19.5	282	228	-5.61 (0.00)	-8.44 (0.00)
153255.11+171901.86	12388 (124)	8.000 (0.000)	14.8	287	225	-5.59 (0.00)	-9.50 (0.00)
153223.82+272503.60	10892 (73)	8.000 (0.000)	30.7	113	92	-5.04 (0.14)	-10.87 (0.00)
153224.22+491453.86	14061 (88)	8.000 (0.000)	15.6	308	243	-5.47 (0.00)	-8.16 (0.00)
153325.60+132537.07	19645 (197)	7.941 (0.049)	19.6	425	325	-4.21 (0.00)	-4.98 (0.00)
153316.76+340803.70	16191 (89)	7.898 (0.067)	20.5	206	168	-5.26 (0.00)	-6.90 (0.00)
153303.95+503245.54	11757 (99)	8.000 (0.000)	20.1	253	198	-5.73 (0.00)	-10.14 (0.00)
153454.99+224918.70	20797 (225)	8.007 (0.038)	23.3	266	212	-4.08 (0.00)	-4.53 (0.00)
153615.72+574902.70	16071 (119)	7.968 (0.092)	14.9	371	276	-5.06 (0.00)	-6.61 (0.00)
153735.17+063848.07	21101 (396)	8.235 (0.060)	13.5	415	296	-3.12 (0.34)	-4.07 (0.00)
153755.31+093249.50	14940 (131)	8.000 (0.000)	10.3	321	235	-5.11 (0.00)	-7.20 (0.00)
153725.51+233719.60	12625 (171)	8.000 (0.000)	10.7	268	213	-5.46 (0.00)	-9.11 (0.00)
153725.72+515126.90	17450 (40)	7.750 (0.032)	29.8	213	164	-3.12 (0.11)	-6.46 (0.00)
153821.66+092006.76	18751 (35)	8.138 (0.024)	37.7	268	195	-3.17 (0.13)	-5.10 (0.00)
153953.06+385520.74	11514 (153)	8.000 (0.000)	13.7	263	211	-5.54 (0.00)	-10.05 (0.00)
153905.51+442951.86	13426 (104)	8.000 (0.000)	14.6	330	261	-5.50 (0.00)	-8.58 (0.00)
154134.50+252329.98	11155 (43)	8.000 (0.000)	50.3	54	42	-5.55 (0.14)	-11.04 (0.00)
154152.20+475253.75	16517 (114)	8.121 (0.070)	17.3	348	270	-5.06 (0.00)	-6.43 (0.00)
154201.50+502532.10	31027 (247)	7.640 (0.030)	31.9	298	229	-2.99 (0.00)	-4.00 (0.00)
154446.06+204654.27	10760 (72)	8.000 (0.000)	39.2	139	106	-6.07 (0.00)	-11.01 (0.00)
154550.28+115958.70	17662 (69)	8.059 (0.035)	32.5	199	144	-5.09 (0.35)	-6.03 (0.00)
154606.89+565059.10	11372 (89)	8.000 (0.000)	24.1	181	134	-5.80 (0.00)	-10.48 (0.00)
154703.53+450053.35	14622 (86)	8.000 (0.000)	15.0	365	283	-5.36 (0.00)	-7.71 (0.00)
154811.34+083613.21	18969 (119)	7.925 (0.045)	20.4	396	276	-4.45 (0.00)	-5.26 (0.00)
155051.40+022511.12	14506 (98)	8.000 (0.000)	12.8	408	265	-5.25 (0.00)	-7.62 (0.00)
155026.70+201951.80	12552 (139)	8.000 (0.000)	12.3	282	212	-5.54 (0.00)	-9.29 (0.00)
155115.33+363742.00	16035 (103)	7.966 (0.077)	17.6	239	186	-5.22 (0.00)	-6.88 (0.00)
155225.07+081919.88	14353 (81)	8.000 (0.000)	16.3	360	247	-5.33 (0.00)	-7.99 (0.00)
155253.52+141334.50	16374 (97)	7.972 (0.071)	18.8	254	182	-5.17 (0.00)	-6.69 (0.00)
155327.56+150545.70	24724 (481)	7.901 (0.048)	18.0	379	273	-3.15 (0.00)	-4.00 (0.00)
155409.03+172124.10	15930 (37)	8.000 (0.000)	31.1	166	121	-4.29 (0.11)	-6.47 (0.18)
155450.28+325413.30	10783 (66)	8.000 (0.000)	38.2	73	56	-5.93 (0.00)	-11.05 (0.00)
155426.22+461707.80	12606 (34)	8.000 (0.000)	47.8	91	69	-4.57 (0.06)	-10.16 (0.00)
155511.87+343350.58	16700 (164)	8.073 (0.108)	10.1	212	163	-4.35 (0.00)	-5.77 (0.30)
155756.04+333603.74	14478 (77)	8.000 (0.000)	16.6	341	260	-5.42 (0.00)	-7.88 (0.00)
155717.36+525623.10	15194 (46)	8.000 (0.000)	24.2	280	205	-4.68 (0.25)	-7.70 (0.00)
155847.35+353113.39	13434 (122)	8.000 (0.000)	12.8	336	255	-5.43 (0.00)	-8.49 (0.00)
155921.08+190407.86	20685 (114)	7.991 (0.017)	49.0	151	109	-3.80 (0.16)	-5.46 (0.00)
160030.97+195734.50	17041 (150)	7.967 (0.093)	13.6	336	243	-4.81 (0.00)	-5.98 (0.00)
160157.26+125133.41	13296 (30)	8.000 (0.000)	50.7	114	78	-5.40 (0.09)	-9.68 (0.00)
160241.83+035814.93	15885 (77)	8.000 (0.000)	14.5	387	243	-4.60 (0.00)	-6.72 (0.00)
160223.11+052239.80	17090 (100)	7.926 (0.065)	19.8	380	242	-5.02 (0.00)	-6.06 (0.00)
160205.60+320419.56	16050 (32)	8.132 (0.024)	55.9	110	83	-5.47 (0.23)	-7.07 (0.00)
160522.47+532220.10	16473 (70)	7.922 (0.051)	25.7	330	236	-5.30 (0.00)	-6.89 (0.00)
160625.19+052821.30	21947 (316)	7.883 (0.041)	22.5	428	269	-3.56 (0.41)	-4.54 (0.00)
160651.52+074752.12	12314 (101)	8.000 (0.000)	18.1	255	163	-5.71 (0.00)	-9.71 (0.00)
160622.04+272017.00	12900 (107)	8.000 (0.000)	16.5	308	225	-5.62 (0.00)	-9.15 (0.00)
160836.24+271132.06	18017 (50)	8.087 (0.017)	59.1	118	85	-4.34 (0.11)	-5.59 (0.00)
160942.44+063049.40	15018 (69)	8.000 (0.000)	17.2	364	227	-5.07 (0.49)	-7.61 (0.00)
160911.61+392150.40	15169 (72)	8.000 (0.000)	16.5	274	202	-4.79 (0.30)	-7.40 (0.00)
160904.90+500555.14	12859 (139)	8.000 (0.000)	11.8	338	243	-5.41 (0.00)	-8.87 (0.00)

Table 1. continued.

SDSSJ	T_{eff} [K]	$\log g$ [cgs]	S/N	d [pc]	z [pc]	[H/He]	[Ca/He]
161003.24+113004.50	17394 (89)	7.997 (0.049)	23.1	235	154	-5.03 (0.00)	-6.24 (0.00)
161000.72+370009.00	19356 (358)	7.990 (0.093)	10.8	418	307	-4.02 (0.00)	-4.61 (0.00)
161038.93+371403.23	11698 (137)	8.000 (0.000)	14.9	296	217	-5.17 (0.29)	-8.41 (0.17)
161054.23+521137.70	16997 (68)	8.063 (0.048)	26.1	306	218	-4.33 (0.21)	-6.51 (0.00)
161009.85+550211.46	32744 (461)	7.640 (0.065)	17.2	859	604	-3.00 (0.00)	-4.00 (0.00)
161210.55+114535.80	19595 (247)	7.710 (0.071)	14.1	364	236	-4.09 (0.00)	-4.80 (0.00)
161200.33+151804.60	19477 (178)	7.926 (0.044)	23.5	245	164	-4.25 (0.24)	-5.29 (0.00)
161243.19+370803.66	15149 (87)	8.000 (0.000)	13.6	411	299	-4.73 (0.00)	-7.23 (0.00)
161252.34+424856.30	19438 (243)	7.913 (0.056)	16.9	282	205	-3.56 (0.39)	-5.01 (0.00)
161218.32+450920.90	14196 (141)	8.000 (0.000)	10.4	327	237	-5.24 (0.00)	-7.79 (0.00)
161331.31+182406.80	14756 (101)	8.000 (0.000)	13.0	269	183	-5.29 (0.00)	-7.55 (0.00)
161320.02+533752.90	12587 (84)	8.000 (0.000)	20.0	287	202	-5.57 (1.12)	-9.62 (0.00)
161544.76+480241.02	19266 (305)	8.138 (0.077)	12.9	446	318	-4.12 (0.00)	-4.55 (0.00)
161643.67+171453.20	13329 (39)	8.000 (0.000)	39.4	174	115	-6.09 (1.48)	-9.54 (0.00)
161756.83+301751.79	17592 (76)	8.217 (0.045)	23.6	262	185	-4.56 (0.32)	-6.01 (0.00)
161735.37+311645.41	19610 (127)	8.071 (0.052)	15.4	484	344	-3.22 (0.29)	-4.53 (0.00)
161701.34+352319.64	16967 (104)	8.061 (0.064)	18.6	335	240	-4.99 (0.00)	-6.21 (0.00)
161834.01+093358.14	19220 (167)	8.066 (0.039)	24.4	310	191	-4.42 (0.47)	-4.73 (0.00)
161853.48+414143.01	12029 (66)	8.000 (0.000)	27.1	184	131	-5.68 (0.26)	-10.19 (0.00)
161859.55+472323.78	13057 (119)	8.000 (0.000)	13.7	334	238	-5.51 (0.00)	-8.86 (0.00)
161927.55+165144.93	14778 (36)	8.000 (0.000)	36.1	210	138	-5.86 (0.00)	-8.21 (0.00)
161941.07+294353.51	18312 (143)	7.922 (0.057)	18.3	414	290	-4.56 (0.00)	-5.48 (0.00)
161932.55+310941.47	18655 (88)	7.905 (0.034)	28.0	311	219	-4.66 (0.00)	-5.70 (0.00)
161953.99+493350.80	16427 (120)	8.129 (0.093)	13.5	384	273	-4.73 (0.45)	-6.25 (0.00)
162332.63+542130.28	20905 (251)	7.963 (0.044)	20.3	404	276	-3.96 (0.00)	-4.51 (0.00)
162425.01+295511.86	22426 (348)	7.776 (0.038)	22.4	377	260	-3.65 (0.00)	-4.36 (0.00)
162546.32+251144.00	11596 (98)	8.000 (0.000)	19.9	162	109	-5.36 (0.21)	-10.29 (0.00)
162650.27+083026.28	11141 (104)	8.000 (0.000)	22.2	205	120	-5.76 (0.00)	-10.56 (0.00)
162635.84+130544.70	17181 (146)	7.871 (0.088)	14.3	354	218	-4.78 (0.00)	-5.93 (0.00)
162621.56+181439.98	13770 (50)	8.000 (0.000)	30.0	207	133	-5.87 (0.00)	-8.96 (0.00)
162646.92+313627.94	13665 (143)	8.000 (0.000)	11.1	367	252	-4.86 (0.36)	-6.60 (0.22)
162740.27+130354.71	19667 (203)	7.939 (0.050)	18.3	498	304	-4.16 (0.00)	-4.88 (0.00)
162703.33+172327.60	15795 (112)	8.000 (0.000)	11.5	300	191	-5.02 (0.00)	-6.66 (0.00)
162711.17+253108.50	17324 (159)	7.852 (0.087)	13.4	427	286	-4.70 (0.00)	-5.80 (0.00)
162844.43+191059.15	20483 (224)	7.905 (0.035)	24.7	387	247	-4.08 (0.00)	-4.89 (0.00)
163133.89+374053.98	18874 (145)	7.887 (0.057)	16.7	471	321	-4.34 (0.00)	-5.13 (0.00)
163100.45+452710.44	21570 (217)	7.995 (0.029)	29.1	272	186	-4.02 (0.00)	-4.76 (0.00)
163259.40+523405.96	13543 (115)	8.000 (0.000)	13.4	311	208	-5.45 (0.00)	-8.44 (0.00)
163322.86+341835.46	18127 (137)	7.880 (0.055)	18.5	390	262	-4.60 (0.00)	-5.56 (0.00)
163334.09+480802.40	12446 (96)	8.000 (0.000)	18.6	249	168	-5.70 (0.00)	-9.61 (0.00)
163401.23+243049.80	12310 (121)	8.000 (0.000)	14.9	232	150	-5.64 (0.00)	-9.61 (0.00)
163411.27+281212.13	17116 (37)	8.040 (0.020)	54.1	130	85	-5.05 (0.16)	-6.17 (0.00)
163520.15+260852.94	15176 (42)	8.000 (0.000)	27.1	218	141	-5.61 (0.00)	-7.82 (0.00)
163654.42+230236.10	17973 (118)	7.752 (0.054)	20.4	299	189	-4.74 (0.00)	-5.84 (0.00)
163654.12+345801.20	13623 (39)	8.000 (0.000)	42.9	115	76	-5.50 (0.14)	-9.35 (0.00)
163621.11+503757.26	12068 (82)	8.000 (0.000)	23.2	194	130	-5.83 (0.00)	-10.06 (0.00)
163841.63+262336.48	11611 (98)	8.000 (0.000)	21.3	227	145	-5.74 (0.00)	-10.26 (0.00)
163824.65+471719.06	15772 (130)	8.232 (0.093)	15.0	321	214	-5.16 (0.00)	-6.83 (0.00)
164007.85+453007.09	16112 (121)	8.040 (0.083)	16.0	361	239	-5.10 (0.00)	-6.65 (0.00)
164056.84+462448.10	10958 (142)	8.000 (0.000)	19.3	170	112	-5.66 (0.00)	-10.54 (0.00)
164240.41+391731.41	13681 (134)	8.000 (0.000)	11.6	275	180	-4.97 (0.40)	-8.29 (0.00)
164340.45+415532.41	19681 (268)	7.939 (0.067)	13.9	537	351	-4.01 (0.00)	-4.61 (0.00)
164432.15+403926.21	16655 (51)	7.898 (0.041)	22.9	344	224	-3.15 (0.13)	-6.51 (0.30)
164814.79+194520.50	17644 (126)	7.897 (0.064)	16.8	411	239	-4.71 (0.00)	-5.75 (0.00)
165052.52+174636.59	14802 (54)	8.000 (0.000)	21.9	281	158	-4.30 (0.17)	-7.91 (0.00)
165003.55+274309.08	18501 (197)	8.144 (0.076)	13.4	470	286	-4.36 (0.00)	-5.01 (0.00)
165015.58+400129.46	15426 (79)	8.000 (0.000)	15.1	422	268	-5.21 (0.00)	-7.11 (0.00)

Table 1. continued.

SDSSJ	T_{eff} [K]	$\log g$ [cgs]	S/N	d [pc]	z [pc]	[H/He]	[Ca/He]
165057.16+404327.30	18855 (134)	8.129 (0.057)	19.4	230	146	-4.54 (0.00)	-5.04 (0.00)
165155.97+182112.80	14863 (94)	8.000 (0.000)	15.8	216	122	-5.45 (0.00)	-7.71 (0.00)
165103.57+290820.67	12601 (71)	8.000 (0.000)	24.4	188	115	-5.85 (0.00)	-9.64 (0.00)
165117.04+432757.35	18336 (142)	7.873 (0.054)	19.5	423	269	-4.58 (0.00)	-5.52 (0.00)
165245.82+290053.20	11553 (159)	8.000 (0.000)	13.2	221	134	-5.54 (0.00)	-10.04 (0.00)
165222.17+322214.10	16796 (103)	8.138 (0.062)	19.1	210	129	-5.11 (0.00)	-6.44 (0.00)
165339.17+174838.84	19403 (288)	8.204 (0.060)	15.0	454	252	-3.98 (0.00)	-4.55 (0.00)
165349.38+274647.30	19803 (290)	7.669 (0.078)	11.8	462	277	-3.88 (0.00)	-4.51 (0.00)
165321.37+331352.85	14407 (93)	8.000 (0.000)	14.3	375	231	-5.34 (0.00)	-7.80 (0.00)
165513.16+333313.60	18296 (177)	7.842 (0.069)	15.5	514	315	-4.45 (0.00)	-5.32 (0.00)
165522.00+433638.56	14949 (54)	8.000 (0.000)	22.2	250	157	-5.32 (0.00)	-7.81 (0.00)
165946.51+393418.30	22489 (532)	7.840 (0.057)	15.0	590	361	-3.43 (0.00)	-4.08 (0.00)
165938.54+614101.20	12852 (71)	8.000 (0.000)	23.4	155	93	-5.87 (0.00)	-9.56 (0.00)
170143.68+384953.60	18391 (139)	7.780 (0.055)	20.2	418	253	-4.61 (0.00)	-5.61 (0.00)
170142.11+643720.70	12272 (66)	8.000 (0.000)	26.8	191	112	-5.94 (0.00)	-10.06 (0.00)
170345.85+212506.20	20500 (370)	7.973 (0.063)	14.0	361	195	-3.85 (0.00)	-4.45 (0.00)
170539.46+241945.10	16713 (79)	8.066 (0.055)	21.8	234	128	-4.54 (0.25)	-6.51 (0.00)
170547.14+315007.70	14274 (33)	8.000 (0.000)	40.7	97	56	-5.59 (0.14)	-8.93 (0.00)
170559.94+383115.60	11016 (82)	8.000 (0.000)	29.3	160	95	-5.87 (0.00)	-10.73 (0.00)
170611.93+404656.64	16371 (102)	8.219 (0.077)	16.6	320	191	-4.48 (0.26)	-6.52 (0.00)
170727.11+203153.25	44920 (668)	7.780 (0.059)	20.9	703	369	-2.73 (0.00)	-4.00 (0.00)
170741.85+390032.10	13761 (97)	8.000 (0.000)	15.7	325	191	-5.52 (0.00)	-8.41 (0.00)
170731.42+395755.04	16973 (93)	8.060 (0.055)	21.2	309	183	-5.06 (0.00)	-6.34 (0.00)
171323.16+280954.20	15948 (124)	8.000 (0.000)	10.2	370	200	-4.89 (0.00)	-6.42 (0.00)
171350.40+380843.14	17160 (118)	8.006 (0.071)	17.2	344	196	-4.88 (0.00)	-6.00 (0.00)
171403.75+365810.56	12016 (98)	8.000 (0.000)	19.3	243	138	-5.20 (0.17)	-8.57 (0.14)
171607.71+285006.98	11012 (197)	8.000 (0.000)	11.6	222	118	-5.47 (0.00)	-10.29 (0.00)
171643.99+305817.80	14270 (57)	8.000 (0.000)	24.1	198	107	-5.20 (0.29)	-8.47 (0.00)
171726.64+422052.73	13192 (137)	8.000 (0.000)	12.4	377	215	-5.49 (0.00)	-8.73 (0.00)
172243.19+603059.70	18572 (163)	8.120 (0.067)	16.6	267	150	-4.53 (0.00)	-5.05 (0.00)
172520.14+244604.94	15721 (78)	8.000 (0.000)	14.9	427	208	-5.12 (0.00)	-6.84 (0.00)
172505.57+312909.49	42344 (839)	7.957 (0.081)	14.0	907	469	-2.65 (0.00)	-4.00 (0.00)
172520.20+345910.86	14945 (70)	8.000 (0.000)	17.9	312	165	-5.41 (0.00)	-7.62 (0.00)
172551.69+633142.50	17950 (140)	8.116 (0.068)	16.8	397	219	-4.70 (0.00)	-5.52 (0.00)
172856.21+325045.60	13709 (68)	8.000 (0.000)	23.0	242	123	-5.79 (0.00)	-8.14 (0.15)
173042.25+540313.30	15492 (93)	8.000 (0.000)	13.4	307	169	-5.18 (0.00)	-7.03 (0.00)
173232.09+335610.40	23011 (699)	7.843 (0.076)	11.0	674	339	-3.09 (0.00)	-4.00 (0.00)
173304.07+645606.00	12885 (139)	8.000 (0.000)	11.7	369	199	-5.13 (0.00)	-8.94 (0.00)
173635.42+642113.90	11198 (89)	8.000 (0.000)	25.0	191	102	-5.15 (0.15)	-10.62 (0.00)
174025.00+245704.50	20444 (144)	8.328 (0.037)	23.6	196	86	-3.31 (0.19)	-4.54 (0.00)
180520.65+225608.40	12618 (42)	8.000 (0.000)	39.9	90	30	-4.86 (0.06)	-10.09 (0.00)
183131.64+420220.30	13057 (43)	8.000 (0.000)	38.8	121	44	-6.46 (0.00)	-9.39 (0.25)
183200.07+420029.80	16142 (91)	8.000 (0.000)	14.2	389	140	-5.07 (0.00)	-6.59 (0.00)
183252.20+421526.10	21396 (266)	7.915 (0.034)	25.4	301	108	-4.03 (0.00)	-4.76 (0.00)
183511.51+405752.10	18322 (211)	8.024 (0.082)	13.3	489	169	-4.46 (0.00)	-5.05 (0.00)
200757.10-120832.00	14202 (35)	8.000 (0.000)	39.3	121	46	-4.63 (0.09)	-8.42 (0.23)
201001.60-124126.10	17525 (113)	7.915 (0.064)	19.1	366	143	-4.90 (0.00)	-6.04 (0.00)
202718.52+763446.60	11865 (148)	8.000 (0.000)	14.3	172	61	-5.62 (0.00)	-9.93 (0.00)
203821.24-053413.30	13564 (93)	8.000 (0.000)	17.1	213	94	-5.64 (0.00)	-8.71 (0.00)
204213.01+764041.10	14703 (107)	8.000 (0.000)	12.5	327	114	-5.27 (0.00)	-7.55 (0.00)
204919.49+765828.90	14437 (123)	8.000 (0.000)	11.0	249	86	-5.23 (0.00)	-7.64 (0.00)
205336.69+764511.20	11816 (134)	8.000 (0.000)	14.3	238	81	-5.43 (0.28)	-9.95 (0.00)
210328.68-004640.60	19584 (356)	8.085 (0.090)	10.7	491	241	-3.96 (0.00)	-4.50 (0.00)
210742.30+102611.70	13439 (101)	8.000 (0.000)	15.8	242	98	-5.38 (0.00)	-8.75 (0.00)
211252.07+102931.40	18475 (190)	8.194 (0.071)	14.3	369	156	-4.04 (0.41)	-5.04 (0.00)
211841.06-080346.90	11515 (152)	8.000 (0.000)	14.6	243	144	-5.61 (0.00)	-10.14 (0.00)
211950.84-064056.20	23234 (767)	7.993 (0.072)	12.1	533	312	-3.16 (0.00)	-4.00 (0.00)

Table 1. continued.

SDSSJ	T_{eff} [K]	$\log g$ [cgs]	S/N	d [pc]	z [pc]	[H/He]	[Ca/He]
212242.66-070417.10	15432 (35)	8.000 (0.000)	32.8	208	124	-5.18 (0.25)	-7.54 (0.00)
212310.79+003518.85	13121 (86)	8.000 (0.000)	18.5	339	184	-5.65 (0.00)	-9.05 (0.00)
212403.12+114230.20	29480 (676)	7.750 (0.093)	11.0	676	301	-2.84 (0.00)	-4.00 (0.00)
212552.77+001918.62	20772 (277)	7.919 (0.049)	18.4	581	321	-3.92 (0.00)	-4.54 (0.00)
212656.72-002423.90	17920 (146)	8.061 (0.070)	16.2	276	155	-4.68 (0.00)	-5.52 (0.00)
212645.06+043138.36	16300 (115)	7.991 (0.088)	15.4	444	231	-5.03 (0.00)	-6.48 (0.00)
212841.49+001231.40	17094 (139)	7.751 (0.080)	15.4	377	212	-4.83 (0.00)	-6.01 (0.00)
212901.32-062924.60	18041 (120)	7.916 (0.046)	25.0	250	153	-4.77 (0.39)	-6.00 (0.00)
213103.40+105956.10	13675 (137)	8.000 (0.000)	11.7	275	130	-5.42 (0.00)	-8.32 (0.00)
213840.11-003337.70	15662 (38)	8.000 (0.000)	31.7	153	91	-4.73 (0.15)	-7.52 (0.00)
214116.86-062959.70	12650 (159)	8.000 (0.000)	11.3	246	160	-5.50 (0.00)	-9.15 (0.00)
214441.71+010029.88	20081 (188)	7.960 (0.031)	29.5	341	205	-4.14 (0.00)	-5.16 (0.00)
214541.77+003147.50	16369 (131)	8.625 (0.084)	14.9	200	122	-4.42 (0.31)	-6.50 (0.00)
214527.11+125256.00	14847 (78)	8.000 (0.000)	17.1	211	104	-5.46 (0.00)	-7.74 (0.00)
214712.52+001903.70	16896 (128)	8.155 (0.081)	15.1	272	167	-4.89 (0.00)	-6.06 (0.00)
215005.31+005552.90	14338 (120)	8.000 (0.000)	10.8	293	181	-4.01 (0.30)	-7.69 (0.00)
215107.29-084829.40	11609 (127)	8.000 (0.000)	15.9	210	145	-5.63 (0.00)	-10.12 (0.00)
215514.44-075833.80	35117 (712)	7.899 (0.072)	15.3	546	380	-2.78 (0.00)	-4.00 (0.00)
220250.26+213120.21	20293 (109)	7.986 (0.020)	48.3	187	83	-4.48 (0.00)	-5.54 (0.00)
220554.02+055252.90	11072 (105)	8.000 (0.000)	23.7	182	112	-5.82 (0.00)	-10.65 (0.00)
220633.02+125910.91	15176 (82)	8.000 (0.000)	14.0	278	153	-4.36 (0.29)	-7.31 (0.00)
220623.74+132556.50	16142 (81)	7.950 (0.061)	22.1	223	121	-5.32 (0.00)	-7.00 (0.00)
220827.84+223636.90	12181 (84)	8.000 (0.000)	22.6	93	41	-5.86 (0.00)	-10.02 (0.00)
220934.85+122336.60	17103 (72)	8.166 (0.043)	28.1	159	89	-5.23 (0.00)	-6.04 (0.17)
221000.09+213719.06	11140 (87)	8.000 (0.000)	26.7	179	82	-5.85 (0.00)	-10.65 (0.00)
221150.49+222139.60	16763 (123)	8.027 (0.072)	16.4	363	166	-5.01 (0.00)	-6.30 (0.00)
221729.25+000833.40	21506 (672)	7.789 (0.080)	11.7	440	306	-3.45 (0.00)	-4.03 (0.00)
221921.99-005202.08	13465 (95)	8.000 (0.000)	16.4	348	246	-5.57 (0.00)	-8.67 (0.00)
221945.63+123554.05	12356 (26)	8.000 (0.000)	65.5	99	58	-4.84 (0.07)	-10.51 (0.00)
222833.82+141037.00	31724 (714)	7.756 (0.085)	10.8	646	380	-2.80 (0.00)	-4.00 (0.00)
223255.40-084044.20	13050 (40)	8.000 (0.000)	39.5	145	115	-6.49 (0.00)	-9.72 (0.00)
224009.33+320828.55	15065 (99)	8.000 (0.000)	12.1	402	163	-5.15 (0.00)	-7.19 (0.00)
224348.66+312239.74	11171 (142)	8.000 (0.000)	17.6	245	99	-5.62 (0.00)	-10.38 (0.00)
224558.86+295245.80	11112 (139)	8.000 (0.000)	16.4	256	99	-5.29 (0.25)	-10.37 (0.00)
224600.40-080424.20	15902 (89)	8.000 (0.000)	13.4	335	273	-5.07 (0.00)	-6.69 (0.00)
224748.78+302251.65	19303 (274)	7.964 (0.068)	13.5	523	219	-4.09 (0.00)	-4.55 (0.00)
224930.38-001623.00	14260 (62)	8.000 (0.000)	23.2	224	172	-5.45 (0.25)	-8.47 (0.00)
224913.64+064410.04	17178 (112)	7.967 (0.068)	17.2	429	304	-4.87 (0.00)	-6.00 (0.30)
225020.91-091425.60	25393 (959)	8.012 (0.071)	11.4	479	398	-2.92 (0.00)	-4.00 (0.00)
225124.08+311627.80	46654 (145)	7.969 (0.063)	18.6	883	371	-3.00 (0.00)	-4.00 (0.00)
225158.75+314936.45	12351 (86)	8.000 (0.000)	21.4	245	101	-5.80 (0.00)	-9.80 (0.00)
225122.13+315628.90	17313 (81)	7.930 (0.045)	25.3	281	115	-5.05 (0.00)	-6.03 (0.00)
225206.14+130831.20	12190 (170)	8.000 (0.000)	11.3	253	164	-5.50 (0.00)	-9.51 (0.00)
225410.48+054419.46	15602 (92)	8.000 (0.000)	13.1	410	297	-5.08 (0.00)	-6.83 (0.00)
225424.73+231515.82	27852 (397)	7.853 (0.053)	16.8	607	323	-3.00 (0.00)	-4.00 (0.00)
225652.76+225738.28	11011 (102)	8.000 (0.000)	23.3	241	130	-5.75 (0.00)	-10.61 (0.00)
230419.08+232518.17	21781 (566)	8.006 (0.072)	12.2	503	277	-3.38 (0.00)	-4.00 (0.00)
230620.01+211118.50	15052 (88)	8.000 (0.000)	14.4	361	209	-5.17 (0.57)	-7.19 (0.58)
230842.14+243753.22	12115 (71)	8.000 (0.000)	26.0	179	96	-5.25 (0.21)	-10.09 (0.00)
230953.03+060820.02	14212 (40)	8.000 (0.000)	33.0	191	143	-3.85 (0.22)	-6.39 (0.12)
231026.38+211204.80	18448 (115)	8.013 (0.042)	24.6	339	198	-4.09 (0.25)	-5.12 (0.00)
231141.59-004100.60	13656 (137)	8.000 (0.000)	11.8	263	214	-5.42 (0.00)	-7.33 (0.29)
231141.44+232707.00	17005 (99)	7.898 (0.062)	20.1	394	220	-5.05 (0.00)	-6.28 (0.00)
231940.36-085037.20	13521 (149)	8.000 (0.000)	10.3	294	259	-5.33 (0.00)	-8.29 (0.00)
231952.98+132242.12	19734 (180)	8.053 (0.046)	21.2	318	220	-4.25 (0.00)	-4.55 (0.00)
232108.40+010433.50	21041 (583)	8.137 (0.073)	13.0	288	234	-3.69 (0.00)	-4.18 (0.00)
232344.88+150858.80	18255 (156)	7.828 (0.060)	17.7	419	284	-4.55 (0.00)	-5.12 (0.00)

Table 1. continued.

SDSSJ	T_{eff} [K]	$\log g$ [cgs]	S/N	d [pc]	z [pc]	[H/He]	[Ca/He]
232548.14+125120.57	14041 (59)	8.000 (0.000)	24.2	236	166	-5.73 (0.00)	-8.60 (0.00)
232711.11+515344.70	18642 (98)	7.931 (0.040)	26.2	199	30	-4.68 (0.00)	-5.73 (0.00)
233232.24+080229.90	16623 (66)	8.091 (0.046)	26.0	231	177	-4.41 (0.19)	-6.54 (0.00)
233305.10+005155.90	21366 (503)	8.001 (0.066)	13.3	403	335	-3.58 (0.00)	-4.03 (0.00)
233725.94+145711.40	17064 (139)	8.304 (0.076)	15.3	308	215	-4.90 (0.00)	-5.99 (0.00)
233817.93+083732.70	11076 (76)	8.000 (0.000)	31.1	156	119	-5.96 (0.00)	-10.79 (0.00)
233913.27+152838.30	16348 (40)	8.221 (0.029)	43.7	125	86	-4.96 (0.13)	-7.04 (0.00)
234137.40+082559.06	14198 (40)	8.000 (0.000)	32.9	191	147	-4.61 (0.11)	-8.73 (0.00)
234143.68+133237.71	12141 (150)	8.000 (0.000)	12.8	305	217	-5.51 (0.00)	-9.55 (0.00)
234459.45+024108.93	17139 (50)	7.915 (0.031)	38.9	210	174	-5.29 (0.00)	-6.11 (0.00)
234754.18+032451.50	12175 (110)	8.000 (0.000)	17.1	287	238	-4.86 (0.19)	-9.74 (0.00)
234820.10+023417.65	11063 (72)	8.000 (0.000)	34.4	121	101	-5.56 (0.22)	-10.81 (0.00)
234814.03-094850.70	19797 (280)	8.020 (0.071)	13.0	535	493	-3.93 (0.00)	-4.50 (0.00)
234848.77+381754.60	23924 (478)	8.065 (0.046)	18.6	240	93	-3.32 (0.00)	-4.00 (0.00)
234920.03+045019.56	19886 (303)	8.104 (0.077)	12.4	470	383	-3.91 (0.00)	-4.45 (0.00)
234923.88+424739.20	13091 (156)	8.000 (0.000)	10.6	310	99	-5.42 (0.00)	-8.71 (0.00)
235139.39+361203.10	13363 (146)	8.000 (0.000)	10.8	418	0	-5.39 (0.00)	-7.82 (0.30)
235245.19+030706.30	12319 (188)	8.000 (0.000)	10.1	317	265	-5.37 (0.00)	-9.23 (0.00)
235336.08+372055.30	15926 (111)	8.000 (0.000)	11.9	510	208	-5.02 (0.00)	-6.61 (0.00)
235410.39-010728.50	16101 (115)	7.762 (0.086)	16.0	297	259	-5.13 (0.00)	-6.75 (0.00)
235719.20+244111.52	14419 (76)	8.000 (0.000)	16.9	332	197	-4.45 (0.22)	-7.96 (0.00)
235844.21-102202.24	19748 (257)	8.464 (0.075)	13.7	349	326	-4.09 (0.00)	-4.51 (0.00)
235825.61+254824.52	12673 (90)	8.000 (0.000)	19.0	261	151	-5.72 (0.00)	-9.47 (0.00)
235959.48+082813.01	16220 (93)	8.376 (0.066)	20.3	204	161	-4.43 (0.15)	-6.79 (0.00)